pennsylvania
DEPARTMENT OF TRANSPORTATION

# Internal Curing with Fine Light Weight Aggregates (FLWA) Created from Unsuitable Coal Combustion Ash (CCA)

FINAL REPORT

9/12/2024

By (PI) Yaghoob (Amir) Farnam
Drexel University

Drexel UNIVERSITY

COMMONWEALTH OF PENNSYLVANIA
DEPARTMENT OF TRANSPORTATION

DEPARTMENT OF TRANSPORTATION
UNITED STATES OF AMERICA

CONTRACT # 4400024510 / 51203
WORK ORDER # DREXEL 001

**Technical Report Documentation Page**

| 1. Report No. | 2. Government Accession No. | 3. Recipient's Catalog No. |
|---|---|---|
| FHWA-PA-2024-007-DREXEL WO 001 | | |

| 4. Title and Subtitle | 5. Report Date |
|---|---|
| Internal Curing with Fine Light Weight Aggregates (FLWA) Created from Unsuitable Coal Combustion Ash (CCA) | 09/12/2024 |
| | **6. Performing Organization Code** |

| 7. Author(s) | 8. Performing Organization Report No. |
|---|---|
| Yousif M. Alqenai, Bankole Tejuoso, Amin Zouyousefain, Thuy Nguyen, and Yaghoob (Amir) Farnam | |

| 9. Performing Organization Name and Address | 10. Work Unit No. (TRAIS) |
|---|---|
| Drexel University<br>3141 Chestnut Street, Curtis 262-B,<br>Philadelphia, PA 19104 | **11. Contract or Grant No.**<br>4400024510 |

| 12. Sponsoring Agency Name and Address | 13. Type of Report and Period Covered |
|---|---|
| The Pennsylvania Department of Transportation<br>Bureau of Planning and Research<br>Commonwealth Keystone Building<br>400 North Street, 6th Floor<br>Harrisburg, PA 17120-0064 | Final Report – 06/13/2022-09/12/2024 |
| | **14. Sponsoring Agency Code:** |

**15. Supplementary Notes**

None


**16. Abstract**

This work studies the potential use of fine lightweight aggregates (FLWA) created from 'as received' landfill condition coal combustion ash (CCA), referred to as CCA-FLWA, for concrete internal curing applications. The innovative CCA-FLWA is manufactured using high-temperature sintering like available industrial kilns. To manufacture CCA-FLWA with desired properties for internal curing, this work first optimizes the manufacturing process and assesses CCA-FLWA properties for concrete applications. Second, concrete samples with CCA-FLWA are prepared and their internal curing performance is assessed in comparison to available FLWA in the market. Finally, a cost analysis and feasibility of implementation for future industrial application of manufactured CCA-FLWA are performed. This work demonstrates that FLWA with desired internal curing properties can be manufactured using CCA waste streams for concrete applications. Not only does CCA-FLWA meet ASTM requirements for FLWA, but also concrete made using CCA-FLWA shows promising fresh and hardened properties for internal curing applications. The industrial manufacturing of CCA-FLWA is also found feasible when compared to commercial FLWA to transfer the technology to the concrete industry.


| 17. Key Words | 18. Distribution Statement |
|---|---|
| Coal combustion ash, concrete, internal curing, lightweight aggregate, and sintering. | No restrictions. This document is available from the National Technical Information Service, Springfield, VA 22161 |

| 19. Security Classif. (of this report) | 20. Security Classif. (of this page) | 21. No. of Pages | 22. Price |
|---|---|---|---|
| Unclassified | Unclassified | 125 | |

**Statement of Credit**

This work was sponsored by the Pennsylvania Department of Transportation and the U.S. Department of Transportation, Federal Highway Administration.

**Internal Curing with Fine Light Weight Aggregates (FLWA) Created from Unsuitable Coal Combustion Ash (CCA)**

**Work Order (WO) 001**

**Contract Number: 4400024510**

# Task 5 – Deliverable 5.2: Final Report

**Submitted To:**
Pennsylvania Department of Transportation (PennDOT)


**Prepared by:**
***Yousif M. Alqenai,*** Ph.D. Candidate, Department of Civil, Architectural, and Environmental Engineering, Drexel University, Philadelphia, PA

***Yaghoob (Amir) Farnam,*** Ph.D. (Principal Investigator) Associate Professor, Department of Civil, Architectural, and Environmental Engineering, Drexel University, Philadelphia, PA

**Undergraduate/Graduate Students:**
***Bankole Tejuoso*** *(MS. Graduate),* ***Zouyousefain Amin*** *(MS. Graduate),* ***Thuy Nguyen*** *(BS. Undergraduate)*


PennDOT Project Manager: Bradley Thomas
PennDOT Technical Advisor: Tyler Culhane

# Table of Contents

## List of Figures

## List of Tables

## 1. Project Overview

This project studied the potential use of fine lightweight aggregates (FLWA) created from 'as received' landfill condition coal combustion ash (CCA), referred to as CCA-FLWA, for concrete internal curing applications. The innovative CCA-FLWA was manufactured using high-temperature sintering like available industrial kilns. To manufacture CCA-FLWA with desired properties for internal curing, three objectives were pursued including optimizing the manufacturing process and assessing CCA-FLWA properties for concrete applications (investigated in Task 1), preparing concrete with CCA-FLWA and assessing the internal curing performance of concrete in comparison to current available FLWA in the market (investigated in Task 2), and performing cost analysis and feasibility of implementation for future industrial application of manufactured CCA-FLWA (investigated in Task 3).

In Task 1, thermodynamic modeling alongside experimental characterization was performed to successfully manufacture CCA-FLWA via sintering to be used for concrete internal curing applications. This was accomplished by first performing material characterization on acquired as received CCA from a Pennsylvania powerplant. The intricate raw CCA blend composition was examined to define oxide contents, glassy phases, particle sizes, and moisture contents of CCAs for CCA-FLWA production processes. This information was used with the thermodynamic modeling necessary to identify the FLWA manufacturing process (i.e., blending proportions with a fluxing agent, fresh pellet preparation, and kiln sintering configuration). Accordingly, the manufacturing process was optimized for successful CCA-FLWA production. A sintering temperature of 1075°C with the addition of 2% sodium hydroxide, by mass, as fluxing agent) was found necessary for manufacturing successful CCA-FLWA for concrete internal curing application. The manufactured CCA-FLWA's engineering properties were assessed in accordance

with ASTM standards including density, porous structure, active amorphous phase, crush strength, water absorption, desorption, and the shape of the CCA-FLWA. All CCA-FLWA engineering properties were compared to commercially available FLWA counterparts in the market. The study showed promising engineering properties of CCA-FLWA meeting ASTM requirements with comparable or superior properties compared with commercially available FLWA.

The work was followed by Task 2, where manufactured CCA-FLWA was used to prepare concrete samples for internal curing performance evaluations. Commercial-FLWA and fine normal-weight aggregates were also used to prepare 'control' conventional concrete samples to comparatively evaluate the internal curing performance of concrete samples. Both fresh and hardened properties of concrete samples were evaluated in accordance with ASTM standards. Samples were manufactured in accordance with Pennsylvania Department of Transportation bridge design criteria. The influence of using pre-saturated FLWA on fresh properties was assessed to indicate the achievement of a satisfactory slump, air content, and density. Additionally, concrete-hardened properties were evaluated including compressive strength, flexural strength, shrinkage, rate of water absorption, freeze-thaw performance, and leachability of COPC in concrete. Concrete made using CCA-LWA showed promising internal curing performance where required ASTM and environmental requirements were fully met. It was also shown that concrete made using CCA-LWA performs relatively like or better than control samples made commercial-FLWA and fine normal-weight aggregates.

Finally, in Task 3, a cost analysis and feasibility study were performed to ensure the practical implementation of CCA-FLWA at an industrial scale. Information acquired from O1 and O2 were utilized along with market research data to identify the successful implementation of CCA-FLWA highlighting three main considerations i) evaluating the security (availability) of suitable CCA

within the region, ii) assessing the facility requirements for hosting production lines, and iii) project personnel for successful execution. The cost analysis considered raw material, capital equipment costs, and manufacturing costs to identify the net and capital costs of producing CCA-FLWA. No major industrial implementation hurdle was found during the investigation indicating CCA-FLWA can be implemented in larger scales.

In summary, this project demonstrated that FLWA with desired internal curing properties can be manufactured using CCA waste streams for concrete applications. Not only did CCA-FLWA meet ASTM requirements for FLWA, but also concrete made using CCA-FLWA showed promising fresh and hardened properties for internal curing applications. The industrial manufacturing of CCA-FLWA was also found feasible when compared to commercial FLWA to transfer the technology to the concrete industry.

## 2. CCA-FLWA Production and Characterization from Unsuitable CCA Local Resources in Pennsylvania (Task 1)

The U.S. Energy Information Administration (EIA) reported in February 2022 that coal was the second largest energy source, generating 22% of the United States' electricity supply [1]. A by-product of burning coal for energy is solid waste, referred to as waste coal combustion ash (W-CCA) [2]. Based on a study conducted in 2016, the American Chemical Society announced that W-CCA was the second most abundant waste material in the US behind household trash [3]. The American Coal Ash Association (ACAA) declared in 2021 that 90 million tons of W-CCA were produced across the United States and only 60% of the produced W-CCA was utilized in 2021 (**Figure 1**) [4]. The 40% W-CCA is usually disposed of in surface ponds and landfills causing a financial burden on power plants and a hazard to the environment and human health [5]. The unutilized W-CCA is usually disposed of in landfills or stored in surface impoundments. Storing

W-CCA has both economic repercussions and negative impacts on the environment and human health. Utilizing W-CCA to produce a beneficial product can significantly reduce its harmful effects and promote a circular economy. Drexel team has shown that manufacturing lightweight aggregates (LWA) from W-CCA can be a viable solution [6–13]. LWA manufactured from W-CCA can be utilized in various applications such as lightweight masonry units, lightweight concrete structures, internal curing of concrete, wastewater treatment, green roof sublayers, and geotechnical backfill for drainage purposes. The conversion of W-CCA into LWA has shown promising results, however, it is associated with many challenges due to its vast range of chemical and physical composition, various manufacturing approaches, and intended industrial use.

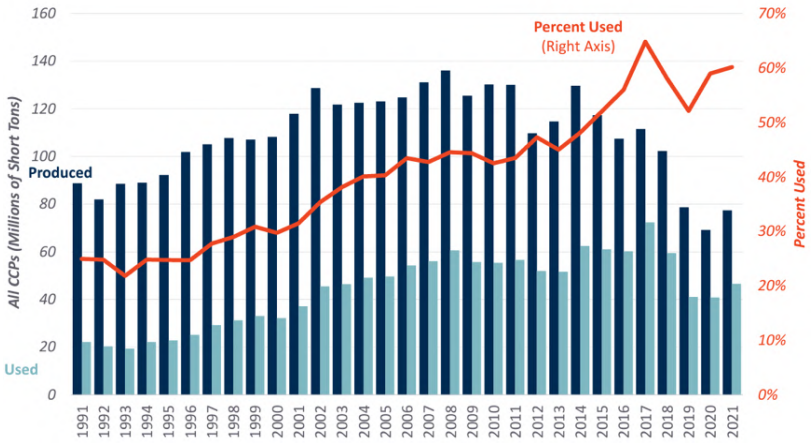


**Figure 1.** All CCPs Production and Use with Percent Used.

This research focuses on converting W-CCA including off-spec fly ash and bottom ash into fine-LWA (FLWA) for internal curing purposes. The project is divided into four main tasks and this study covers the scope of task 1. Task 1 consists of a literature review, acquisition/experimental characterization of W-CCA from a Pennsylvania resource, the production of CCA-Fine-LWA (CCA-FLWA), and finally the mechanical and physical characterization of the produced CCA-FLWA. In the following, activities conducted under Task 1 are discussed in detail:

### 2.1. Literature Review

This section first discusses challenges associated with the manufacturing of CCA-FLWA for internal curing purposes. It further explores manufacturing parameters that may influence the properties of FLWA. Additionally, it investigates the importance of internal curing for concrete durability and performance. Finally, it discusses the necessary engineering properties of FLWA required when CCA-FLWA is used for concrete internal curing. The properties include compressive strength for sustaining structural integrity during the concrete mix, water absorption/desorption capacity for internal water supply, and particle size distribution (PSD) for efficient distribution of CCA-FLWA within a concrete mix.

A wide variation and range of elemental concentrations have been reported for W-CCA chemical and physical compositions [14]. W-CCA can have variations in its saturation degree (wet and dry conditions). W-CCA samples can have variations in their particle size, shape, and distribution [15]. It has been documented that W-CCA chemical properties have demonstrated variations in oxide content among different samples [14]. A previous investigation indicated that W-CCA samples can have elemental concentration ranges of $SiO_2$ between 13% and 80%, $Al_2O_3$ between 1.6% and 46%, CaO between 0.12% and 29%, and $Fe_2O_3$ between 0.60% and 69% (by mass) [14]. Additionally, the amount of glassy (amorphous) phase, carbon residue, and constituents of potential concerns can also vary substantially in W-CCA [16]. Faced with this variation, creating a robust CCA-FLWA manufacturing process has been reported to be challenging and demands a thorough understanding of these interactions for manufacturing [16].

By characterizing and implementing W-CCA physical and chemical properties in the manufacturing process, researchers have been able to manufacture the desired CCA-FLWA. Xiong et al. 2019 investigated the effect of fly ash particle size on the strength and pore structure of CCA-

FLWA made using cold binding manufacturing technology with ordinary Portland cement [17]. Their research examined the mechanical and physical properties of CCA-FLWA manufactured from various W-CCA particle sizes. Their research demonstrated that W-CCA with a particle size range of 0.125-0.25mm achieved optimum chemical reaction degree thereby producing more C-S-H, fewer micro-holes, fewer cracks, higher strength performance, and more uniform pores in manufactured CCA-FLWA [17]. Balapour et al. 2021 were able to utilize the W-CCA properties to assist in thermodynamic modeling and parametric experimentation to achieve successful CCA-FLWA [10,11]. Their investigation performed X-ray fluorescence (XRF) and X-ray diffraction (XRD) of W-CCA for phase identification and oxide composition. This information was used during thermodynamics modeling to predict the change and formation of stable phases during sintering. By understanding the CCA-FLWA thermal behavior during sintering, they were able to identify the required sintering temperature to achieve successful FLWA with desired engineering properties [10,11].

While desired CCA-FLWA can be produced, there is little known about its performance when used in concrete for internal curing. Accordingly, it is critical that its performance is evaluated for the internal curing of concrete [13]. The utilization of CCA-FLWA for the internal curing of concrete requires a thorough understanding of its addition to concrete. Internal curing is used in concrete to enhance its performance and durability by increasing the cement's degree of hydration [18]. Concrete is a porous material that requires water for the proper hydration of cement particles. During the curing process, concrete can lose moisture due to evaporation, leading to self-desiccation [18]. This self-desiccation can hinder proper hydration, resulting in reduced strength development, increased cracking, and decreased durability [19]. Internal hydration techniques, such as incorporating saturated CCA-FLWA, provide an internal water resource that replenishes

the moisture lost through self-desiccation [20]. By maintaining an adequate internal water supply, internal hydration mitigates self-desiccation, reduces concrete shrinkage, enhances its durability, and ensures efficient cement hydration [21]. Several parameters need to be considered when designing an internally cured concrete mixture using CCA-FLWA. Factors that must be considered are the CCA-FLWA absorption capacity, desorption capacity, size, and distribution within a mix-design [18].

The absorption and desorption capacity (sorption behavior) of the CCA-FLWA can influence the internal curing performance in a concrete mixture. The sorption behavior is the ability of CCA-FLWA to hold and release water prior to and post-concrete mixing [22]. It is important to know the absorption capacity of the CCA-FLWA being used and consider it when calculating the water demand of the concrete mixture. The absorption capacity will also define the amount of CCA-FLWA to be added to internally cured concrete. The CCA-FLWA amount used in a concrete mixture will directly indicate the amount of water supplied during the hydration process. **Equation 1** is recommended by Bentz and Weiss [18] to calculate the amount of LWA to be added for internal curing of concrete:

$$M_{LWA} = \frac{C_f \times CS \times a_{max}}{\mathrm{S} \times \phi_{max}} \qquad \textbf{Equation 1}$$

This analytical approach (Equation 1) considers parameters associated with both CCA-FLWA and cement properties. The variables considered in this equation include $C_f$ = cement factor, $CS$ = chemical shrinkage, $a_{max}$ = maximum cement degree of hydration, S = CCA-FLWA degree of saturation, and $\phi_{max}$ = CCA-FLWA absorption capacity. This equation can be then used to quantify the mass of dry CCA-FLWA ($M_{LWA}$) per unit volume of concrete necessary to achieve successful concrete internal curing [18].

Gradation is another physical property of CCA-FLWA that can influence its internal curing performance [23]. The particle size distribution (PSD) of the CCA-FLWA affects the workability, mechanical properties of the concrete, and packing density during a concrete mixture. It is recommended to use FLWA in accordance with ASTM C1761/C1761M [24]. The effect of the spatial distribution of CCA-FLWA on internal curing has been thoroughly investigated [18]. A finer gradation of CCA-FLWA indicates a higher quantity of smaller size aggregates relative to the total mass of CCA-FLWA used [25]. This results in an increased surface area of the aggregate particles. With a larger surface area, there is more contact between the CCA-FLWA and the concrete, leading to a more homogeneous water supply distribution throughout the mixture [25]. By achieving a more uniform distribution of CCA-FLWA, the internal water supply within the concrete is enhanced. The optimal distribution of CCA-FLWA allows desorbed water to have more contact with surrounding cementitious materials. This facilitates a more efficient internal hydration process, where water can readily diffuse and react with cement particles, leading to improved performance and durability of the concrete [25]. Furthermore, the increased surface area provided by the finer gradation of CCA-FLWA allows for more water to be desorbed from the aggregates and made available for internal curing. This ensures that a higher volume of water is distributed throughout the concrete, enhancing its hydration, and contributing to improved strength development, reduced shrinkage, and enhanced long-term durability [25].

### 2.1.1. Research Methodology

To address the necessary parameters that dictate the applicability of CCA-FLWA for internal curing, the research team begins by compiling information regarding waste CCA's chemical and physical properties from a local resource in Pennsylvania. The team then manufactures CCA-FLWA based on the W-CCA characterization analysis and thermodynamic/experimental design.

Engineering properties are finally evaluated to ensure the manufactured CCA-FLWAs meet specific classification criteria and are applicable for the internal curing of concrete.

The acquisition and experimental characterization of W-CCA from a local resource in Pennsylvania involved conducting various tests to comprehensively characterize the chemical and physical properties of the W-CCA. These tests included but were not limited to x-ray fluorescence (XRF), x-ray diffraction (XRD), thermogravimetric analysis (TGA), and laser particle size analysis. Additionally, other characterization techniques and tests were performed to gather more specific information about the W-CCA samples. The comprehensive chemical/physical characterization aimed to define the oxide contents, identify the glassy phase, determine particle sizes, and assess the moisture contents of the coal combustion ash. These characterization results serve as crucial data for the CCA-FLWA production processes, providing insights into the suitability of the ash for lightweight aggregate production and guiding the development of optimized manufacturing methods.

The manufacturing process of CCA-FLWA required both analytical and experimental investigations to produce a fully functioning product ready for use in the market. Understanding and optimizing the manufacturing process of CCA-FLWA will reduce wasted energy, time, and material. Enhancing the physical and mechanical properties of the resultant CCA-FLWA will produce an effective product that best fits its intended industrial applications. The analytical investigation of CCA-FLWA involves a thermochemical analysis guided by thermodynamic modeling software to predict the required material formulation for manufacturing the required CCA-FLWA properties. The experimental investigation of the manufacturing process involves three main phases: (a) mixing CCA, water, and fluxing agent (NaOH) to create CCA paste, (b)

pelletizing CCA paste to create spherical green aggregates, and (c) sintering green pellets for particle fusion and solidification.

The engineering properties of the manufactured CCA-FLWA were characterized to determine their classifications and applicability for concrete internal curing. Properties such as unit weight, specific gravity, sorption capacity, particle size distribution, strength, porosity, and shape of the CCA-FLWA were studied and compared to an existing traditional FLWA available in the market. American Society for Resting and Materials (ASTM) standards were followed to ensure the manufactured CCA-FLWA were classified as industrial FLWA material. These standards help maintain quality control, provide consistency in physical and chemical properties, and enable the appropriate use of CCA-FLWA for concrete internal curing.

### 2.2. Acquisition and experimental characterization of W-CCA from PA local Resource

The W-CCA samples were acquired from a CCA resource within the state of Pennsylvania to encompass various types of W-CCA including off-spec fly ash and bottom ash samples. The location of the powerplants landfill providing the W-CCA was in York Haven, PA. Using x-ray fluorescence (XRF), x-ray diffraction (XRD), thermogravimetric analysis (TGA), and laser particle size analysis, a comprehensive chemical/physical characterization was conducted to define oxide contents, glassy phase, particle sizes, and moisture contents of W-CCAs for CCA-FLWA production.

#### 2.2.1. Raw Waste Coal Combusted Ash (W-CCA) Properties

The raw W-CCA used for testing was obtained from TALEN Energy, Brunner Island Steam Electric Station located at 1400 Wago Rd, York Haven, PA (**Figure 2**). The landfill that supplied the tested raw W-CCA was from basin #6.

**Figure 2.** TALEN Energy, Brunner Island Steam Electric Station.

Basin #6 is a large coal ash landfill that has been expanded and stored ash for more than 10 years (**Figure 3.** Aero view of the Basin #6 Landfill). Basin #6 is an uncovered landfill and has been exposed to the ambient environment. The W-CCA in this landfill has been kept moist to prevent W-CCA dust migration when exposed to high winds. A few barrels (50 gals ~ 190 liters each) were collected from basin #6 for this project.

**Figure 3.** Aero view of the Basin #6 Landfill.

### 2.2.2. Raw CCA Preparation

**Figure 4** depicts the field retrieved W-CCA sample with a high moisture content which is mainly due to long-term outdoor storage and exposure to the natural environmental conditions. Also, excess water was applied to field W-CCA to avoid dust generation as a safety measure to control heavy metals.

**Figure 4.** Raw CCA retrieved from landfill basin #6.

A moisture analysis was performed by determining the oven-dry condition of retrieved raw W-CCA. To reach oven-dry condition, a raw CCA sample was placed in a stationary oven at 105ºC, and its mass was measured at different time intervals until a constant mass was achieved (**Table 1**). The Oven dry condition was reached when raw CCA remained in the oven for about 10 hours (**Figure 5**).

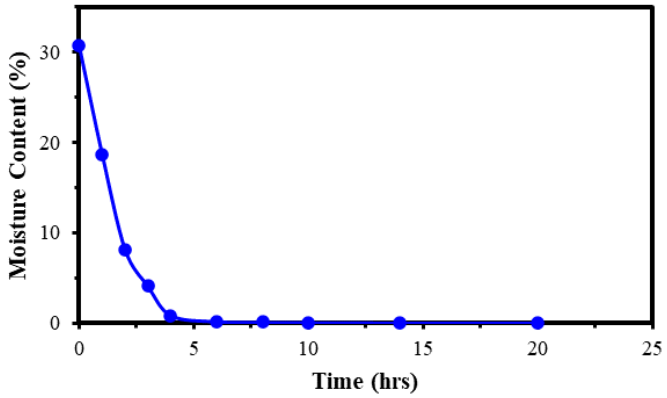


**Figure 5.** Moisture Content Analysis for raw field CCA from basin #6.

**Table 1.** Moisture Analysis for raw field CCA.

| Raw CCA | Time (hr) | Mass (g) | Moisture Content (%) |
|---|---|---|---|
| | 0 | 1000.1 | 30.71 |
| | 1 | 908.2 | 18.70 |
| | 2 | 827.4 | 8.14 |
| **TALEN** | 3 | 796.3 | 4.08 |
| **Raw CCA** | 4 | 771.6 | 0.85 |
| **Placed in oven** | 6 | 766.5 | 0.18 |
| **at 105ºC** | 8 | 765.9 | 0.10 |
| | 10 | 765.6 | 0.07 |
| | 14 | 765.3 | 0.03 |
| | 20 | 765.1 | 0 |

### 2.2.3. Field Debris Analysis

After removing the excess moisture, oven-dry raw W-CCA was sieved under a fume hood using sieve #30 to remove any field debris. The retained field debris contained stone, large particles, stems, vegetation, roots, and shells (**Figure 6**). To determine how much field debris was contained in raw W-CCA, a field debris analysis using the sieve test was performed on four samples (**Table 2**).

**Figure 6.** Field debris was removed from CCA.

**Table 2.** Field debris analysis using sieve #30.

| Test | Initial Mass (g) | Passing CCA (g) | Retained Field Debris (g) |
|---|---|---|---|
| **1** | 907.14 | 808.61 | 98.02 |
| **2** | 948.68 | 844.83 | 92.29 |
| **3** | 973.84 | 897.16 | 75.49 |
| **4** | 920.89 | 849.88 | 69.81 |
| **Mean** | 937.64 | 850.12 | 83.90 |

After sieving the raw W-CCA samples, both the passing W-CCA and retained field debris mass were measured. The raw W-CCA contained approximately ~10% field debris. The debris fraction of W-CCA was stored in sealed containers for future use. The passing W-CCA fraction of the material was used to manufacture CCA-FLWA.

### 2.2.4. Scanning Electron Microscopy (SEM) of Raw W-CCA

Oven-dry sieved W-CCA was examined using scanning electron microscopy (SEM) to further understand the coal ash morphology. The SEM images revealed that there are traces of bottom ash, fly ash, and small field debris (sand, rocks, vegetation, roots, etc.) based on their shapes and sizes. The scale of the images taken was 200 micrometers and 100 micrometers, as can be seen in **Figure 7 (a) and (b)**, respectively.

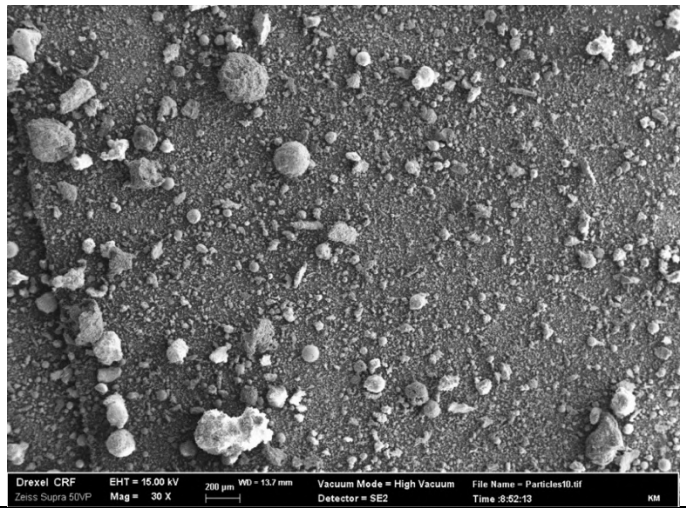


a) SEM Image with scale of 200µm

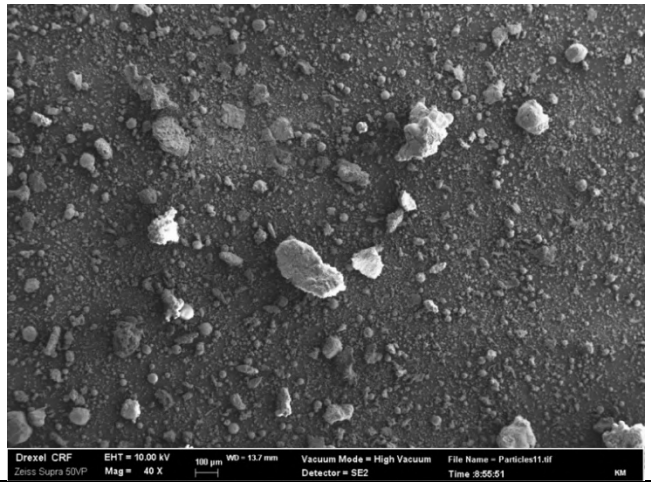


b) SEM Image with scale of 100µm

**Figure 7.** SEM image analysis of raw W-CAA showing traces of bottom ash, fly ash, and field debris.

### 2.2.5. Particle Size Distribution (PSD) of Raw CCA

To measure the particle size distribution (PSD) of the raw CCA, laser diffraction particle size and distribution analyses on four sieved samples (using sieve #30) were performed. The tests were run on a Horiba LA950-V2 Partica analyzer using a wet cell module with methanol as the dispersion solvent. To prepare the samples for analysis, a small amount of the powder was dropped into a beaker and a few mL of methanol was added. A spatula was used to deagglomerate and incorporate the powder into a thin slurry to test for wetting / floating. The sample was further diluted to develop a dispersion that could be pipetted into the analysis cell. The system was aligned and calibrated to the circulating methanol bath before each sample set was measured. The sample was introduced into the bath and reasonable stability was noted, indicated by a settled response in the real-time histogram. The sample was treated with the internal ultrasonic horn for 60 seconds to help deagglomerate the samples. After stability was noted, a measurement of the particle size distribution was then taken. Three measurements were conducted on the sample to assure repeatability. After the third measurement, the data were checked for consistency. An average data set for the three runs was calculated and the graphic report was generated for the samples tested. The graphical data is shown in **Figure 8** and indicates the results for the four samples tested. It indicates that a wider range of PSD for fly ash was available and indicates three peaks showing higher frequency and amount of specific ash size at each peak region.

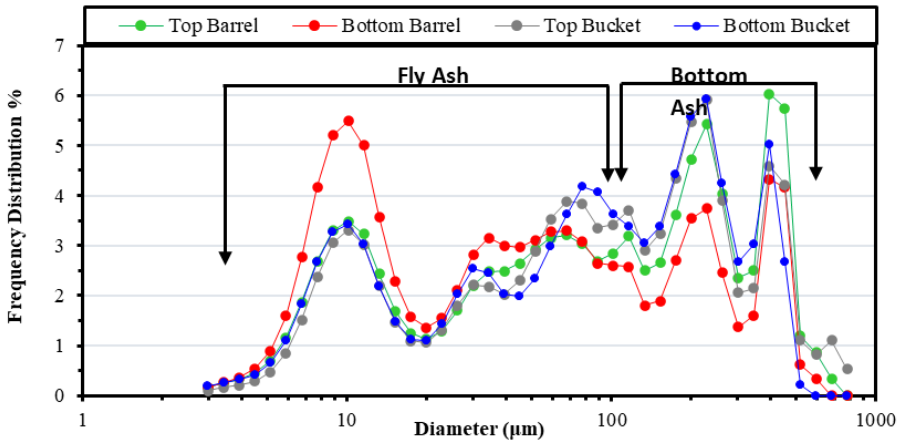


**Figure 8.** Particle Size Distribution (PSD) of W-CCA acquired from PA source.

### 2.2.6. Semi-quantitative X-ray Fluorescence (XRF) Analysis of Raw CCA

To assess the oxide chemical composition of the raw CCA, four sieved samples (using sieve# 30) were examined using a semi-quantitative XRF analysis. The samples were taken from each of barrel collected to obtain a more precise chemical composition. The oxide amount in four samples is relatively consistent with $Fe_2O_3$ having the highest variability of ±0.6. The Loss on Ignition (LOI) was determined by heating the samples at 950°C in air for 1 hour, allowing them to cool to room temperature, and measuring the weight losses. The XRF samples were then prepared by blending 1 gram of the post LOI sample with 10 grams of a lithium borate flux (LiM 49.75/LiT49.75/LiBr 0.5). The mixtures were heated to 1050°C in platinum crucibles and the resulting melts were poured into standard 40mm molds and allowed to harden. The XRF test was run on a Panalytical MagiX PW-2403 Wavelength Dispersive X-ray Fluorescence Spectrometer using Rh radiation. This is a sequential analyzer that examines one element at a time between Na and U and optimizes the test conditions for each element. The XRF spectra were evaluated using the Fundamental Parameters standardless quantification software associated with the XRF system. This approach uses established sensitivity factors for pure elements and considers fluorescence yield, absorption, and enhanced excitation effects. The results of the analyses have been

normalized to equal 100% including the LOI. The percentage of the chemical compositions and their average values are listed in **Table 3.**

**Table 3.** Average chemical oxides proportion of CCA from XRF analysis.

| Sample | $Al_2O_3$ | CaO | $Fe_2O_3$ | MgO | $K_2O$ | $SiO_2$ | $Na_2O$ | $TiO_2$ | $P_2O_5$ | LOI |
|---|---|---|---|---|---|---|---|---|---|---|
| **1** | 24.60 | 1.14 | 16.00 | 0.76 | 2.21 | 44.50 | 0.25 | 1.39 | 0.28 | 8.53 |
| **2** | 24.80 | 1.13 | 14.80 | 0.72 | 2.22 | 44.10 | 0.27 | 1.42 | 0.30 | 9.79 |
| **3** | 24.60 | 1.19 | 16.10 | 0.69 | 2.24 | 44.60 | 0.29 | 1.33 | 0.28 | 8.24 |
| **4** | 25.30 | 1.17 | 15.6 | 0.69 | 2.25 | 44.60 | 0.33 | 1.36 | 0.30 | 7.94 |
| **Average** | 24.83 (±0.33) | 1.16 (±0.03) | 15.63 (±0.59) | 0.72 (±0.03) | 2.23 (±0.02) | 44.45 (±0.24) | 0.29 (±0.03) | 1.38 (±0.04) | 0.29 (±0.01) | 8.63 (±0.81) |

*The ± represents the standard deviation obtained using four samples

### 2.2.7. X-ray Diffraction (XRD) Analysis of Raw CCA

To quantify the mineral phases of the raw W-CCA, X-ray diffraction was performed using Rigaku MiniFlex Smart Lab device. A 1g sieve sample of the W-CCA was first ground using a pestle and mortar and then passed through sieve #200. This was performed to ensure consistent particle size and accurate results achieved. The test was performed on nominally 0.02º steps in the range of 10º to 70º. Rutile ($TiO_2$) was used as a reference material for the internal quantification standard added as 20% by mass of raw W-CCA. The phase identification and Rietveld refinements (**Figure 9**) were performed using the Profex 5.1.0 software and the phase content was measured and presented in **Table 4**.

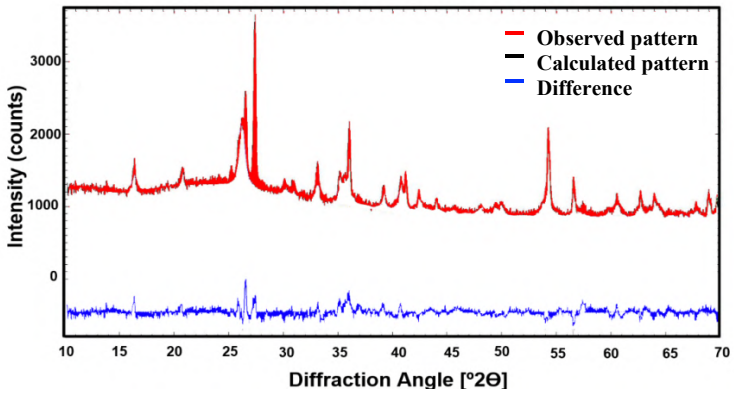


**Figure 9.** X-ray Diffraction (XR) phase identification and Rietveld refinements.

**Table 4.** Quantitative X-ray Diffractometry (XRD) of CCA by mass percent.

| Phase | Phase Formula | Mass (%) |
|---|---|---|
| **Quartz** | $SiO_2$ | 6.0 (±1.9) |
| **Mullite** | $3Al_2O_3 \cdot 2SiO_2$ | 37.2 (±3.5) |
| **Calcite** | $CaCO_3$ | 7.7 (±4.5) |
| **Katoite** | $Ca_3Al_2(SiO_4)_{(3-x)}(OH)_{4x}$ (x=1.5-3) | 2.0 (±0.1) |
| **Anhydrite** | $CaSO_4$ | 2.5 (±0.1) |
| **Hematite** | $Fe_2O_3$ | 2.3 (±0. 55) |
| **Augite** | $(Ca,Na)(Mg,Fe,Al,Ti)(Si,Al)_2O_6$ | 7.3 (±0. 95) |
| **Gypsum** | $CaSO_4 \cdot 2H_2O$ | 2.7 (±1.5) |
| **Dolomite** | $CaMg(CO_3)_2$ | 1.9 (±0.4) |
| **Anatase** | $TiO_2$ | 2.2 (±2.3) |
| **Anorthite** | $CaAl_2Si_2O_8$ | 5.8 (±1.1) |
| **Amorphous** | | 22.4 (±3.2) |

*The number after ± shows one standard deviation of three replicates.

### 2.2.8. Thermogravimetric Analysis (TGA) of Raw CCA

A thermogravimetric analysis (TGA) test was performed on the raw CCA to measure the free carbon content. This was performed by grinding a sample of raw CCA and passing it through sieve #200 (size 75 μm) to achieve consistent particle size. The sample was heated to 750ºC under a nitrogen atmosphere, then cooled down and finally reheated to 1075ºC under a normal air atmosphere (**Figure 10**). This sequence and environmental gas arrangement were performed to separate the oxidization of carbon from other decomposition reactions occurring in the same range of temperatures. The results indicated a 4.73% mass loss attributed to the burnt pure carbon in the raw W-CCA sample (**Figure 11**).

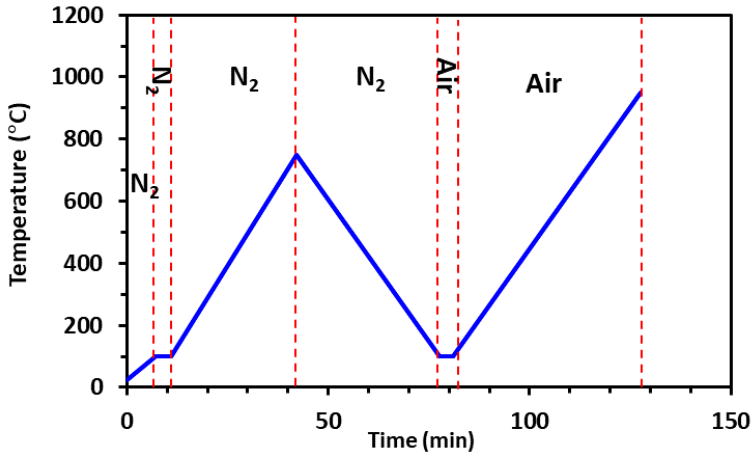


**Figure 10.** The TGA atmosphere and temperature were performed on raw CCA.

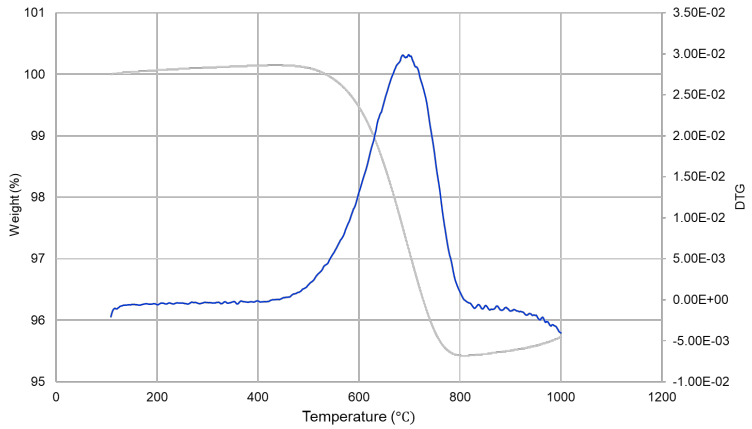


**Figure 11.** TGA results of raw CCA: weight loss over temperature.

### 2.3. Production of CCA-FLWA from selected W-CCA source

The manufacturing process of FLWA produced from W-CCA requires both analytical and experimental investigations. The analytical investigation involves a thermochemical analysis guided by thermodynamic modeling (FactSage[å] software) [26] to predict material formulation and sintering temperature that can generate an appropriate slag/solid ratio to produce CCA-FLWA with the required properties. The experimental investigation of the manufacturing process involves three main phases: (1) mixing raw W-CCA, D.I. water, and a fluxing agent (NaOH) to create W-CCA paste, (2) pelletizing W-CCA paste to create spherical green pellets, and (3) sintering for green pellets fusion and solidification.

### 2.3.1. Analytical Thermodynamic Design of CCA-FLWA Sintering

The analytical investigation involves a thermochemical analysis using the FactSage® model to predict the changes in slag content and chemical compositions at different sintering temperatures. The analytical design determines the ideal amount of fluxing agent to be used for the desired sintering temperature for the successful manufacturing of CCA-FLWA (Figure 12). Our previous research indicated that a minimum of 35% slag content with suspension viscosity greater than 100 pascal-seconds (Pa.s) is required to produce successful CCA-FLWA using W-CCA and NaOH solution for concrete applications [12]. Using data shown in (Table 3 and Table 4) and adding NaOH solution at a weight percent of 0, 1, 2 wt.%, phase diagrams were generated through the FactSage model. A predicted slag content of 38% was achieved at a sintering temperature of 1075°C using 2wt.% NaOH solution. This slag content meets a minimum 35% slag content requirement to produce CCA-FLWA using obtained W-CCA [12].

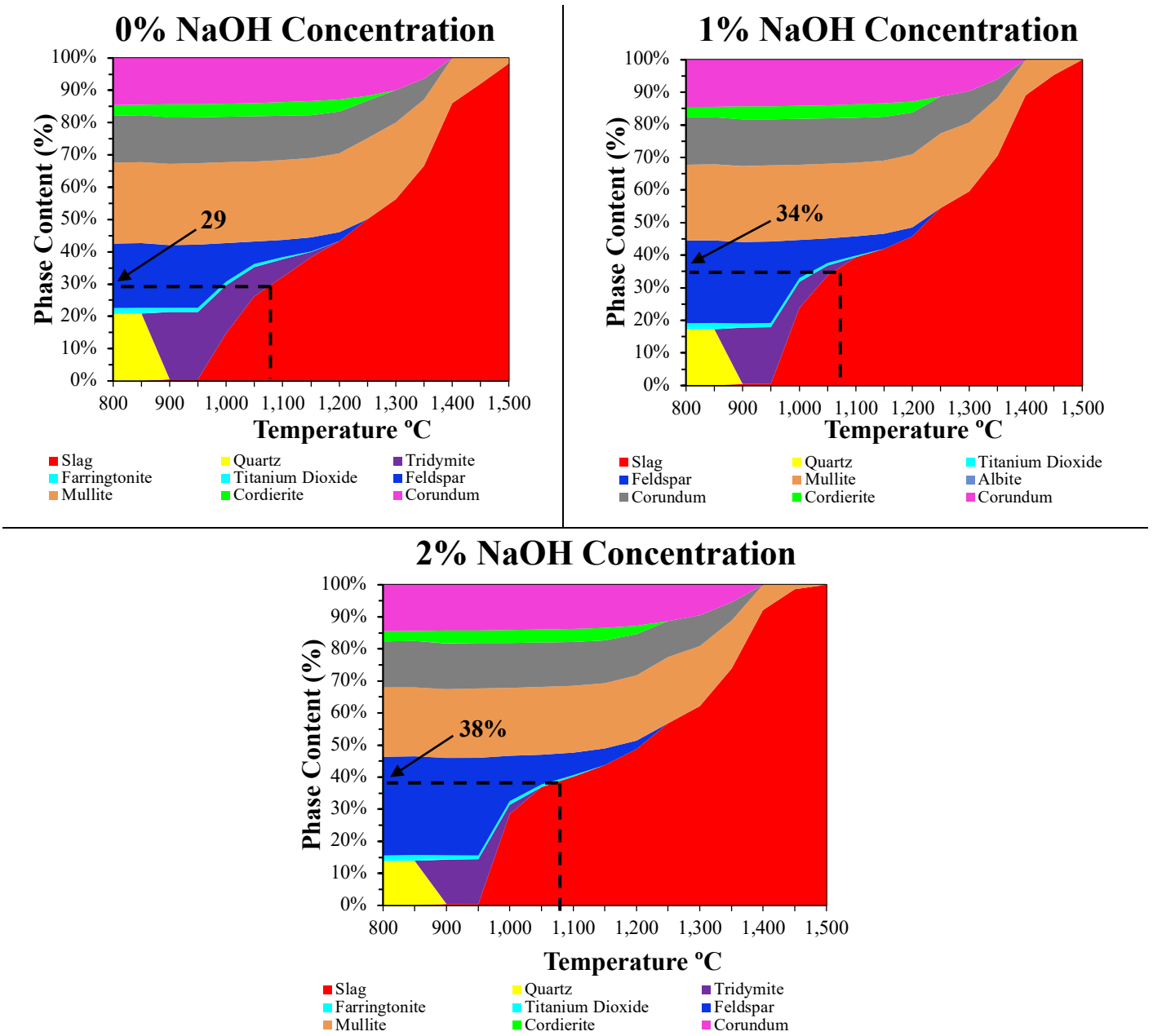


**Figure 12.** Predicted phase diagrams for W-CCA with 0, 1, 2 wt.% NaOH concentration.

The viscosity of the solid/liquid mixture (i.e., suspension) was calculated using various models developed specifically for FLWA manufactured from CCA. The empirical viscosity model developed by Browning et al. 2003 [27] (Equation 2) was used for estimating the viscosity of the liquid phase in CCA-FLWA. The second model introduced by Urbain, 1987 and Kalmanovitch, 1988 [28,29] (Equation 3) was used to calculate a wide range of liquid phase viscosity in CCA-

FLWA. CCA-FLWA are composed of both liquid and solid phases which makes the suspension's composite viscosity dependent on the volume fraction of the solid phase. Therefore, a third model developed by Krieger and Dougherty, 1959 [30] (Equation 4) was employed to estimate the viscosity of the liquid-solid suspension using Equation 2 and Equation 3 The viscosity of solid/liquid mixture at a sintering temperature of 1075°C and 2wt.% NaOH solution was calculated to be $10^{10}$ Pa.s, (Figure 13), meeting the minimum 100 Pa.s viscosity required to produce spherical CCA-FLWA for concrete application [12].

$$\log\left(\frac{\eta L}{T-Ts}\right) = \frac{14788}{T-Ts} - 10.931 \qquad \text{Equation 2}$$

Where:

$$Ts = 306.63 \cdot \ln A - 574.31$$

$$A = \frac{3.19Si^{4+} + 0.855Al^{3+} + 1.6K^{+}}{0.93Ca^{2+} + 1.50Fe^{n+} + 1.21Mg^{2+} + 0.69Na^{+} + 1.35Mn^{n+} + 1.47Ti^{4+} + 1.91S^{2-}}$$

$$Si^{4+} + Al^{3+} + Ca^{2+} + Fe^{n+} + Mg^{2+} + Na^{+} + K^{+} + Mn^{n+} + Ti^{4+} + S^{2-} = 1$$

$$\eta = aTe^{\frac{1000b}{T}} \qquad \text{Equation 3}$$

Where:

$$Ln(a) = -0.2812b - 11.8279$$

$$b = b_0 + b_1N + b_2N^2 + b_3N^3$$

$$b_0 = 13.8 + 39.9355\beta - 44.049\beta^2$$

$$b_1 = 30.481 - 117.1505\beta + 129.9978\beta^2$$

$$b_2 = -40.9429 + 234.0486\beta - 300.04\beta^2$$

$$b_3 = 60.7619 - 153.9276\beta + 211.1616\beta^2$$

$$\beta = \frac{CaO + MgO + Na_2O + K_2O + FeO + TiO_2}{Al_2O_3 + CaO + MgO + Na_2O + K_2O + FeO + TiO_2}$$

$$\eta_s = \eta_L\left(1 - \frac{\phi}{\phi_m}\right)^{-(\eta)\phi_m} \qquad \text{Equation 4}$$

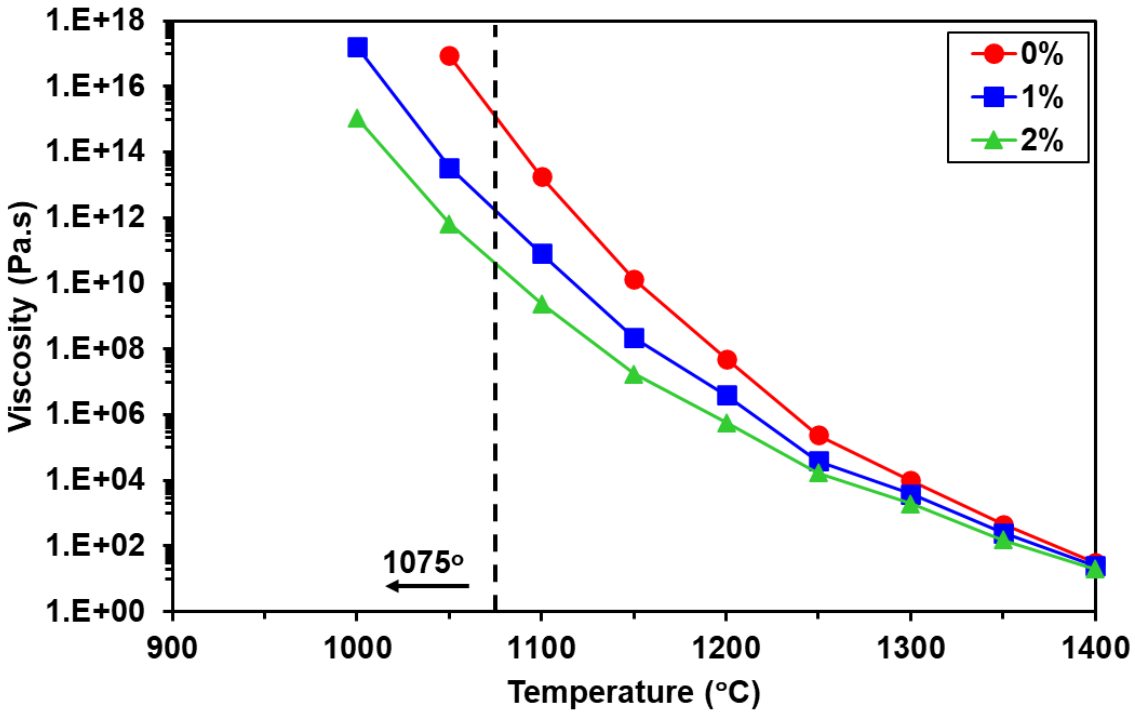


**Figure 13.** Liquid phase viscosity calculations for CCA-FLWA produced with 0, 1, 2% NaOH concentration.

### 2.3.2. CCA-FLWA Manufacturing Process

The manufacturing process involves three main phases: 1) W-CCA paste preparation (mixing W-CCA, water, and fluxing agent NaOH), 2) pelletizing W-CCA paste with a pelletizer to create spherical green pellets, and 3) finally sintering green pellets through a rotary furnace for particle flow, fusion, and solidification.

**Phase-1: W-CCA Paste Preparation:** W-CCA paste was prepared through multiple steps. NaOH-pellets (fluxing agent) (Figure 14a) were initially mixed with DI water to create a 2 weight percent (wt.%) NaOH solution, by mass of W-CCA (Figure 14b). The 2%-NaOH solution was then mixed with oven-dry sieved W-CCA (Figure 14c) to create W-CCA paste. Initial hand mixing (Figure 14d) was performed, then placed into a mechanical mixer (Figure 14e) to achieve thorough mixing. Afterward, the W-CCA paste (Figure 14f) was ready for phase-2 pelletization.

a) NaOH pellets

b) 2% NaOH Solution

c) Raw W-CCA + NaOH Solution

d) Hand mixing

e) Mixer

f) W-CCA Paste

**Figure 14.** Phase 1: W-CCA paste preparation.

**Phase-2: Pelletization:** This Phase consists of pelletizing W-CCA paste to create spherical pellets. A pelletizer device (Figure 15) was used with a pan that was set to a 45º angle for optimum pelletizing. The rotational rate was set to 10 rpm to ensure sufficient pellet formation and rolling to achieve sphericity. Through testing, spherical pellets were achieved after 6 to 7 minutes of pelletizing, meaning that it takes 6-7 minutes to pelletize approximately ~ 1000g of W-CCA paste.


**Figure 15.** Pelletizer with adjusted angle 45º and set speed 10 rpm.

The pelletizing process starts with W-CCA paste placed into the pan to create spherical pellets (Figure 16a). During the pelletizing, oven dry (OD) W-CCA was added as a coating material to prevent the agglomeration of spherical pellets (Figure 16b). The minimum coating amount of 10% (mass-based) was achieved through a parametric study by adding 1% (mass-based) increments of OD W-CCA to the mixture until agglomeration of pellets was no longer observed. The final spherical pellets were then placed into the stationary oven at 105 °C (Figure 16c) for 2 hours to remove excess moisture and achieve OD green spherical pellets (Figure 16d).

a) Paste into pelletizer's pan

b) Coating addition

c) Stationary oven

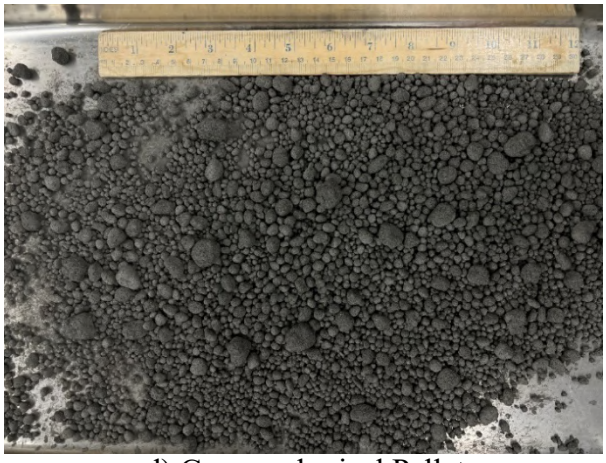

d) Green-spherical Pellets

**Figure 16.** Pelletization process.

**Phase-3: Sintering:** The rotary furnace and associated apparatus and components were configured to allow a continuous flow process, as illustrated in Figure 17. After the green pellets were OD for 2 hours and no moisture was left, the dried green pellets were placed into a feeder. The feeder

discharged green pellets onto a conveyor belt. The conveyor belt transported the green pellets to a shooter that fed the green pellets into a rotary furnace. The green pellets traveled through the rotary furnace tube at a defined mean residence time (MRT) at a sintering temperature of 1075 ºC. The sintered green pellets were discharged at the collecting end as CCA-FLWA. An exhaust hood was placed at the elevated end of the rotary furnace to discharge any gaseous carbon fumes. These fumes are a result of sintering and escape through the feeding end of the rotary furnace due to the drag effect.

The furnace consists of two heating zones that can reach temperatures up to 1500°C. The rotary furnace has a tilting range from -5° to 35° and a rotational speed from 0 to 7 rpm. The dimensions of the furnace tube are 1200 mm long and a diameter of 60 mm. The rotary furnace was operated at a specific configuration (angle, rotation speed) to reach a specific MRT of green pellets passing through the rotary furnace tube. Our previous study indicates that an optimum MRT to successfully produce enough molten phase for successful CCA-FLWA production is 15 minutes [31]. To obtain the optimum manufacturing parameters, a detailed parametric study was conducted that is presented later in this report.

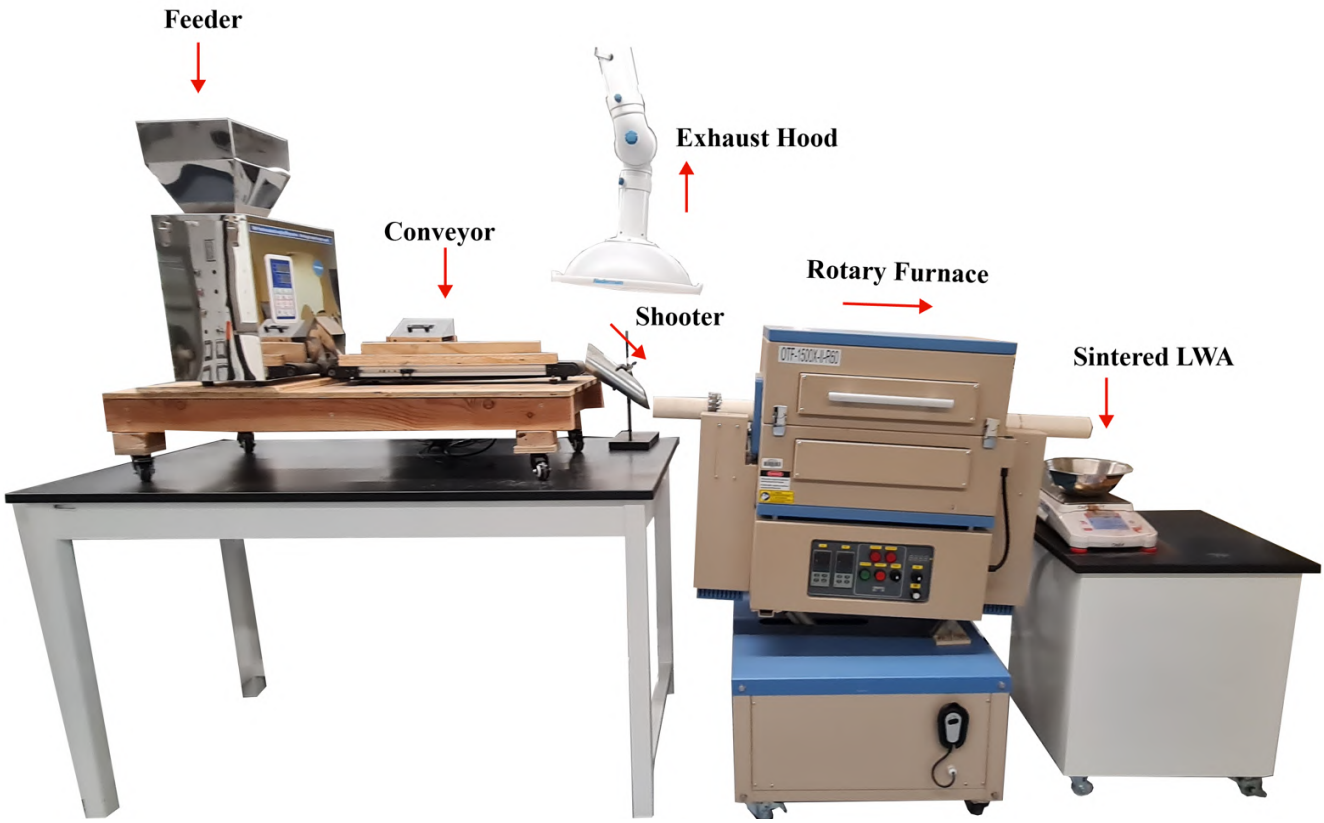


**Figure 17.** Sintering apparatus and flow of production

Once green pellets entered the rotary furnace tube, they were instantly rotated to allow the rolling of pellets through the rotary furnace. The furnace contains two heat chambers that were maintained at the same temperature of 1075 ºC (± 20 ºC) as shown in Figure 18. This temperature was selected as commercial large-scale furnaces for traditional CCA-FLWA are usually set to temperatures ranging from 1050 to 1200 ºC. Beyond the heat chambers, the temperature decreases gradually. This means the green pellets experienced a gradual thermal change as they rolled through the rotary furnace.

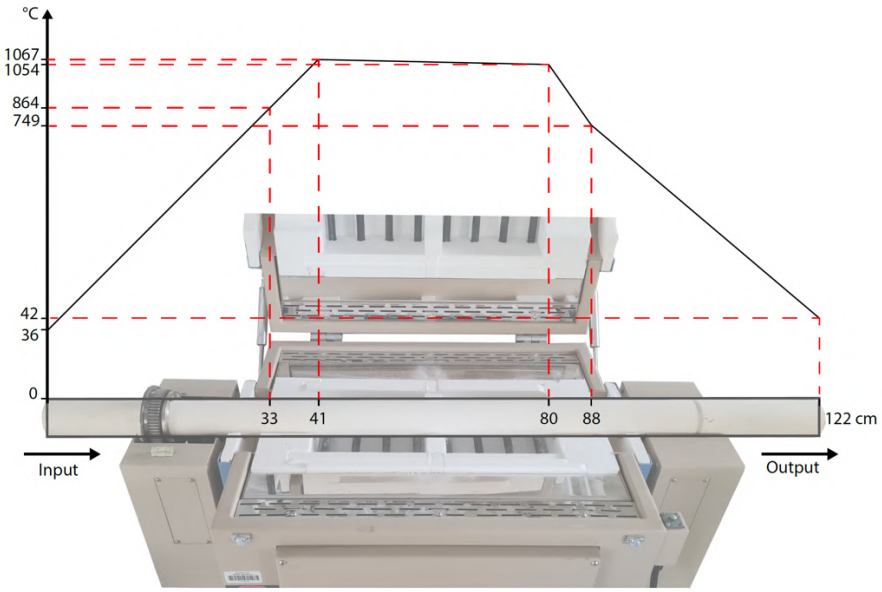


**Figure 18.** Rotary furnace heat zone analysis: Furnace temperature as a function of distance from the beginning of the rotary tube (tube diameter = 6 cm, length = 122 cm).

### 2.3.3. Optimization of CCA-FLWA's manufacturing process

To optimize the manufacturing parameters for CCA-FLWA production, further investigation was performed to understand their influence on the CCA-FLWA's physical and mechanical properties. Three necessary considerations were investigated during CCA-FLWA production including engineering particle size distribution (PSD), reducing furnace clogging observed during sintering, and maintaining an MRT of 15 minutes.

#### 2.3.3.1. Particle Size Distribution (PSD) Optimization of CCA-FLWA

The ASTM C1761/C1761M standard on FLWA used for internal curing of concrete indicates that FLWAs must meet the assigned grading requirements range. The grading range is provided based on the PSD mass percentage of a FLWA batch (Table 5). The moisture content associated with W-CCA paste preparation before pelletization was found to control the PSD of the manufactured CCA-FLWA. The W-CCA paste proportions were referred to as the liquid/solid

(L/S) ratio and only the moisture content in the liquid ratio was adjusted to achieve the required PSD necessary to meet ASTM C1761/C1761M standard.

**Table 5.** ASTM grading requirement for FLWA used for internal curing of concrete.

| FLWA Nominal Size Designation | 12.5mm (1/2in.) | 9.5mm (3/8in.) | 4.75mm (No.4) | 2.36mm (No.8) | 1.18mm (No.16) | 300µm (No.50) | 150µm (No.100) | 75µm (No.200) |
|---|---|---|---|---|---|---|---|---|
| **4.75mm to 0 (No.4 to 0)** | --- | 100 | 65-100 | --- | 15-80 | 0-35 | 0-25 | --- |

A parametric study was performed to determine the required L/S ratio necessary to achieve the ASTM C1761/C1761M gradation range. Four L/S ratios at 0.36, 0.35, 0.34, and 0.33 were tested and their FLWA-PSD (Figure 19). It was noted that a higher L/S ratio produced more coarser aggregates and a lower L/S produced finer aggregates. Figure 19 indicates that the produced FLWA-PSD using a L/S ratio of 0.34, 0.35, and 0.36 did not comply with ASTM required gradation boundaries. It was noted that as the L/S ratio was reduced, the FLWA gradation approaches the necessary ASTM gradation boundary conditions. The L/S ratio was optimized at a L/S ratio of 0.33 (Figure 20), however, the achieved FLWA gradation resulted in clogging of sintered LWA in the rotary furnace ceramic tube; the clogging further obstructed continuous CCA-FLWA production flow. Clogging issues are often observed in lab-scale production of CCA-FLWA as the size of rotary furnace tubes is relatively small in comparison to the size of CCA-FLWA. To alleviate the clogging issue observed, further investigation was conducted as described later in this report.

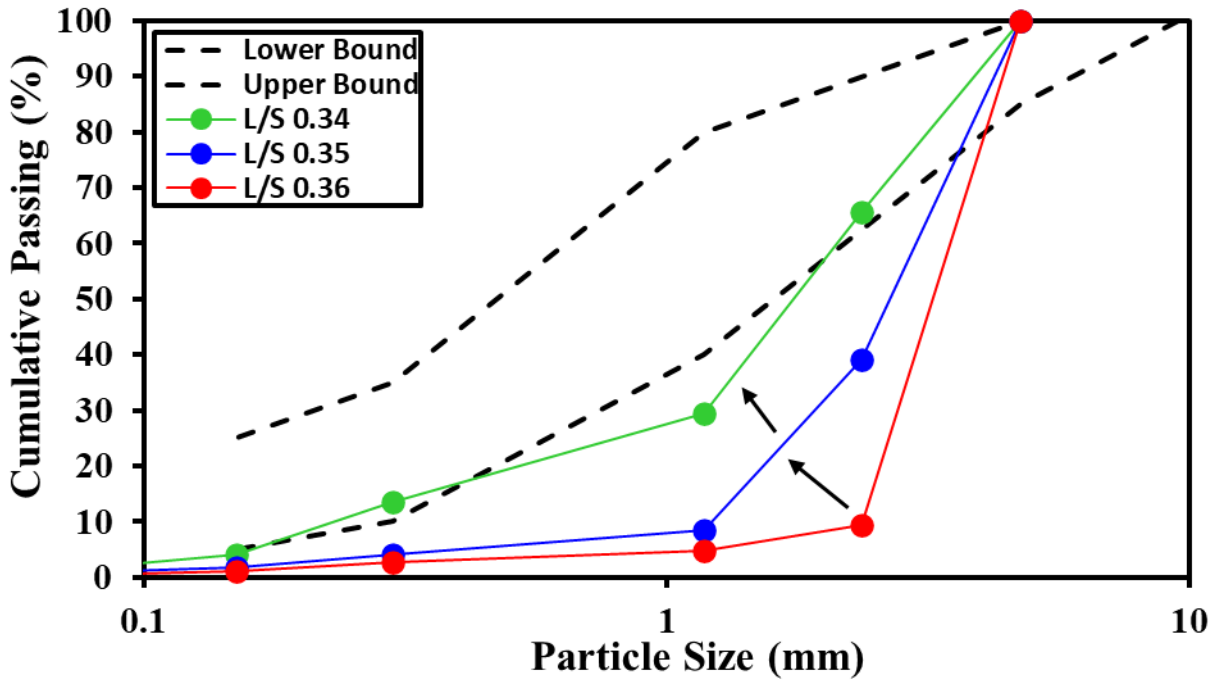


**Figure 19.** Gradation curves for CCA-FLWA manufactured using L/S ratio of 0.34, 0.35, and 0.36, indicating that as L/S ratio is reduced the FLWA-PSD approaches ASTM C1761/C1761M PSD boundaries.

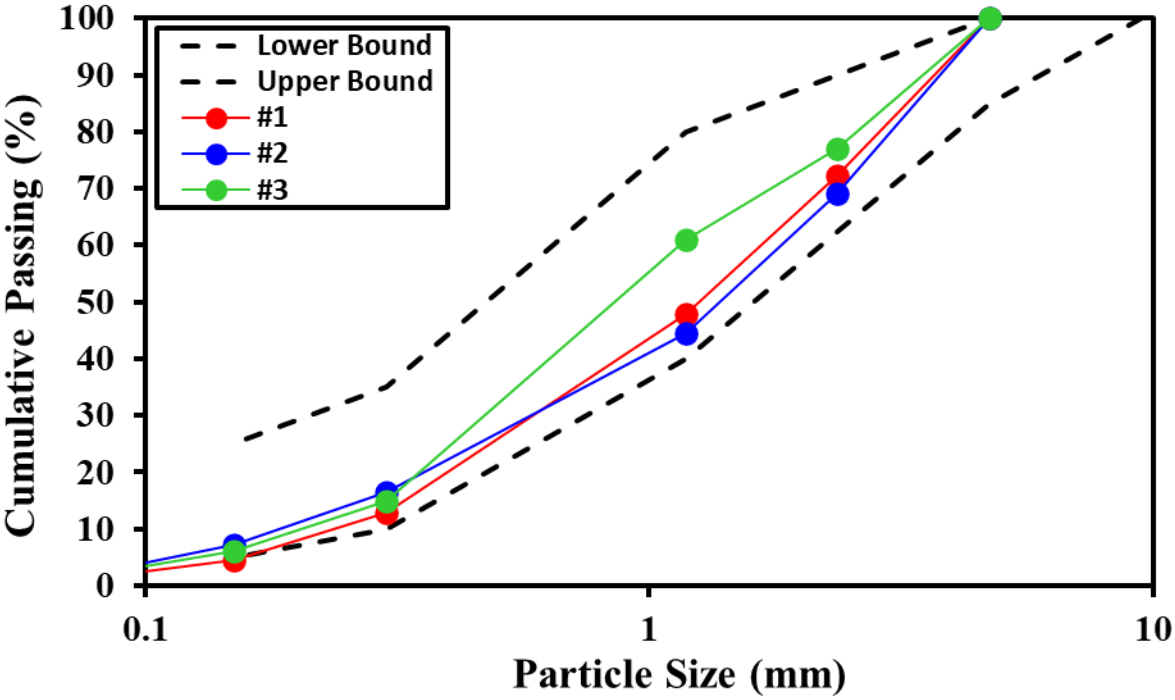


**Figure 20.** Gradation of CCA-FLWA manufactured using a L/S ratio of 0.33 complying with ASTM C1761/C1761M PSD boundaries, performed for three tests for reproducibility verification.

#### 2.3.3.2. Clogging

Clogging was observed during sintering in phase-3 of the manufacturing process and occurred in a ring-like shape around the inner surface of the rotary furnace tube (Figure 21). The clogging prevents a smooth passage of pellets through the rotary furnace tube. It was discovered that clogging occurred due to an increase in pellets sizes below 1.18 mm in diameter which are retained in sieve size No. 50 and No. 100. The increase in the number of smaller pellets increased the total surface area of the batch and indicated that the coating amount was insufficient to cover the entire pellets surface area (Figure 22).

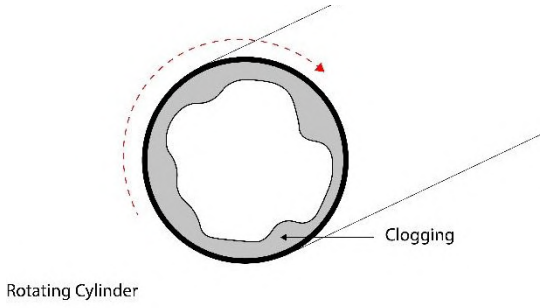


**Figure 21.** Clogging of the rotary furnace tube.

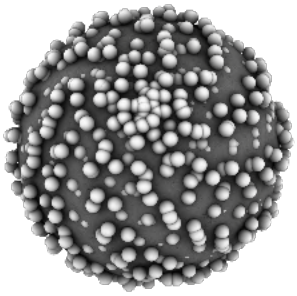

**Figure 22.** Coating distribution on spherical pellet based on SEM observation.

The coating effect on clogging was examined by adjusting the coating quantity in phase 2-pelletization. The initial minimum amount of coating used was 10% (mass-based) of the W-CCA mass used to prepare the CCA-FLWA. At this coating amount, it was noticed that 90g of sintered CCA-FLWA was produced before clogging occurred. When coating was increased to 20% (mass-based), it was noted that the clogging occurred after producing 150g of sintered CCA-FLWA (Figure 23). The increase in coating amount did not eliminate clogging, however, it was able to enhance the production level. Clogging is believed to occur due to the size limitations of the laboratory-scale rotary furnace. In pilot-scale CCA-FLWA production, clogging is resolved by

striking the furnace tube to agitate the clogged aggregates and allow for continuous CCA-FLWA production. flow.

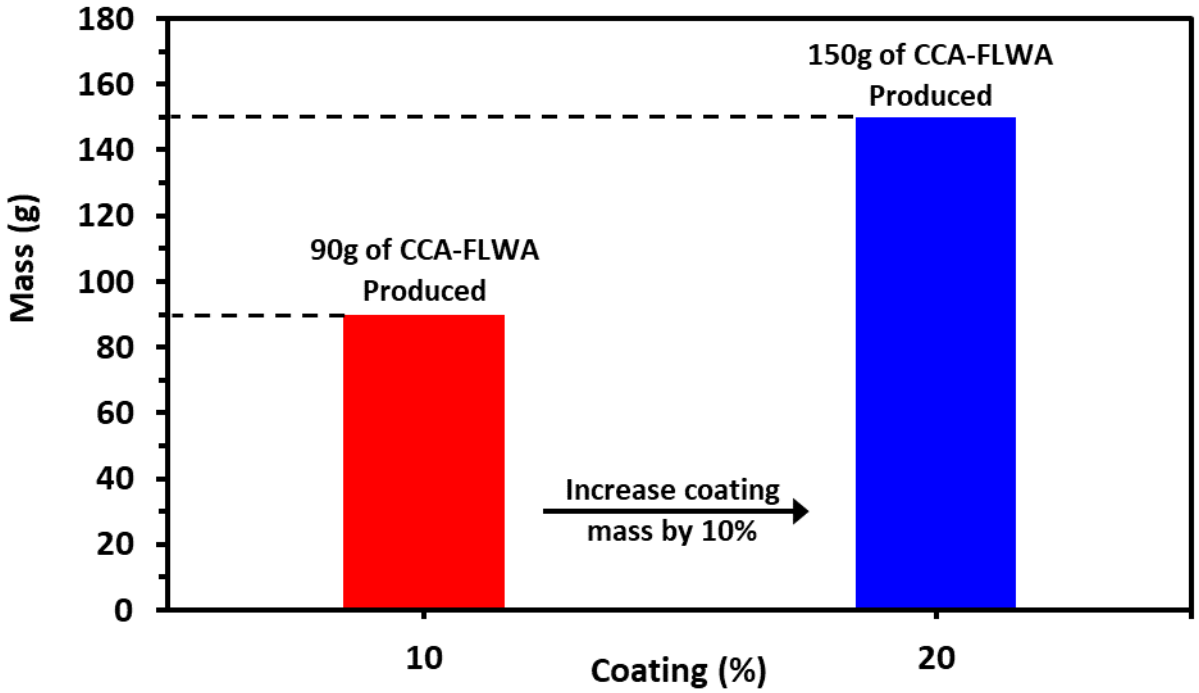


**Figure 23.** Coating analysis based on coating amount and production.

A solution for clogging was further explored by investigating the effect of feeding mass, rate, and frequency.

The effect of feeding mass on clogging was studied by initially setting the feeding rate at 5g/314sec and then increased to 10g/314sec, while monitoring the production of CCA-FLWA and clogging behavior (Figure 24). The results indicated that increasing the feeding mass resulted in higher production of CCA-FLWA before clogging was observed. Specifically, at a feeding rate of 5g/314sec, 90g of CCA-FLWA was produced before clogging occurred. However, when the feeding mass was increased to 10g/314sec, the production of CCA-FLWA increased further to 120g before encountering clogging issues. Although the increase in feeding mass did not eliminate the occurrence of clogging, it did contribute to increased productivity.

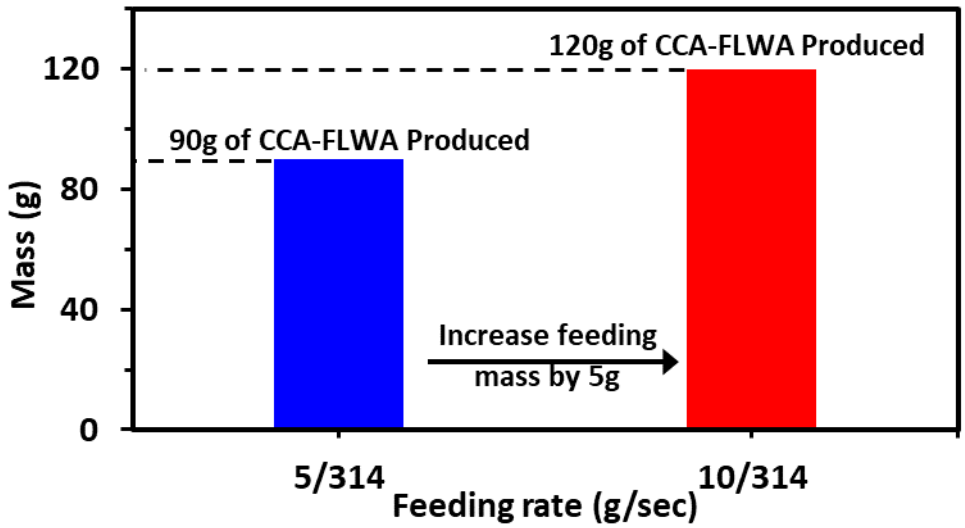


**Figure 24.** The effect of feeding mass on CCA-FLWA production and clogging.

The impact of feeding rate on clogging was also investigated by experimentally testing three various rates (5g/100sec, 5g/157sec, and 5g/314sec). Figure 25 illustrates the production rate of CCA-FLWA for each feeding rate. The results indicate that at 5g/100sec feeding rate only 40g of CCA-FLWA was produced before clogging was observed. This indicates that the system experienced blockages after a relatively small amount of production. However, when the feeding rate was reduced to 5g/157sec, the production rate of CCA-FLWA increased to 90g before clogging occurred. This indicates that a lower feeding rate resulted in an extended period of production before encountering clogging issues. Lastly, when the feeding rate was further decreased to 5g/314sec, there was no observed change in the production of CCA-FLWA before clogging was observed. This suggests that reducing the feeding rate beyond 5g/157sec did not provide any additional benefit in terms of prolonging the production duration before clogging occurred.

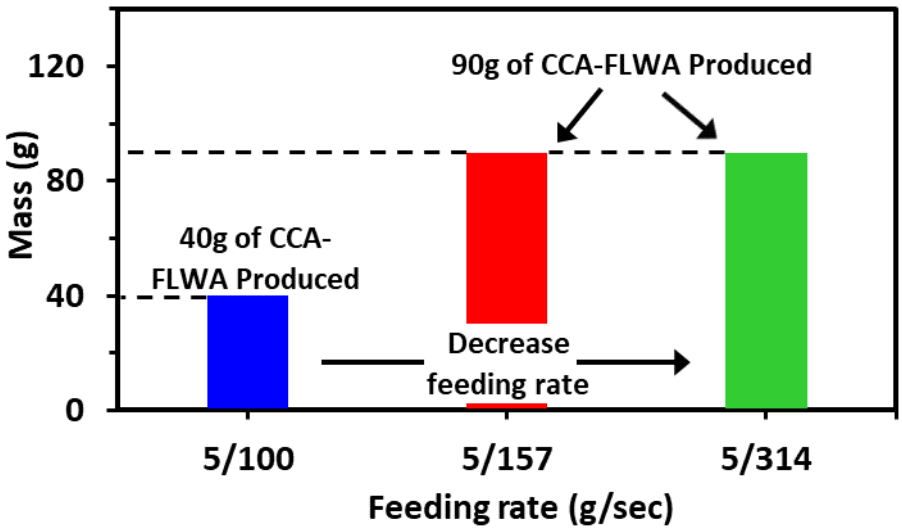


**Figure 25.** The effect of feeding rates on CCA-FLWA production and clogging.

The effect of feeding frequency on CCA-FLWA production and clogging was investigated. Two feeding frequencies were tested, 5g/157sec and 10g/314sec, and their impact on CCA-FLWA production and clogging behavior were analyzed. Figure 26 illustrates that when the feeding frequency was set at 5g/157sec, the production of CCA-FLWA reached 90g before clogging was observed. This implies that the system could sustain a relatively high production rate before facing issues with clogging. When the feeding frequency was changed to 10g/314sec, the production of CCA-FLWA increased to 120g before clogging became noticeable. This indicates that increasing the feeding frequency had a positive impact on the production rate, allowing for a higher amount of CCA-FLWA to be produced before experiencing clogging issues. The findings suggest that the feeding frequency can play a significant role in enhancing the production rate of CCA-FLWA and reducing the impact of clogging. Increasing the frequency of feeding resulted in a greater quantity of CCA-FLWA being produced before clogging occurred.

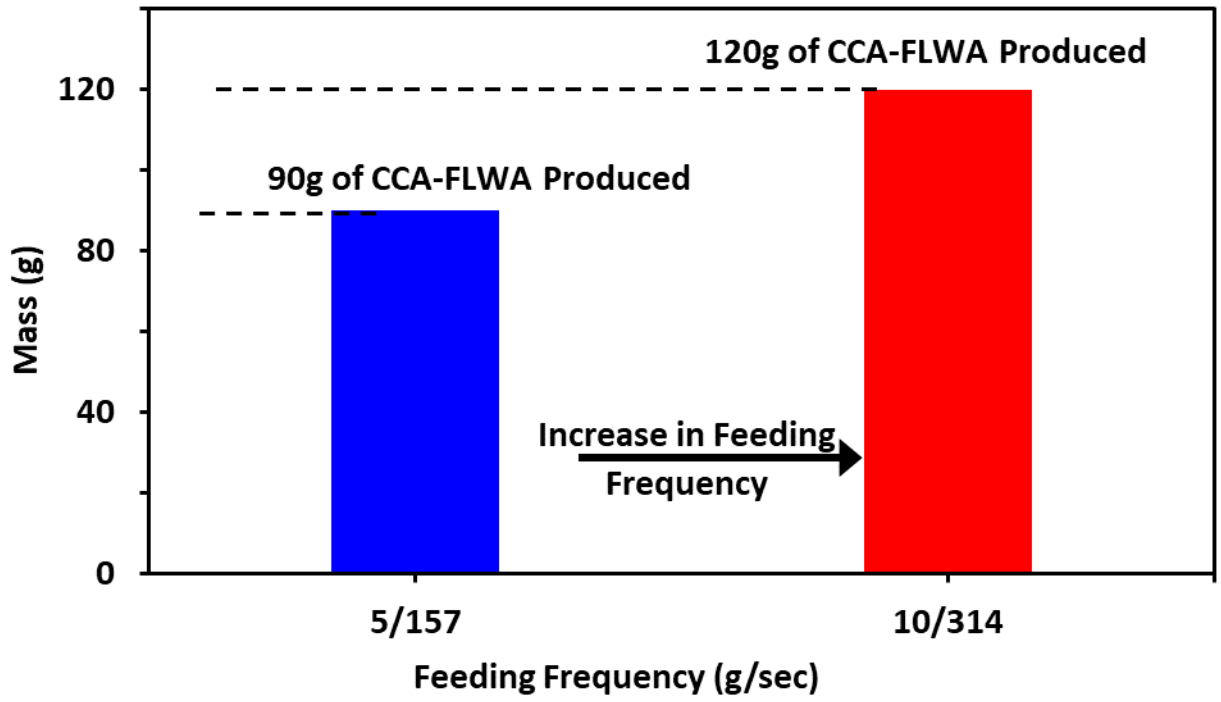


**Figure 26.** The effect of feeding frequency on CCA-FLWA production and clogging.

#### 2.3.3.3. Mean Residence Time (MRT)

The mean residence time (MRT) is the average time that a green pellet spends inside the rotary furnace tube. This dictates the length of time that a green pellet will experience sintering. MRT can have significant effects on the final CCA-FLWA's properties such as strength, porosity, and fusion bonding of W-CCA particles. The MRT value varies with the rotary furnace configuration which includes feeding rate, rotary speed, and angle of the rotary furnace. The MRT can be calculated by dividing retained mass in the rotary furnace ($m_{Retained}$) by the feeding rate ($\dot{m}$) of green pellets.

$$\text{MRT} = \frac{m_{Retained}}{\dot{m}}$$

The required MRT desired for this project was selected based on Drexel's previous work where an MRT of 15 minutes was found necessary to achieve sufficient CCA-FLWA [31]. Based on the

PSD of green pellets and coating quantity, the 15 minutes of MRT was achieved with furnace configurations of 7º angle, 7rpm rotational speed, and 4g/min feeding rate with 20% coating materials (Figure 27).

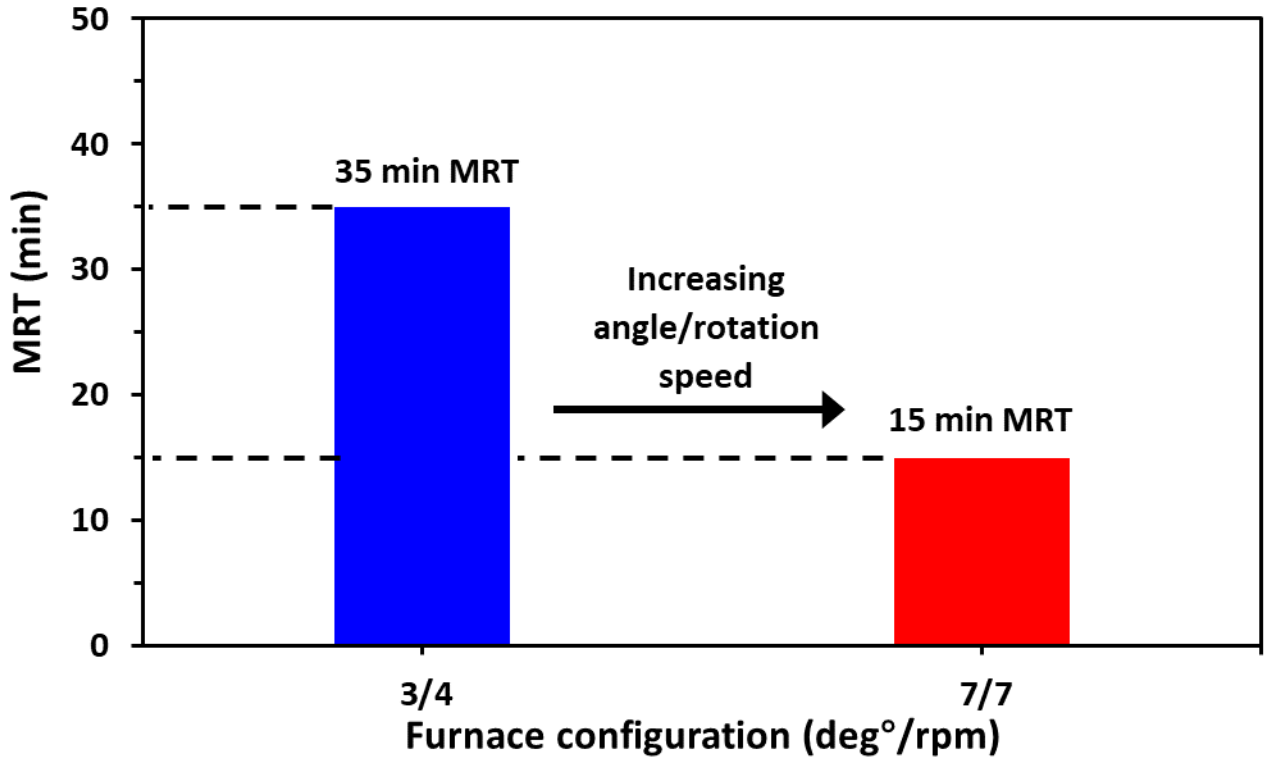


**Figure 27.** The effect of the rotary furnace configuration on the MRT of CCA-FLWA with 205 coating materials.

### 2.3.4. Optimum Manufacturing Parameters for FLWA Production

The optimized manufacturing parameters were determined according to parametric studies described earlier and CCA-FLWA production was initiated for further CCA-FLWA property analysis. The design parameters included material proportioning, mechanical configuration, and experimental duration. Table 6 summarizes the three main phases of the manufacturing process and the necessary proportioning and configuration required to achieve successful CCA-FLWA.

**Table 6.** Manufacturing parameters for CCA-FLWA production include material proportion, mechanical configuration, and time.

| Phase | Parameter | Proportion to manufacture ~ 1kg of CCA-FLWA |
|---|---|---|
| **Mixed Material** | Raw OD W-CCA | 900g |
| | Sodium Hydroxide NaOH (2%) | 18g |
| | Water (L/S 0.33) | 279g |
| | Coating (20%) | 180g |
| **Pelletization** | Angle | 45° |
| | Rotational Speed | 10 rpm |
| | Duration | 6 min |
| | Coating Added | 1 min |
| **Sintering** | Angle | 7° |
| | Rotational Speed | 7 rpm |
| | Feeding Rate | 4g/min |

### 2.4. Mechanical and Physical Characterization of Manufactured CCA-FLWA

Experimental characterizations were performed on the manufactured CCA-FLWA to investigate engineering properties such as density, porous structure, crush strength, water absorption, and the shape of the CCA-FLWA. A comparative analysis was performed for the manufactured CCA-FLWA with commercial FLWA available in the market approved by PennDOT. The tests performed complied with the standard methods of the American Society for Testing and Materials (ASTM) and the British Standard Institute (BSI). The inner structure of FLWA specimens was further evaluated using microscopy techniques to examine the internal fusion bonding and solidification. In addition, the internal structure was observed using microscopy images and X-ray micro computed tomography to study the internal fusion, solidification, and pore formation of CCA-FLWA.

### 2.4.1. Unit Weight

The unit weight was measured following the ASTM C29/C29M testing procedure. A standard cylinder with a known volume and weight was filled with CCA-FLWA at three intervals and rodded 25 times in each interval to ensure compaction. The mass of the aggregates in the cylinder with known volume was measured and the unit weight was calculated. The unit weight of CCA-FLWA manufactured with various kiln configurations was determined to verify their agreement with ASTM standards classification of FLWA. The maximum requirement for ASTM unit weight classification of FLWA is 1120 kg/m$^3$. The unit weight test results indicate that the achieved unit weight for CCA-FLWA manufactured with 4º, and 3 rpm was 808 kg/m$^3$, and the unit weight for CCA-FLWA manufactured with 7º and 7 rpm was 1020 kg/m$^3$ both complying ASTM (Figure 28).

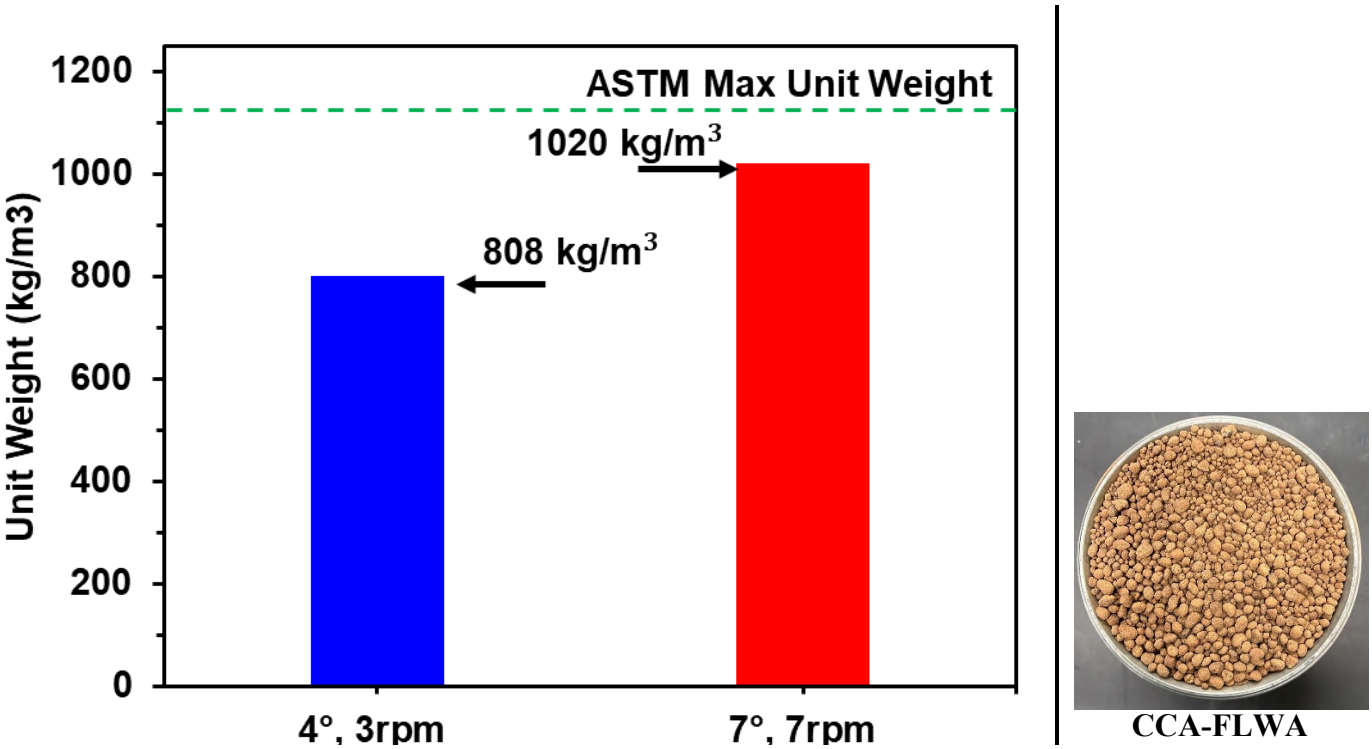


**Figure 28.** Unit Weight results for CCA-FLWA following ASTM C29/C29M.

### 2.4.2. Specific Gravity

The Specific Gravity test was performed according to ASTM C127/C128. CCA-FLWA manufactured with various kiln configurations were immersed in water for 72 hours. After soaking, the aggregates were dried using a heat gun. Using the cone method by tamping aggregates, the SSD condition was reached and measured once there was partial slumping in the aggregates. A graduated cylinder (1000 ml) was filled with water and weighed. The graduate cylinder was then filled with CCA-FLWA and water until 1000 ml was achieved and weighed. The three weighed measurements were then used to calculate the specific gravity of oven dry, saturated surface dry, and apparent conditions. The maximum requirement for ASTM apparent specific gravity classification of FLWA is 2.2. The achieved apparent specific gravity for CCA-FLWA manufactured with 4º, and 3 rpm was 2.08, and the apparent specific gravity for CCA-FLWA manufactured with 7º and 7 rpm was 2.12 (**Figure 29**).

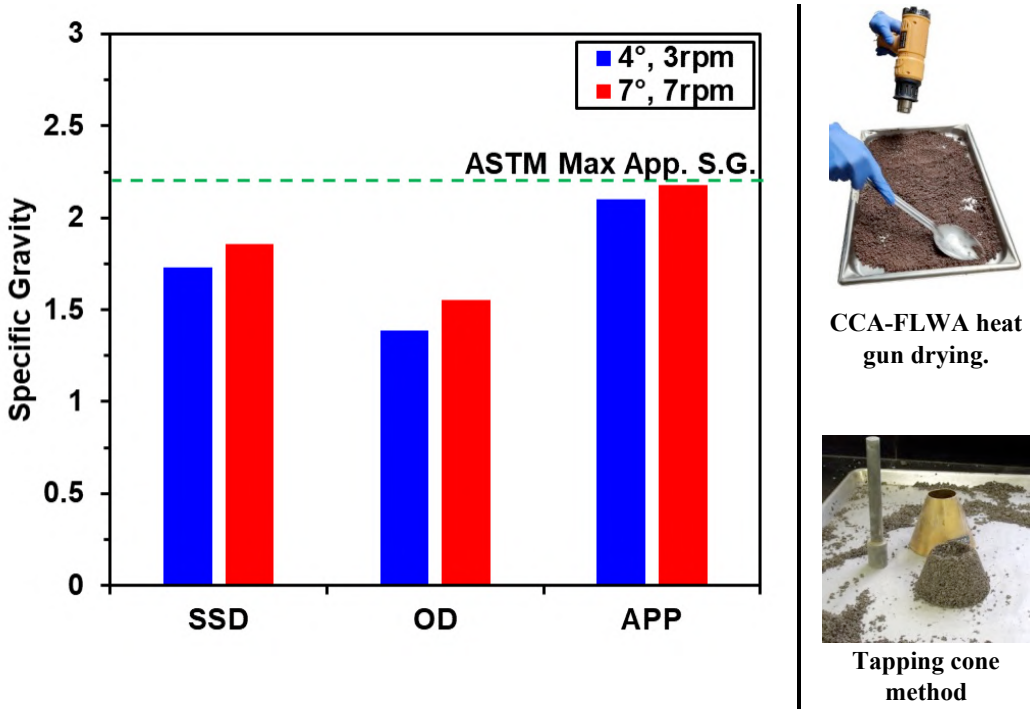


**Figure 29.** Specific gravity comparison between SSD, OD, and App S.G. for different kiln configurations of CCA-FLWA.

### 2.4.3. Water Absorption

Water absorption was measured following ASTM C127/C128 testing procedure. A 500g sample of sintered CCA-FLWA was immersed in water for 72 hours. The soaked aggregates were drained and weighted. Once CCA-FLWA reached oven-dry conditions they were weighed again, and the water absorption capacity was measured. Two aggregate batches manufactured with different kiln configurations were evaluated to assess their agreement with ASTM's minimum water absorption requirement for CCA-FLWA. The minimum requirement for ASTM water absorption classification of FLWA is 5%. The achieved water absorption for CCA-FLWA manufactured with 4º, and 3 rpm was 26.2%, and the water absorption for CCA-FLWA manufactured with 7º and 7 rpm was 20.1% (Figure 30).

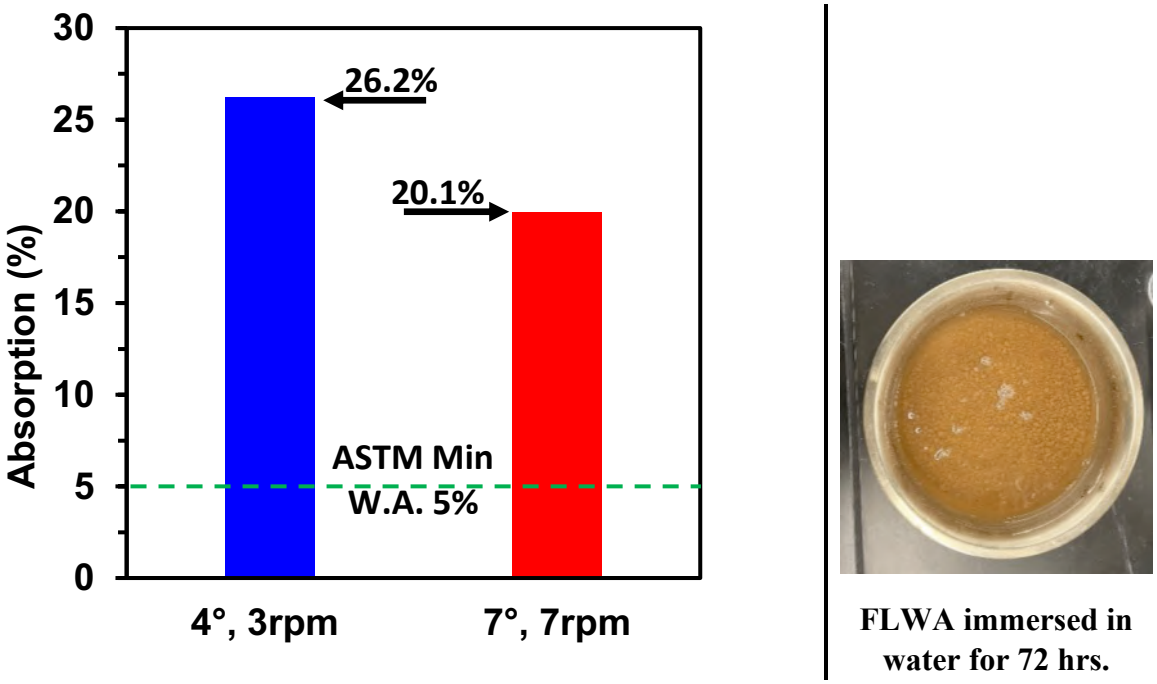


**Figure 30.** Water absorption tested of CCA-FLWA immersed in water for 72hrs. of CCA-FLWA manufactured from both kiln configurations.

### 2.4.4. Comparison analysis between manufactured CCA-FLWA and commercial FLWA

Water absorption over time, vacuum absorption, and compressive strength were tested for CCA-FLWA and compared with commercial FLWA properties. Water absorption and compressive strength of FLWA can be attributed to many factors such as pore volume, size, quantity, tortuosity, and connectivity. The increase in pore structure, quantity, and connectivity can all contribute to higher absorption capacity. Conversely, the increase in pores results in a higher void/solid ratio within the FLWA structure resulting in reduced compressive load resistance.

#### 2.4.4.1. Vacuum absorption and water absorption over time

Vacuum water absorption is used to determine the maximum possible water absorption capacity of FLWA. Vacuum absorption was measured using a vacuum pump and chamber. The FLWA was dried in an oven at 105 °C ± 5 °C for 24 hrs. to measure OD mass. ~1000 mL water was de-aerated in the vacuum pump for 1 h to remove the gas inside the water. The pump was then turned off and the deionized water container was removed from the chamber of the vacuum pump and covered with a lid for later procedures. The oven dried FLWA was de-aerated in a vacuum pump at a pressure of 1.33 kPa ± 0.33 kPa for 3 hrs. to remove any gas in the pores. After 3 hrs. and still under vacuum conditions, the previously de-aerated deionized water was introduced to the FLWA. The process lasted for an additional 1 hr. until the FLWA were fully submerged in the water. The vacuum pump was then turned off, and the beaker was taken out of the chamber and kept in atmospheric conditions for 24 hrs to fully saturate the pores in FLWA. After vacuum saturation, the tapping cone method was used to measure the SDD conditions. After determining the SSD and OD mass, the vacuum water absorption was calculated.

Water absorption over time was measured by first placing FLWA into a stationary oven to measure their oven dry mass. The FLWA were then immersed in water for specified saturation intervals. After achieving the purposed FLWA saturation time (6, 12, 24, 48, 72, 128 hrs.), the SSD condition was measured using the tapping cone method. The SSD and OD mass were used to measure the water absorption at each specified saturation interval (Figure 31).

The results for both vacuum absorption and water absorption over time tests indicate that the CCA-FLWA possessed higher water absorption capacity than commercial-FLWA. SPoRA achieved a vacuum absorption capacity of 31.6% and commercial-FLWA achieved a vacuum absorption capacity of 27.3%. The water absorption over time test indicated that CCA-FLWA was able to achieve higher absorption capacity in less time than commercial-FLWA.

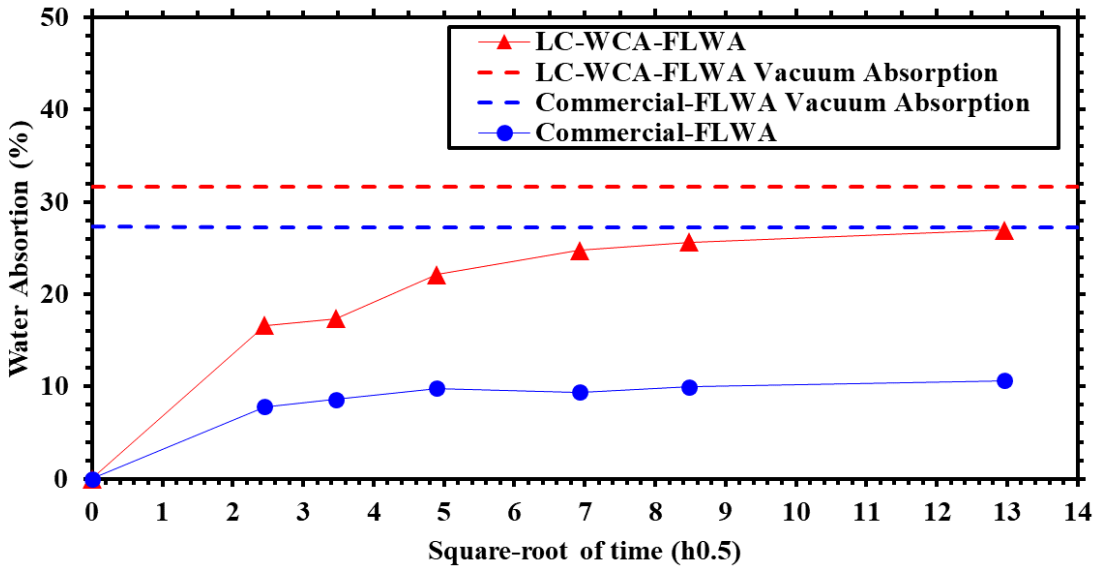


**Figure 31.** Water absorption over time and vacuum absorption of CCA-FLWA versus Commercial-FLWA.

#### 2.4.4.2. Compressive Strength

The confined compressive strength was measured in accordance with British Standard Institutes [32] testing procedure. This was performed on CCA-FLWA and commercial Commercial-FLWA. The test was performed by placing aggregates in a steel cylinder and ensuring

aggregates were tightly compacted through vibration for 1 minute. After vibration, the aggregates were subjected to compressive loading through a load cell (Figure 32). The compressive load was applied at a rate of 0.06±0.002 kN/s until a displacement of 10% was reached. The compressive strength measured at 10% displacement was defined as the confined compressive strength of the CCA-FLWA.

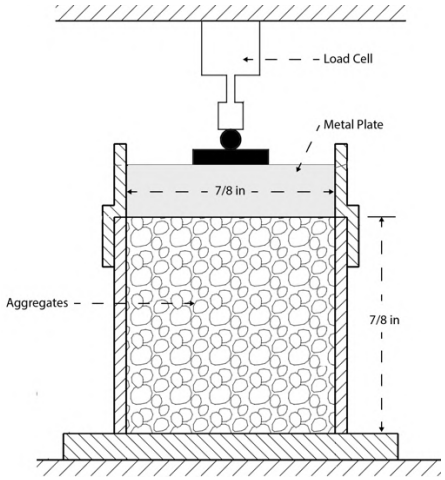


**Figure 32.** Confined compressive strength test – Load cell diagram.

The compressive strength test was performed for both CCA-FLWA and commercial-FLWA. The PSD of both samples was reversed engineered to follow ASTM C1761/C1761M PSD grading requirement. This was to ensure the samples had the same packing density for accurate comparative analysis. The results for the samples tested are presented in Figure 33 and indicate that at 10% displacement (equivalent to 20mm) CCA-FLWA achieved a compressive strength resistance of 47.5 kN and commercial-FLWA achieved a compressive strength resistance of 72.8 kN. FLWAs are considered fill material in concrete design and their compressive resistance capability does not necessarily contribute to concrete overall strength, instead, it is needed to maintain FLWA structural integrity during the mixing, handling, and casting stages of concrete.

CCA-FLWA compressive strength resistance of 47.5kN indicates necessary strength to sustain their structural integrity during a concrete mix, handling and placing.

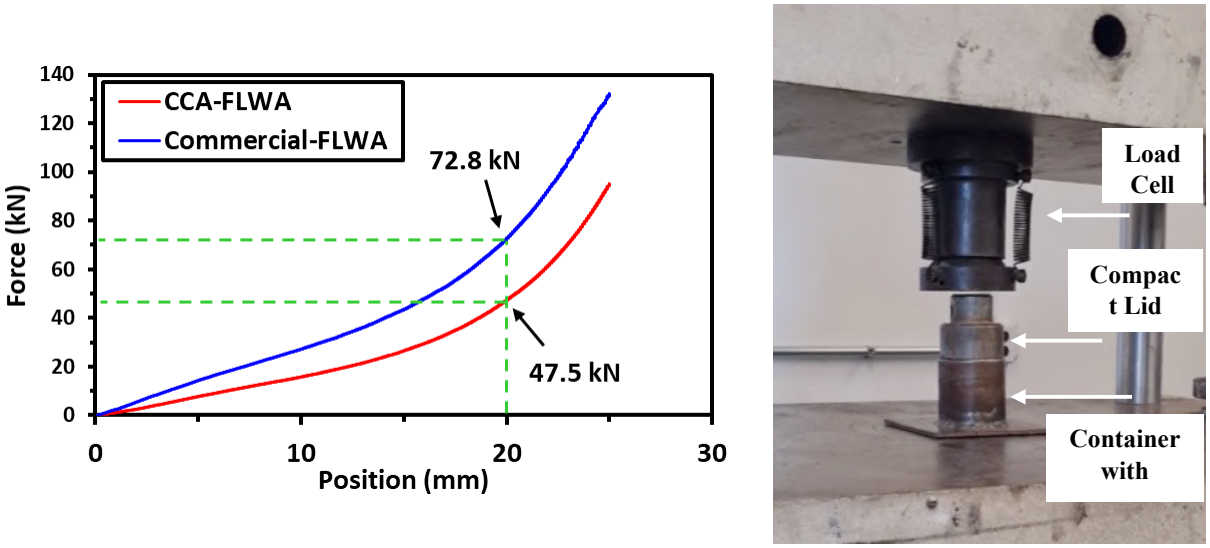


**Figure 33.** Compressive strength test performed for CCA-FLWA and commercial-FLWA.

#### 2.4.4.3. Sorption behavior

The desorption/absorption of the FLWA were characterized using a Dynamic Vapor Sorption Analyzer (DVSA). A sintered FLWA with approximately the same mass ~ 55g and shape ~0.3mm diameter was used for testing in the DVSA instrument. FLWAs were saturated for 72hrs before DVSA testing. After saturation the samples were surface dried using paper towel to achieve SSD condition. The SSD samples were placed in a quartz pan at a constant temperature of 23°C for both the desorption and absorption cycle. The relative humidity (RH) was initially set to 97.5 % and decreased in increments of 1.5 % down to 96 %, then down to 90 % with increments of 2 %, then down to 80 % with increments of 5 %, and finally decreased all the way to 0% with increments of 10 %. After each increment, the RH was kept constant to reach equilibrium for either 96 h or, if the mass change was less than 0.001 mg over 15 min. The instrument then proceeded to the next RH value. This procedure was applied in reverse to increase the RH to 97.5 % for the absorption cycle. CCA-FLWA achieved a desorption capacity of 39.8% and commercial-FLWA achieved a

desorption capacity of 5.9% (**Figure 34**). This indicates that CCA-FLWA possesses a higher capacity to release water in a concrete mix than Commercial-FLWA. For internal curing purposes, it is suggested by ASTM C1761 that FLWA should give off 85% of their absorbed water as the RH decreases to 94%.

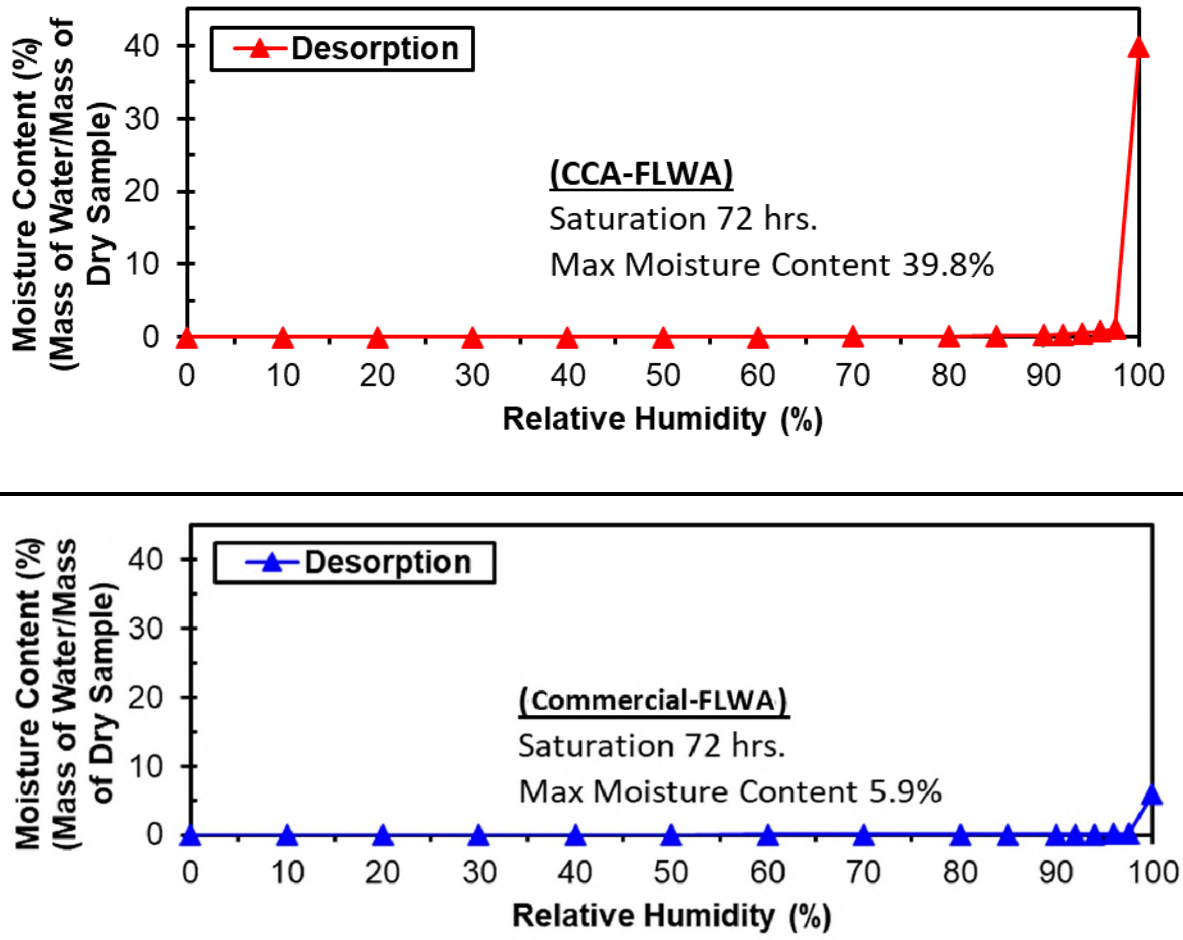


**Figure 34.** Desorption of the CCA-FLWA and Commercial-FLWA characterized using DVSA.

### 2.4.5. CCA-FLWA Internal Structure and Pore Analysis

Scanning electron microscopy (SEM) along with X-ray micro computed tomography (X-Ray microCT) were performed on CCA-FLWA to characterize the pore structure at microscale. Thermogravimetric analysis was used to sinter green pellets and evaluate gas liberation as

temperature was increased. Gas liberation was believed to be the main contributor to pore formation in sintered LWA. The combination of image analysis and quantification of gas release provided an understanding of CCA-FLWA internal structure and porosity characterization.

#### 2.4.5.1. Scanning electron microscopy (SEM)

The scanning electron microscopy (SEM) was performed on CCA-FLWA to examine its pore structure at a micro-scale level. The CCA-FLWA specimen was placed in a container, and a vacuum was applied for approximately 20 minutes. This step removes any trapped air or gases from the specimen and its pores. After the vacuum step, the vacuum was removed, and low-viscosity epoxy was added to the container, covering the entire FLWA specimen. The epoxy serves as a filler and helps preserve the structural integrity of the specimen during the subsequent preparation and imaging steps. The samples, now immersed in epoxy, were subjected to another vacuum treatment for approximately 30 minutes. This step helps to remove any air bubbles or trapped gases within the sample and ensures proper penetration of epoxy filling all pores in the specimen. Following the vacuum treatment, the samples were returned to atmospheric pressure and room temperature for approximately 24 hours to allow the epoxy to cure. During this time, the epoxy hardens, solidifies, and securely binds the specimen, enabling subsequent processing and handling. Once the epoxy was fully cured, the samples were sectioned at their midplane using a diamond saw. This step involves cutting and exposing the internal structure of the CCA-FLWA for further analysis. The sectioned samples were subjected to a series of polishing steps to obtain a smooth and flat surface suitable for SEM imaging. The polishing preparation procedure include wet polishing on SiC paper (i) grit 400 (22 micron) for 2 min under approximately 22 N force, (ii) grit 600 (15 micron) for 13 min under approximately 18 N force, (iii) grit 800 (10 micron) for 20 min under approximately 9 N force, (iv) and finally polishing on grit 1200 (5 micron) for 30 min

under approximately 4 N force. This step ensures a smooth and mirror-like surface, minimizing any surface artifacts that may interfere with the SEM imaging (Figure 35). Finally, the polished samples were sputter-coated with platinum. Sputter coating involves depositing a thin layer of platinum onto the sample surface using a high-voltage electrical discharge. This platinum coating helps to enhance the sample's conductivity, reduce charging effects during SEM imaging, and improve the quality of the obtained images. The coating layer thickness achieved was approximately 10 nm. After completing these steps, the CCA-FLWA samples were ready for SEM imaging, allowing for a detailed examination of the pore structure at a micro-scale level.

a) Aggregates in container

b) Immerse aggregate in epoxy

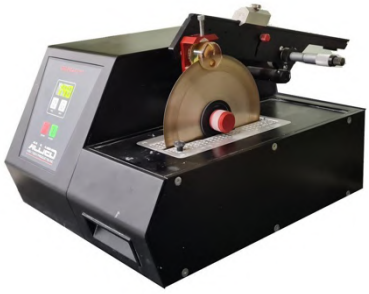

c) Cutting cross-section

d) Grinding/polishing sample

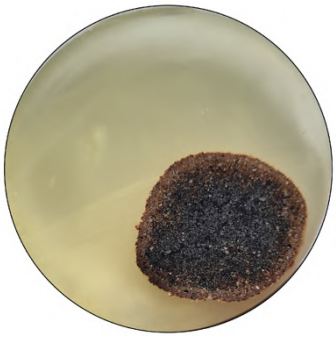

e) SEM sample

**Figure 35.** SEM sample preparation cutting, grinding/polishing.

The SEM images of the interior structure of the CCA-FLWA revealed the presence of various pore structures, indicating a range of pore sizes from the nano to micro scale (Figure 36).

Additionally, it was observed that the pore morphology varied across the sliced surface, and three distinct pore shapes were identified using SEM images analysis (Figure 37):

- Spherical pores: These pores appear as rounded, round-shaped voids within the material. They are attributed to the capturing of liberated gas during the sintering process. During sintering, certain gases can be generated or released, and if they are trapped within the material, they can form spherical voids.
- Irregular-shaped pores: These pores have an irregular or non-uniform shape. They are typically formed due to the diffusion of particles, which causes interlocking grain boundaries and creates connected voids throughout the FLWA. The diffusion of particles can result in the formation of complex and irregular pore shapes.
- Elongated channeled pores: These pores exhibit a channeled or elongated shape, resembling elongated voids or channels within the material's internal structure. They are believed to be created from primary void spaces that were occupied by a solution before the sintering process. These void spaces are relatively large, preventing diffusion from occurring during sintering and resulting in the formation of larger channeled voids within the FLWA's internal structure.

The presence of these different pore shapes suggests variations in the formation processes and conditions that the CCA-FLWA underwent. The spherical pores indicate the presence of trapped gases, while the irregular and channeled pores point to particle diffusion and solution occupation, respectively. These pore structures contribute to the overall porosity and can affect the material's properties, such as permeability, mechanical strength, and surface area. Understanding and

characterizing these pore structures is crucial for evaluating their performance and optimizing their applications.

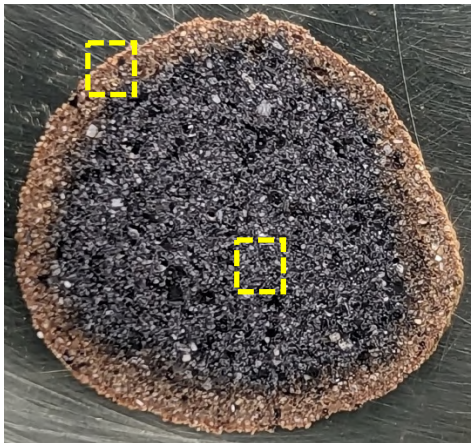

**Figure 36.** Sectioned SPoRA-FLWA exposing internal surface and region of interest (shell, core).

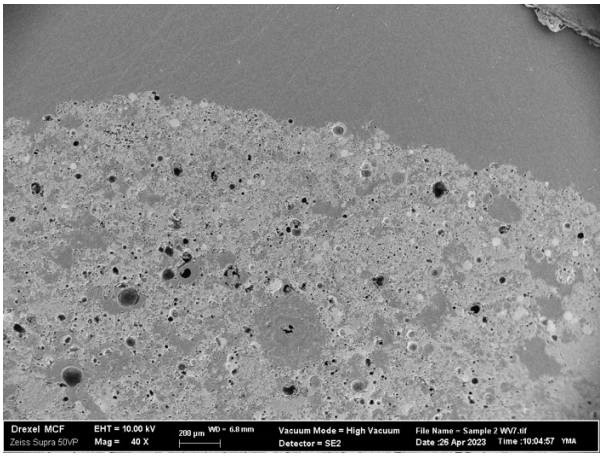


a) Shell investigating region of interest focusing on pore characterization.

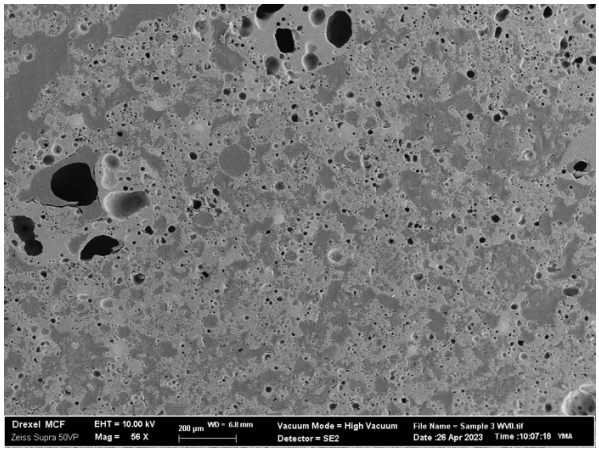


b) Core investigating region of interest focusing on pore characterization.

**Figure 37.** SEM analysis of SPoRA-FLWA internal structure studying pore characterization.

#### 2.4.5.2. X-ray micro Computed Tomography (X-ray mircoCT)

X-ray micro computed tomography (X-ray microCT) was used to characterize porosity, pore size distribution, and predicted permeability of the FLWA. The Skyscan 1172 X-ray micro-CT system was utilized to perform X-ray microCT and characterize the pore structure of the CCA-

FLWA samples that were previously tested by DVSA (Figure 38). The Skyscan 1172 X-ray microCT system can generate high-resolution 3D images of the internal structure of samples using X-ray technology. During sample testing the X-ray tube of the X-ray microCT system was set to a voltage of 100 kV (kilovolts) and a current of 100 μA (microamperes). These settings determine the intensity of the X-ray beam used to scan the sample. The voxel size was set to 2.73 μm (micrometers). The voxel size refers to the three-dimensional pixel size of the reconstructed image. During scanning, an Al + Cu (aluminum plus copper) filter was used. Filters are employed to modify the X-ray beam's energy spectrum, allowing for better contrast and image quality. For one step of the rotation during scanning, which covered 180° in total, the exposure time per step was approximately 3.245 seconds. This duration determines the time the X-ray beam is projected onto the sample during each rotation step. 2D projections of the CCA-FLWA samples were acquired using the X-ray microCT system. These projections are multiple X-ray images captured from different angles around the sample. The software supplied with the Skyscan 1172 (N-Recon software) was used to perform tomographic reconstruction, which involved processing the 2D projections to generate a 3D volume dataset. The N-Recon software was employed for visualization and calculations based on the reconstructed X-ray microCT data. N-Recon is a software tool used for advanced visualization, analysis, and quantification of 3D imaging data, such as micro-CT scans. By combining X-ray microCT with DVSA results, complementary information about the pore structure of the CCA-FLWA samples was gathered. The X-ray microCT analysis provided high-resolution 3D images, allowing for a detailed characterization and evaluation of the internal pore network. The pore structure and type documented in the 3D images reconciled with the observed pores in the SEM analysis. All three types of pores including spherical, irregular, and elongated channel pores were observed in the 3D images. This indicates

that these pore typologies are distributed throughout the entire structure of the CCA-FLWA examined.

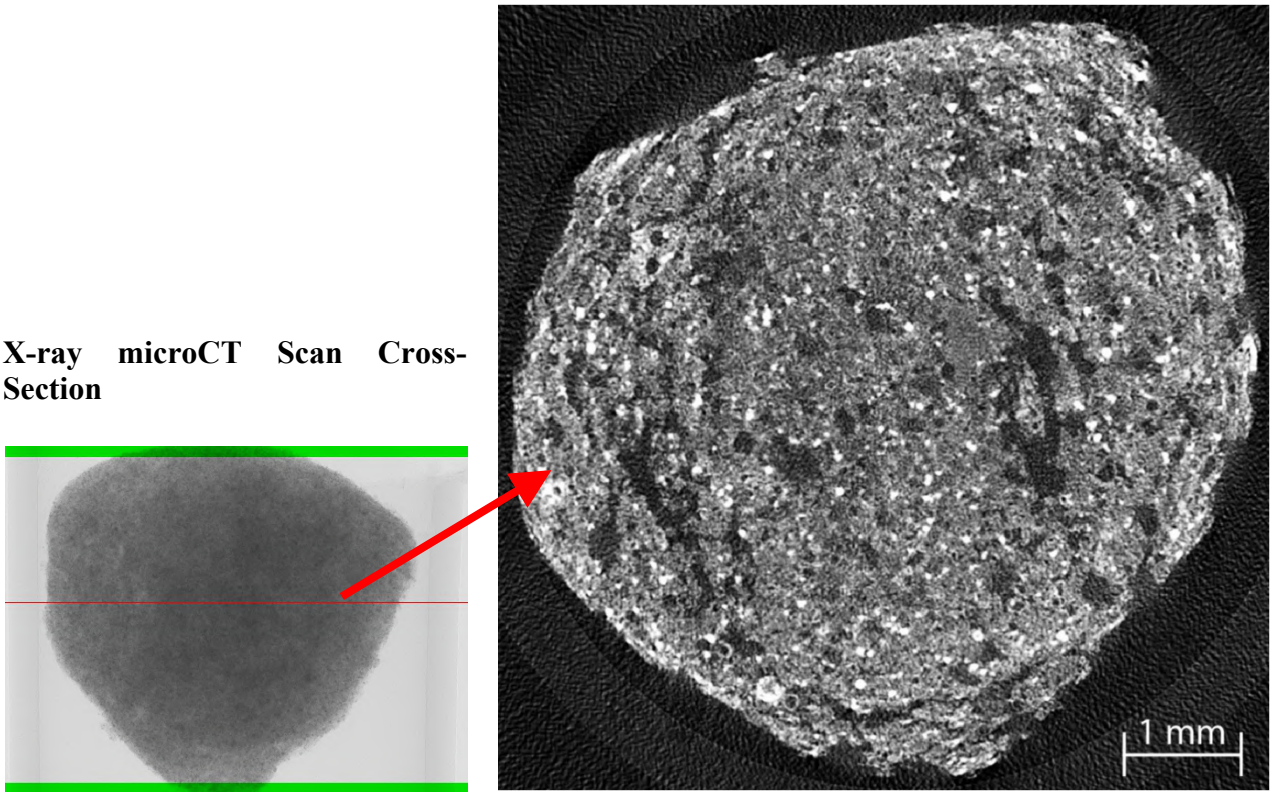


**Figure 38.** X-ray microCT of CCA-FLWA indicating cross-section cut and exposing interior structure.

### 2.5. Summary of Task 1

This report studied the necessary parameters for the successful production and characterization of CCA-FLWA using W-CCA from a local source in Pennsylvania. The investigation consists of a comprehensive literature review of previous work conducted in this area of research. It then proceeds by performing acquisition and experimental characterization of W-CCA from a local PA source. The W-CCA is then used to manufacture CCA-FLWA. Finally, the manufactured CCA-FLWA is tested for mechanical and physical characterization. The following summarizes the major activities performed in Task 1:

- Task 1.1: The literature review consists of understanding the problems associated with coal ash production and storage. Exploring various negative impacts W-CCA may inflict on the environment and human health. It further studies how the utilization of this waste material can mitigate its harmful effects and create a circular economy. Finally, this study attempts to recognize associated challenges when working with this material such as variation in W-CCA physical and chemical composition.
- Task 1.2: The acquisition and characterization of the W-CCA acquired from a local PA source is performed to identify the material's physical/chemical composition. Materials properties of obtained W-CCA are characterized and were used to assist the CCA-FLWA manufacturing design. Raw field condition analysis is performed including moisture analysis, field debris quantification, physical characteristics identification (SEM), PSD for particle size range, XRF for oxides composition, LOI to identify hydrocarbon sources and impurities, XRD for mineral phase identification, and TGA for free carbon content quantification.
- Task 1.3: The manufacturing of CCA-FLWA from unsuitable W-CCA requires both analytical and experimental investigations. The analytical investigation involves a thermochemical analysis guided by thermodynamic modeling (FactSage[â] software) and a viscosity investigation to verify that the design criteria meet the necessary conditions for successful CCA-FLWA production. It is concluded that the addition of 2% NaOH with a sintering temperature of 1075ºC provides the necessary conditions to produce successful CCA-FLWA. The experimental investigation includes three phases: mixing, pelletizing, and sintering. The optimum manufacturing process for CCA-FLWA batch production is found to have mixing parameters of OD W-CCA 900 g, NaOH 2% (18 g),

L/S 0.33 (water 279 g), and 20% coating (180g). The pelletization parameters include angle 45˚, rotational speed 10 rpm, duration 6 minutes, and coating added after 1 minute of pelletizing. The sintering parameters are found to have a rotary furnace angle of 7˚, rotational speed of 7 rpm, and feeding rate of 4 g/min.

- Task 1.4: The mechanical and physical characterization of the manufactured CCA-FLWA is analyzed. The tests performed include unit weight, specific gravity, water absorption, vacuum absorption, absorption over time, compressive strength, sorption behavior, SEM, and X-CT. These tests are performed to ensure the manufactured CCA-FLWA (1) meets ASTM requirements, (2) are comparable to commercial FLWA, (3) can sustain their structural integrity during concrete mixing, handling, and casting, and (3) possesses the necessary performance criteria for internal curing.

The manufactured CCA-FLWA in Task 1 shows promising performance to be used in concrete for internal curing. Additionally, sufficient CCA-FLWA was produced in Task 1 to be consumed in the remainder of the project to prepare concrete samples for further characterization for internal curing performance.

### 3. Evaluation of Internally Cured Concrete Made Using CCA-FLWA (Task 2)

Appropriate curing of concrete structures is critical to ensure structural performance is achieved, and long-term durability is sustained [33]. When concrete internal curing is insufficient it is susceptible to bulk shrinkage, cracking due to deformation when restrained, self-desiccation, high permeability, and reduction in overall structural durability [18]. The inclusion of internal curing technology can help mitigate or reduce depleting internal hydration impacts on concrete properties [18]. The main goal of this study is to utilize CCA-FLWA, serve as a hydrating reservoir for the internal curing of concrete, and compare its internal curing performance with commercial FLWA,

and control samples. To achieve this goal for **Task 2**, this study will address the following sub-tasks:

- **2.1:** Evaluation of mechanical and fresh properties of internally cured concrete made using CCA-FLWA
- **2.2:** Evaluation of freeze-thaw performance
- **2.3:** Evaluation of Leaching Potential of Constituent of Potential Concern (COPC)

### 3.1. Preparation of concrete samples and evaluation of mechanical/fresh properties

Concrete samples will be made using CCA-FLWA produced during Task 1. Fresh properties (e.g., slump, air content, and density), as well as hardened properties (e.g., compressive strength and density) of concrete made using CCA-FLWA, will be evaluated and compared to reference samples made using traditional FLWAs. For the demolition and rubblization process, flexural testing of concrete samples will be conducted. Additionally, the shrinkage of concrete made using CCA-FLWA will be evaluated. Concrete samples will be prepared for subtasks 2-2 and 2-3 to evaluate the freeze-thaw and leaching potential of heavy metals when CCA-FLWAs are used in concrete. The experimental program following planned tests are presented in **Table** *7*.

**Table 7.** Experimental program for evaluating fresh properties, hardened properties, freeze-thaw performance, and leaching.

| Evaluation of Internal Cured Concrete | Test -ASTM | Curing age | Specimen Quantity | Specimen Size |
|---|---|---|---|---|
| **Fresh Properties** | Slump C143M | - | Measured when producing concrete mix | - |
| | Air Content C231-22 | - | | - |
| | Density C138-17 | - | | - |
| **Hardened Properties** | Compressive Strength C39-21 | 14, 28, 56 | 9 Cylinders | 4 x 8 inch |
| | Flexural Strength C78-21 | 14, 28, 56 | 9 Beams | 3 x 3 x 11.25 inch |
| | Strain (Shrinkage) C157-17 | 56 | 3 Beams | 3 x 3 x 11.25 inch |
| **Freeze-thaw Performance** | Rate of Absorption C1585-13 | 14, 28, 56 | 3 Cylinders | 4 x 8 inch |

| | | | | |
|---|---|---|---|---|
| | Longitudinal Guarded Comparative Calorimeter E1225 and D5470 | 56 | 9 Cylinders | 2 x 1 inch (15 specimens) |
| **Leaching** | L.E.A.F | 63 days (after 56 days curing) | 4 Cylinders | 2 x 4 inch |

### 3.1.1. Design Considerations and Material Conditioning

This section is composed of a concrete mix design that considers material proportioning according to design criteria recommended by PennDOT section 704 [34]. Section 704 recommends design parameters for bridge deck design with a maximum w/c ratio of 0.45, a slump of 6 inch $\pm 1$ inch, and air content of 7% ±1%. The material considered includes Keystone Portland cement type 1, fine aggregates (Type A), coarse aggregates (siliceous unreactive Type A – maximum size No.8), water (in accordance with section 720.1), and admixtures (Air Entrainer type MasterAir AE90 [35], Dosage: 16-260 ml/100 kg of cement and Workability Retainer type MasterSure Z60 [36], Dosage: 130-780 ml/100 kg of cement). The FLWA considered includes CCA-FLWA (manufactured in-house) according to Task 1 production parameters, and traditional commercial FLWA.

The aggregate properties are listed in **Table *8*** and specifications were measured according to ASTM C127 [37] and ASTM C128 [38] test method for relative density (specific gravity) and absorption of fine/coarse aggregates. ATM C29 [39] was followed to measure coarse aggregate bulk density (dry unit weight) and fineness modulus was measured following ASTM C33 [40].

**Table 8.** Properties of aggregates used for concrete specimen manufacturing.

| Material Properties | Coarse | Fine | CCA-FLWA | Commercial-FLWA |
|---|---|---|---|---|
| **Oven Dry Specific Gravity** | 2.015 | 2.635 | 1.551 | 1.808 |
| **Saturated Surface Dry Specific Gravity** | 2.047 | 2.653 | 1.860 | 1.988 |

| | | | | |
|---|---|---|---|---|
| **Apparent Specific Gravity** | 2.082 | 2.682 | 2.246 | 2.206 |
| **Water Absorption (%)** | 1.603 | 0.660 | 24.62 | 9.987 |
| **Maximum Aggregate Size** | 3/8" | - | - | - |
| **Dry Unit Weight** | 103 | - | - | - |
| **Bulk Specific Gravity** | 2.015 | 2.635 | 1.551 | 1.808 |
| **Fineness Modulus** | - | 3.081 | - | - |
| **Absorption (24 Saturation) (%)** | - | - | 24.62 | 9.987 |
| **Vacuum Absorption (%)** | - | - | 28.27 | 10.83 |

Concrete mixing proportions were calculated for 3 concrete types CCA-FLWA concrete, Commercial-FLWA concrete, and control specimens (normal weight aggregates). Key Stone Type I Ordinary Portland Cement (OPC) with a Blaine fineness of 400.5 m2/kg, compliant with ASTM C150 was used for the specimen preparation in this study; **Table *9*** outlines the chemical and Bogue composition of the Type I OPC. The design parameters used in this study include a W/C ratio of 0.42, slump 6 inch $\pm$ 1 inch, and air content 7 % $\pm$ 1%.

**Table 9.** Chemical composition, Bogue composition, and relevant properties of Type I OPC.

| Item | Mass (%) | Properties | |
|---|---|---|---|
| Silicon Dioxide ($SiO_2$) | 19.22 | Air Content (%) | 9.93 |
| Aluminum Oxide ($Al_2O_3$) | 5.92 | Blaine ($m^2$/kg) | 400.5 |
| Ferric Oxide ($Fe_2O_3$) | 2.73 | % Pass 325 Mesh | 96.62 |
| Calcium Oxide (CaO) | 62.59 | 14-day C 1038 Expansion % | 0.006 |
| Magnesium Oxide (MgO) | 2.76 | % Autoclave Expansion | 0.09 |
| Loss on Ignition (LOI) | 2.7 | | |
| Sulfur Trioxide ($SO_3$) | 4.15 | Compressive Strength | |
| Sodium Oxide ($Na_2O$) | 0.34 | 1-Day (psi) | 2872 |
| Potassium Oxide ($K_2O$) | 1.04 | 3-Day (psi) | 4033 |
| Total Alkali | 1.02 | 7-Day (psi) | 4620 |
| Insoluble Residue | 0.24 | 28-Day (psi) | 5613 |
| Limestone | <=5.0 | | |
| L color | 59.14 | Time of Set (minutes) | |
| $C_3S$ (Bogue) | 53.3 | Initial | 117 |
| $C_2S$ (Bogue) | 14.9 | | |
| $C_3A$ (Bogue) | 11.1 | | |
| $C_4AF$ (Bogue) | 8.3 | | |

### 3.1.2. Concrete Mix Design

*Fresh Properties*

To optimize the concrete mix design for internal curing, enough pre-wetted CCA-FLWA inclusion was calculated following Bentz equation [41]. Secondly, incorporating Commercial-FLWA was performed as a volumetric substitution, and concrete trial batches were examined for the required fresh properties (air content and slump) based on the addition of superplasticizer and air entrainment admixtures. To optimize workability and air content, specifically for CCA-FLWA and Commercial-FLWA concrete mixes, small batches of concrete were prepared (≈0.5 $ft^3$) for testing slump according to ASTM C143M [42] and air content following ASTM C231-22 [43]. Incremental ±5 ml adjustments were made to admixtures dosage until required flow and air content was achieved. For large-scale concrete preparation procedure, the cement and normal weight aggregates (NWA) were in dry condition (absorption of water was accounted for by the total volume of water used). In a concrete rotary drum mixer, NWA aggregates were then blended with a portion of water to allow dry NWA aggregates to reach saturation. Afterward, cement powder was added to the drum mixer followed by addition of chemical admixtures and remainder of water. The entire blend was blended for 90 seconds, rested for 60 seconds, and then blended for another 90 seconds before the concrete was cast in-place. For CCA-FLWA, and Commercial-FLWA in SSD condition, they were simply treated as fine aggregates replacement and the same concrete procedure was followed as described earlier. Furthermore, Afterward, several iterations of slump tests and air content tests were performed by preparing concrete batches (≈3 $ft^3$) until desired fresh properties were attained. **Table *10*** shows the final concrete mix proportions, and fresh properties measured (i.e., unit weight, slump, and air content) of CCA-FLWA, Commercial-FLWA, and Control samples concrete mixes.

**Table 10.** Concrete mix design for CCA-FLWA, Commercial-FLWA, and Control Samples.

| Material | Specific Gravity | Volume Fraction (0 to 1) | | | Control (lb/yd3) | Commercial -FLWA (lb/yd3) | CCA-FLWA (lb/yd3) |
|---|---|---|---|---|---|---|---|
| | | Control | Commercial -FLWA | CCA-FLWA | | | |
| **Cement (Type-I)** | 3 | 0.164 | 0.164 | 0.164 | 869 | 869 | 869 |
| **Water** | 1 | 0.217 | 0.217 | 0.217 | 386 | 386 | 386 |
| **CA (SSD)** | 2.02 | 0.36 | 0.36 | 0.36 | 1223 | 1223 | 1223 |
| **FA (SSD)** | 2.64 | 0.19 | 0.5 | 0.05 | 839 | 240 | 240 |
| **CCA-FLWA** | 1.56 | - | - | 0.135 | - | - | 423 |
| **Commercial-FLWA** | 1.99 | - | 0.135 | - | - | 423 | - |
| **Air Content (%)** | - | 7.8 | 7.4 | 6.8 | 7.8 | 7.4 | 6.8 |
| **Slump (inch)** | - | 6.6 | 6.5 | 7.3 | 6.6 | 6.5 | 7.3 |
| **w/c** | - | 0.42 | 0.42 | 0.42 | 0.42 | 0.42 | 0.42 |
| **Fresh Unit Weight (Kg/m3)** | - | - | - | - | 138.6 | 120.9 | 125.3 |
| **Air Entraining Admixture, (ml/100 kg of cement)** | - | - | - | - | 260 | 260 | 260 |
| **Water-reducing admixture (ml/100 kg of cement)** | - | - | - | - | 255 | 265 | 290 |

*** CA (OD) - Coarse Aggregates in Oven Dry Condition**

*** FA (OD) - Fine Aggregates in Oven Dry Condition**

*** CCA-FLWA (SSD) - Fine Lightweight Aggregates in Saturated Surface Dry Condition**

*** Commercial-FLWA (SSD) - Fine Lightweight Aggregates in Saturated Surface Dry Condition**

*** CCA-FLWA and Commercial-FLWA inclusion in volume substitution**

The Commercial-FLWA addition to the concrete mix was based on volume substitution relative to CCA-FLWA volume. This was carried out for a more comparative assessment based on volumetric substitution and performance relative to FLWA added to the system. Bentz et al. 1999 [41] was used to calculate the mass of CCA-FLWA needed to substitute fine aggregates for effective internal curing. Parameters considered including: i) Cement factor = 869.048 lb/yd$^3$, ii) chemical shrinkage of cement = 0.08106 (calculated using cement phase fraction for $C_3S$, $C_2S$, $C_3A$, $C_4AF$), maximum degree of hydration = 1, CCA-FLWA saturation level after 24hr saturation = 81.2 %, and CCA-FLWA absorption capacity = 24.6%. The mass of fine aggregates was volume substituted by 71.4 % of CCA-FLWA. Once all three concrete mix designs were mixed, they were

poured into their appropriate molds and cured under moist conditions for 24 hrs. They were then demolded and placed in a curing chamber at relative humidity of 50 % ± 4% and 23 ºC ± 1 ºC, for required curing age before testing (**Figure *39***).

CCA-FLWA Concrete | Commercial-FLWA Concrete | Control Concrete

**Figure 39.** Concrete cast specimens for CCA-FLWA, Commercial-FLWA, and control concrete.

### 3.2. Hardened Properties

The hardened properties investigated for CCA-FLWA, Commercial-FLWA, and control concrete include compressive strength, flexural strength, shrinkage, and rate of absorption. The experimental procedures followed the ASTM Standard.

#### 3.2.1. Compressive Strength

##### 3.2.1.1. Experimental Procedure

The compressive strength of lightweight concrete (LWC) specimens was measured following ASTM C39-21 [44]. This test method determines the compressive strength of cylindrical concrete specimens by applying axial load to specimens at a loading rate of 0.25 MPa/s ±0.05 MPa/s until concrete failure is achieved. The testing machine type used is a Tinius Olsen-Super L with 400K lbf compressive capacity. Both upper and lower bearing blocks were used during testing. LWC specimens were tested at 3 curing ages 14, 28, and 56 days, testing 3 samples at each curing age for standard deviation (**Figure *40***). The tested specimens were cast in cylindrical form with a diameter of 4 inch ±0.08 inch and a height of 8 inch ±0.16 inch.

$$f_{cm} = \frac{4000P_{max}}{\pi D^2}$$ **Equation 5**

The compressive strength was calculated using **Equation 5** provided by ASTM C39-21 [44], where $f_{cm}$ = compressive strength, MPa [psi], $P_{max}$ = maximum load, kN [lbf], and D = average measured diameter, mm [in.].

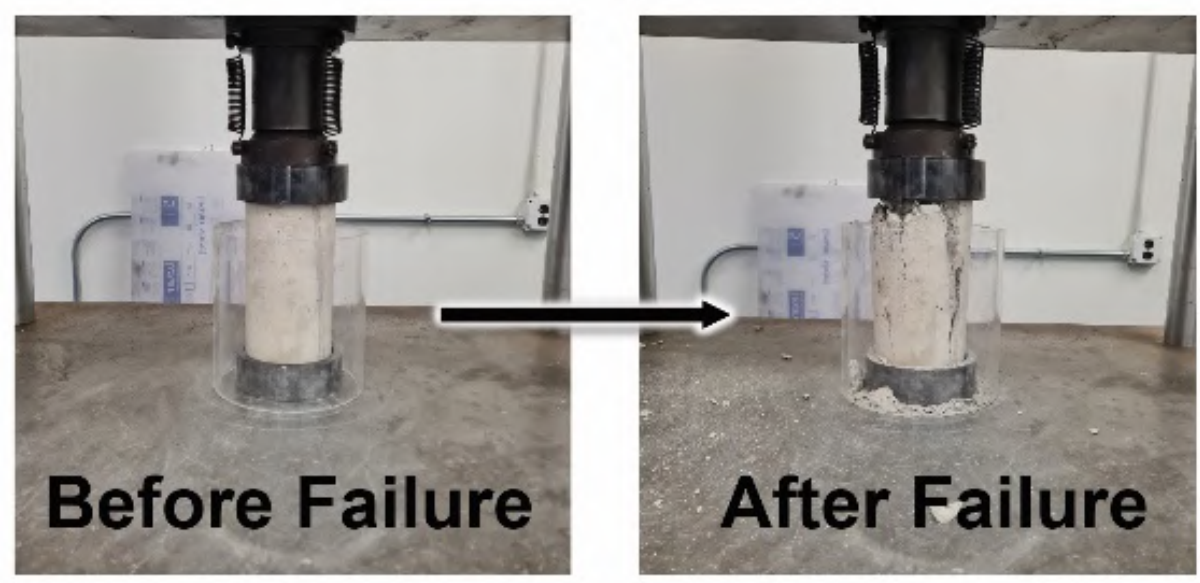


**Figure 40.** Compressive Strength specimen testing experimental set-up.

#### 3.2.1.2. Results and Conclusion

The calculated compressive strength of all LWC specimens cured at 14, 28, and 56 days is plotted in **Figure *41***. The compressive strength results revealed that concrete made using CCA-FLWA demonstrated higher compressive strength resistance. At curing age of 14 days compressive strength was relatively similar for all 3 concrete samples. As curing progressed to 28 days concrete made using CCA-FLWA possessed higher compressive strength relative to Commercial-FLWA concrete and the control sample. After 56 days of curing CCA-FLWA concrete possessed 35.4 MPa compressive resistance (Highest), Commercial-FLWA concrete had 32.5 MPa of compressive resistance, and control specimen had the lowest compressive resistance of 32.0 MPa.

This was attributed to internal curing and enhanced internal hydration forming a denser internal structure and overall higher compressive strength resistance. Other attributes that could be investigated further include the pH of CCA-FLWA influence on accelerating the chemical reactions within the concrete and thereby enhancing compressive strength. Another aspect that needs further investigation is the effect of the spherical shape of aggregates causing an arch effect and potentially mitigating concentrated stresses that can enhance concretes compressive strength resistance.

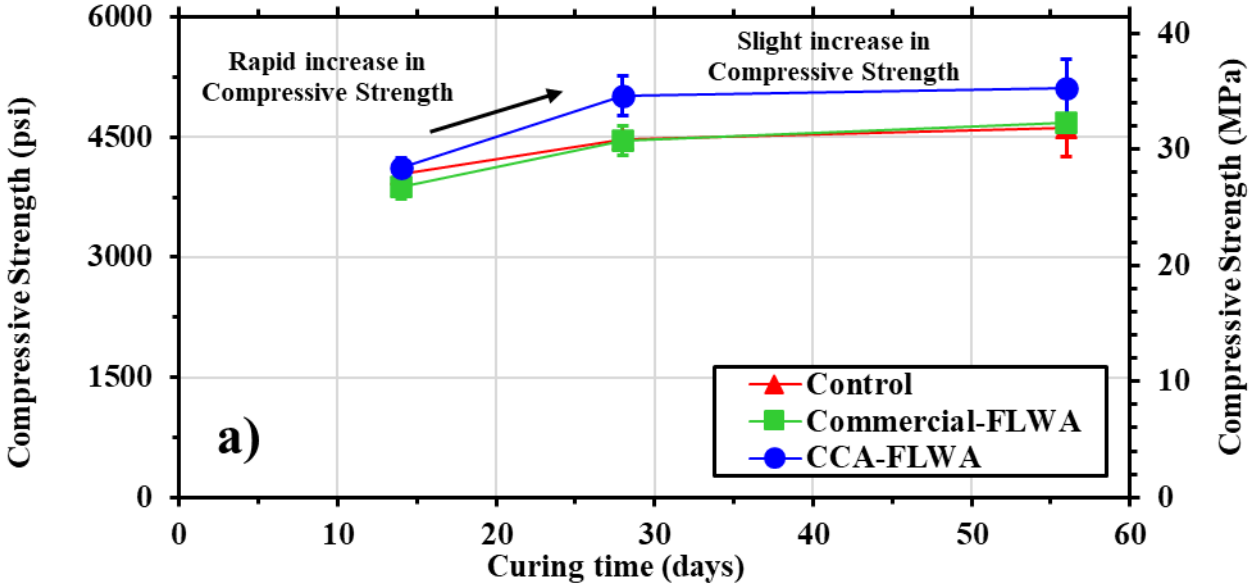


**Figure 41.** Compressive Strength of LWC with curing ages of 14, 28, and 56 days, for CCA-FLWA, Commercial-FLWA and Control concrete specimens.

### 3.2.2. Flexural Strength

#### 3.2.2.1. Experimental Procedure

The flexural strength of lightweight concrete (LWC) specimens was measured following ASTM C78-22 [45]. This test method covers the determination of the flexural strength of concrete using a simple beam with third-point loading. The test applies continuous loading at a constant rate constantly increasing the maximum stress on the tension face between 0.9 MPa/min and 1.2

MPa/min [125 psi/min and 175 psi/min] until concrete rupture occurs. Once rupture is achieved, results are calculated and reported as the modulus of rupture. The testing machine type used is a Tinius Olsen-Super L with 400K lbf load capacity. The support blocks used are composed of steel rods and were free to rotate and maintained in a vertical position. The tested beam specimen dimensions were 3×3×11.25 inch. LWC specimens were tested at 3 curing ages 14, 28, and 56 days, testing 3 samples at each curing age for standard deviation (**Figure *42***).

$$R = \frac{PL}{bd^2} \qquad \textbf{Equation 6}$$

The modulus of rupture was calculated using **Equation 2,** where R = modulus of rupture MPa [psi], P = maximum applied load indicated by the testing machine N [lbf], L = span length mm [in.], b = average width of specimen mm [in.] at the fracture, and d = average depth of specimen mm [in.] at the fracture.

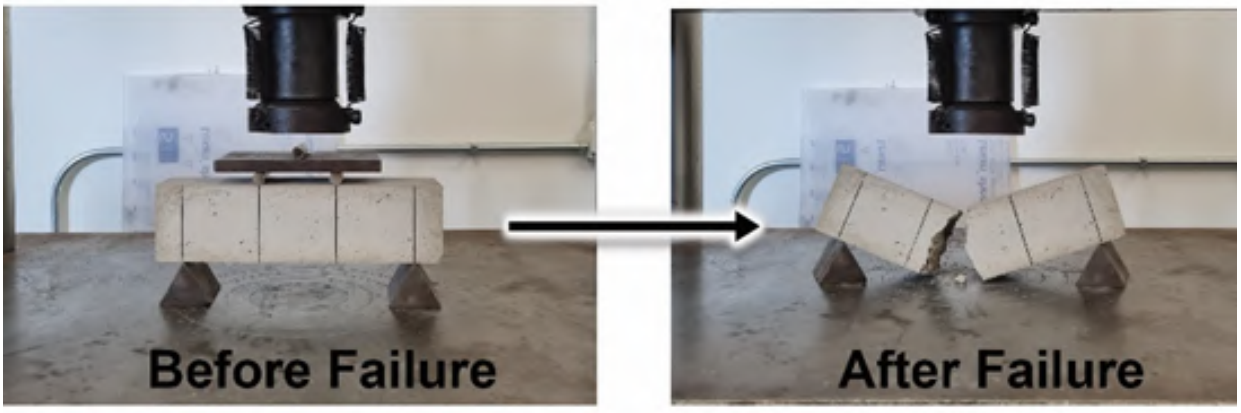


**Figure 42.** Flexural Strength specimen testing experimental set-up

#### 3.2.2.2. Results and Conclusion

The calculated flexural strength of all LWC specimens cured at 14, 28, and 56 days is plotted in **Figure *43***.The flexural strength results demonstrated the inverse performance where the control

sample possessed higher strength than CCA-FLWA and Commercial-FLWA concrete. However, as curing age progressed and reached 56 days, all three samples possessed relatively close flexural strength with CCA-FLWA concrete = 7.2 MPa, Commercial-FLWA concrete = 7.4 MPa, and control = 7.5 MPa. The gain in flexural strength in both CCA-FLWA and Commercial-FLWA concrete was attributed to internal curing enhancing the internal structure development through extended hydration.

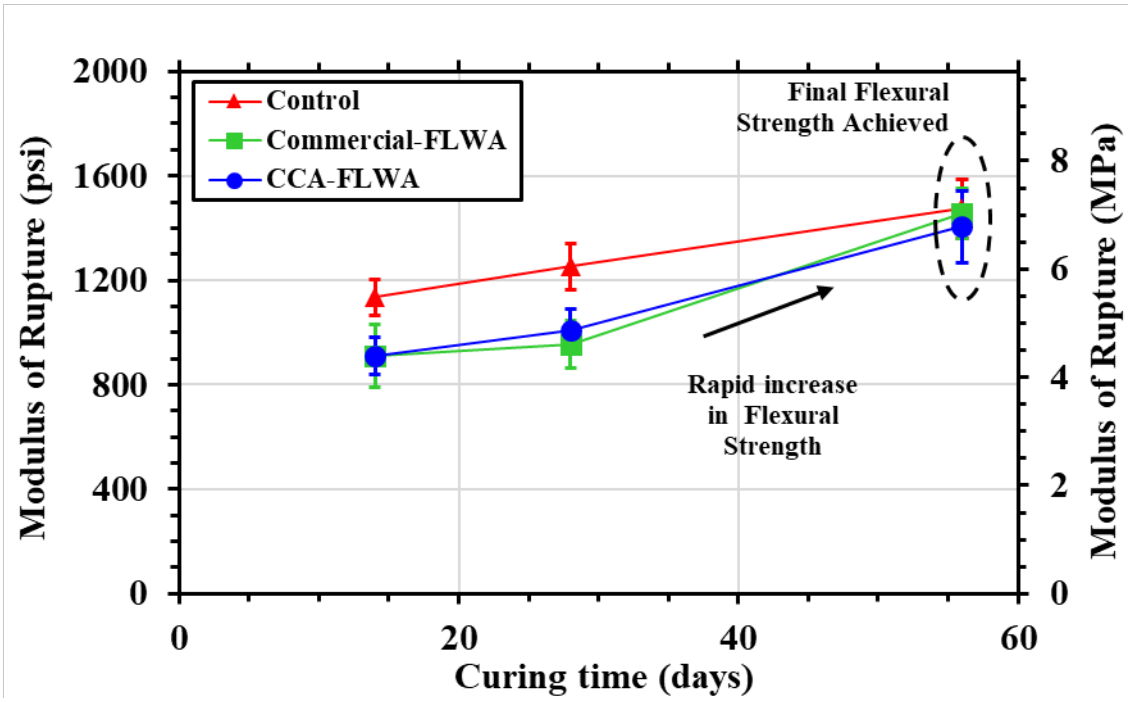


**Figure 43.** Flexural Strength of LWC with curing ages of 14, 28, and 56 days, for CCA-FLWA, Commercial-FLWA and Control concrete specimens.

### 3.2.3. Shrinkage

#### 3.2.3.1. Experimental Procedure

Restrained concrete can experience internal stresses that can cause concrete cracks and failure due to shrinkage. Assessing internally cured concrete by documenting shrinkage provides an understanding of concrete performance in responses to stresses caused by shrinkage. The shrinkage test was performed on all LWC specimens following ASTM C157-17 [46]. This test method covers

the determination of the length changes that are produced by causes other than externally applied forces and temperature changes in hardened concrete specimens made in the laboratory and exposed to controlled conditions of temperature and moisture. Measurement of length change permits assessment of the potential for volumetric expansion or contraction of concrete. Three test specimens in beam form (prism) of 3×3×11.25 inch, were cast for each concrete typology. The samples were stored into a desiccator with constant relative humidity of 50 % ± 4% and 23 ºC ± 2 ºC. Strain measurements were taken daily for 90 consecutive days by calibrating the strain gauge before every measurement.

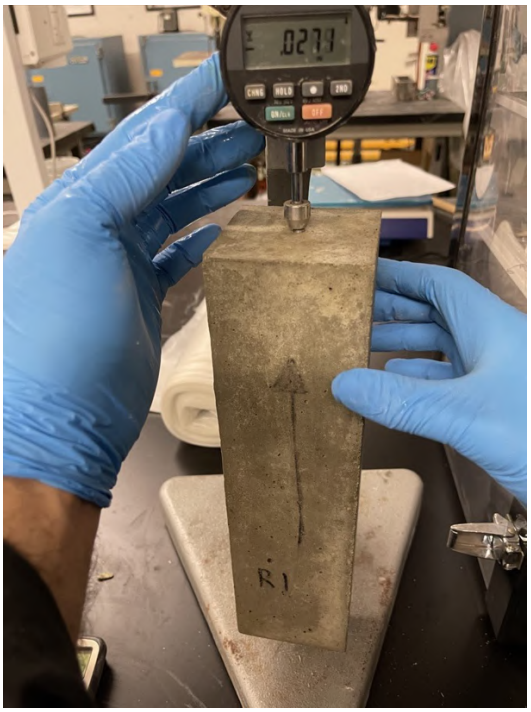


**Figure 44.** Shrinkage measurement for all specimens at specified curing age.

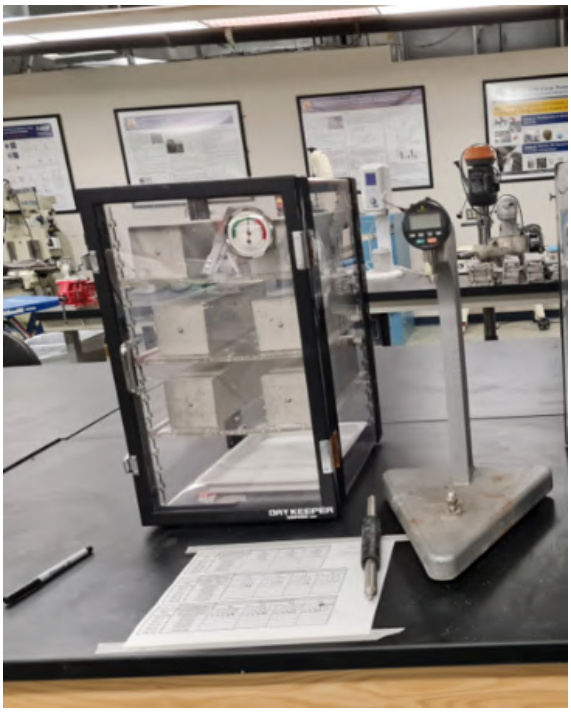

**Figure 45.** Specimens stored in desiccator for consistent curing conditions.

#### 3.2.3.2. Results and Conclusion

The calculated strain (με) of all LWC specimens for 90 days of curing is plotted in **Figure *46***. The shrinkage results demonstrated the CCA-FLWA concrete possessed lower strain than both

Commercial-FLWA and control concrete. This is very beneficial in practical practice as restrained concrete with low-strain properties will experience less internal stress and cracking. CCA-FLWA concrete demonstrated 33.5% lower strain than normal concrete and 26.7% lower strain than commercial-FLWA concrete. The lower strain measurements observed in CCA-FLWA concrete are attributed to internal curing through the increase in degree of hydration of hydration anticipated and significantly reducing chemical and drying shrinkage.

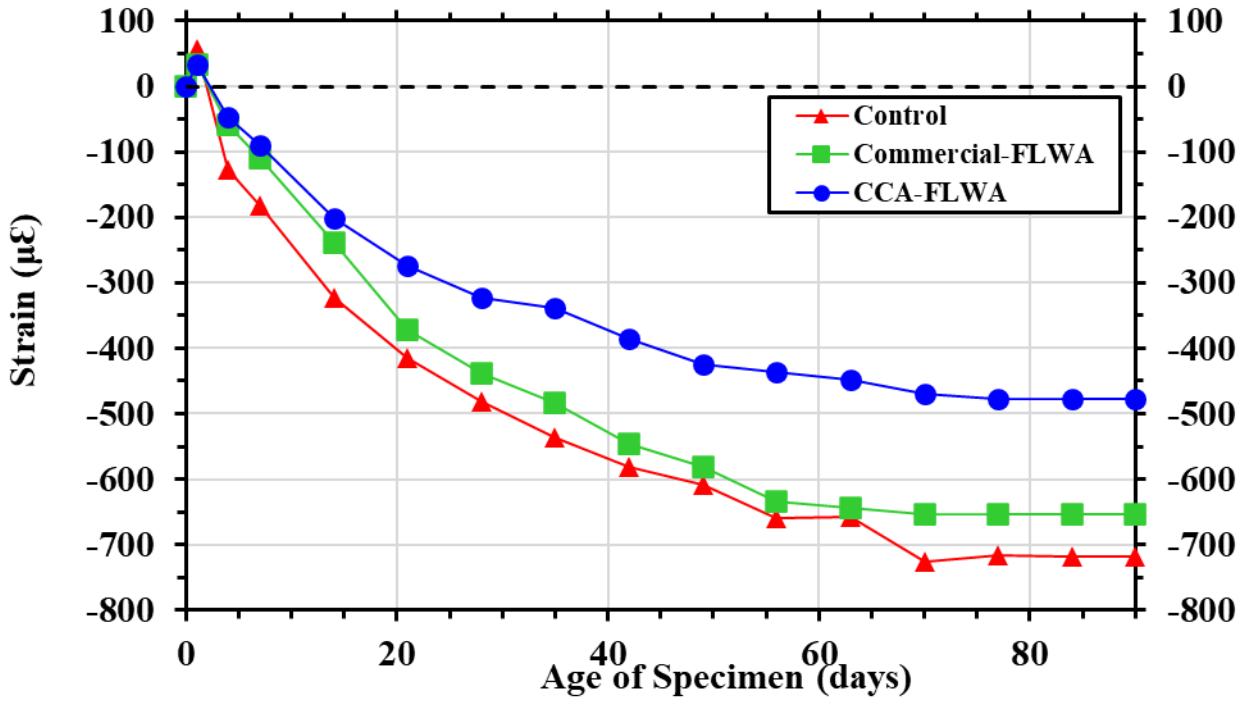


**Figure 46.** Specimens continuous strain (με) measurements for 90 days curing on CCA-FLWA, Commercial-FLWA, and control concrete.

### 3.2.4. Rate of Absorption

#### 3.2.4.1. Experimental Procedure

The durability of concrete can be enhanced through its permeability. The permeability of concrete can be assessed through its absorption rate. Water transport throughout the porous network of concrete happens via three mechanisms of capillary suction: (i) permeability, diffusion, and

absorption. All three mechanisms are directly influenced by the volume of pores, pore size distribution, and pore connectivity. ASTM C1585-13 [47] test method was followed to determine the rate of water absorption (i.e., sorptivity) of water by measuring the increase of mass of concrete specimens over time. For that purpose, three 101.6 mm × 50.8 mm (4" × 2") concrete cylinders cores (i.e., three each for CCA-FLWA, Commercial-FLWA, and control concrete samples) were conditioned at 50 ± 2 ºC and 80 % relative humidity (RH) in an environmental (EV) chamber for 14 days to induce a consistent moisture distribution in the capillary pore system. The significance behind the conditioning parameters was established by Castro et al. [48]; the authors discovered that RH of concrete specimens kept at field under different exposure conditions was within 80-100 % RH; at 80 % RH, moisture is removed via evaporation process from the capillary pores ($r \geq 10$ nm) whereas the gel pores ($r \leq 10$ nm) remain water-filled. **Figure *47*** shows the experimental setup for the water absorption test. Each concrete specimen was coated with 24 hour set epoxy adhesive around the outer circumference and the top surface was sealed with plastic wraps to prevent moisture loss during the experimentation. This pre-conditioning setup allows the water to move at a unidirectional method (i.e., bottom to top) influenced by the concrete specimen's ability to uptake water under the mechanism of absorption, diffusion, and permeability. Absorption tests require recording incremental changes of mass at pre-determined time intervals during the first 6 hours after the specimens were placed in contact with water. Subsequently, incremental mass measurements were carried out for the next 56 days. The amount of water absorbed is divided by the volume of each respective specimen.

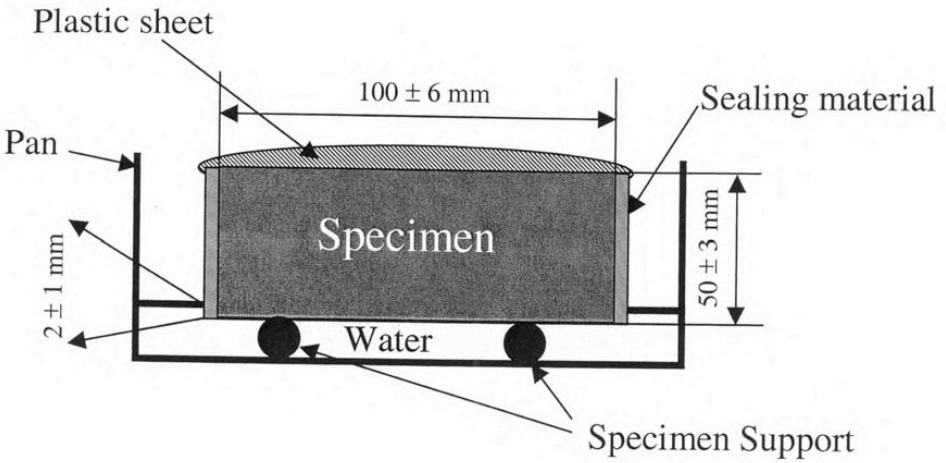



**Figure 47.** Rate of absorption test performed on all specimens demonstrating experimental and laboratory set-up.

#### 3.2.4.2. Results and Conclusion

The measured rate of absorption of all LWC specimens cured at 14, 28, and 56 days are plotted in **Figure *48***. It is noticed that CCA-FLWA concrete demonstrates lower absorption rate than both Commercial-FLWA and control concrete specimens. The initial absorption rate is usually attributed to capillary suction, and the secondary absorption rate is attributed to the percolation of

the Interfacial Transition Zone (ITZ - the zone surrounding the aggregate). The results demonstrate the CCA-FLWA concrete contains lower amounts of capillary pores, and the aggregates have a denser ITZ resulting in lower permeability. The result in **Figure *48*a** demonstrates the rate of absorption for samples cured for 14 days, however, as concrete curing age progressed to 28 and 56 days (**Figure *48* b and c**), (where internal curing is most effective) an even larger decrease in absorption rate was noticed. This was attributed to internal curing enhancing internal cement hydration. During cement hydration, the hydration products occupy a volume that is approximately 10% smaller than the initial reactant [49]. This results in the creation of vapor filled voids inside the concrete [50]. These vapor-filled voids grow with increased hydration and penetrate smaller and smaller pores. Pre-wetted FLWA can supply water to replenish the water demanded by the hydrating cement paste thereby reducing the vapor filled voids reducing capillary pores and reducing overall concretes rate of absorption [51].

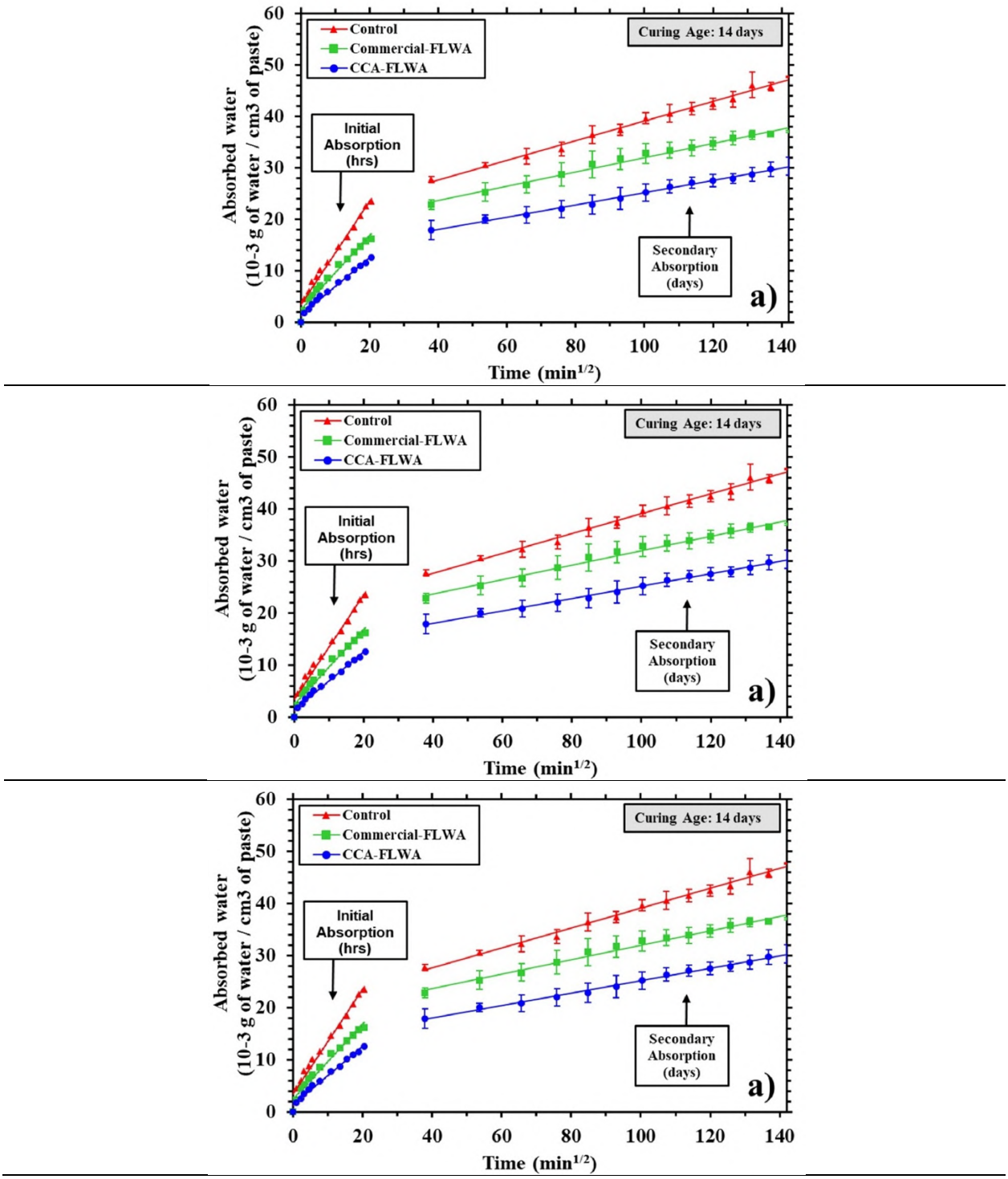


**Figure 48.** Rate of absorption for all specimens cured at **a)** curing age 14 days, **b)** curing age 28 days, and **c)** curing age 56 days.

### 3.3. Evaluation of freeze-thaw performance

This subtask will evaluate the freeze-thaw performance of concrete made using CCA-FLWA as a function of the degree of saturation. While traditional ASTM C666 [52] provides a comparative freeze-thaw performance of concrete samples with respect to control samples, it cannot be fully used to predict the service life of concrete structures exposed to freeze-thaw cycles and moisture exposure. As suggested by several studies [53–55], the freeze-thaw performance and service life of a cementitious system are mainly related to its degree of saturation and the time at which the cementitious system reaches the critical degree of saturation ($DOS_{cr}$). $DOS_{cr}$ is a level of saturation beyond which freeze-thaw damage begins to develop. The time to reach $DOS_{cr}$ (i.e., $t_{cr}$) varies as the pore size and the chemical compositions of a cementitious system changes. By determining $t_{cr}$ and $DOS_{cr}$, service life of a concrete system exposed to the freeze-thaw cycle and moisture exposure can be predicted. Accordingly, in this project, $t_{cr}$ and $DOS_{cr}$ will be measured using water sorption method (modified ASTM C1585-13) and longitudinal guarded comparative calorimetry (LGCC) testing method; and the results will be compared to reference samples made commercial Commercial-FLWA. The damage developed during freeze-thaw testing using Longitudinal Guarded Comparative Calorimeter (LGCC) will be evaluated by the acoustic emission (AE) method. The rate of damage increase will also be evaluated as DOS increases beyond $DOS_{cr}$.

#### 3.3.1. Sample Conditioning

The specimens made from CCA-FLWA, Commercial-FLWA and control concrete were cast in a prism mold with 3×3×11.25-inch dimension. The specimens were cured for 56 days in a curing chamber with a constant relative humidity of 50% ±4% and a temperature of 23°C ±2°C. after achieving the desired curing age the prism samples were carefully cut using a wet table saw into smaller specimens with a constant size of 1×1×2-inch. The cut samples were then placed in a

vacuum oven at 50°C with a vacuum pressure of 1.33 kPa ± 0.33 kPa to achieve oven dry conditions and remove any internal moisture without effecting the samples microstructure. For the samples to achieve 100% DOS, water was de-aerated in the vacuum pump for 1 hr to remove any gas inside the water. The pump was then turned off and the deionized water was stored in a sealed container. The oven-dry samples were then de-aerated in a vacuum pump with a pressure of 1.33 kPa ± 0.33 kPa for 3 hrs. After 3hrs under vacuum conditions, the previously de-aerated deionized water was introduced into the samples without stopping the vacuum. After the samples were fully submerged and remained under vacuum the process lasted for an additional 1 hr. The vacuum pump was then turned off and the samples remained submerged under water for 7 days. This assured that the samples reached 100% DOS. To achieve lower DOS the samples were placed on a scale and moisture was allowed to escape the surface. The samples mass was monitored until the desired DOS was achieved. Lower DOS was calculated by subtracting the necessary amount of water released necessary to achieve the required DOS by the mass of sample at 100% DOS. After achieving the desired DOS (100, 95, 90, 85, and 80%), the samples were carefully wrapped using plastic film wrap (saran wrap) and placed in double Ziplock bags to prevent excess moisture loss.

### 3.3.2. Experimental Set-up

LGCC technique is a well-established steady state method to measure thermal conductivity and heat evolution from a cut-bar specimen. This method is also known as cut-bar and/or divided bar method. The cut bar specimen (i.e., concrete, mortar) is stacked between two reference bars of known thermal conductivity and change in temperature is allowed in an axial direction (i.e., bottom to top). Several temperature sensors are placed at defined locations to measure the temperature difference (ΔT) between specified distances. The samples are laterally stacked over a cold plate which is set at freezing and thawing temperature cycles. AE sensors are positioned on opposite

sides of the sample to capture any energy release during cracking caused by freeze thaw exposure. Acoustic emission is a non-destructive testing method to detect and assess damage by capturing energy release and signals during cracking. The stress wave generated by cracking can be captured and used to quantify damage. The amplitude of waveform is the maximum absolute value. The acoustic energy is the absolute value of the integral of the voltage versus time. The number of acoustic events and cumulative acoustic energy could be used to evaluate the extent of damage [56]. The LGCC with AE sensors were experimental set-up according to ***Figure 49***. Furthermore, ultra-sonic velocity UPV measurements were documented before and after every conducted experiment to measure the damage index of each sample exposed to freeze-thaw cycles.

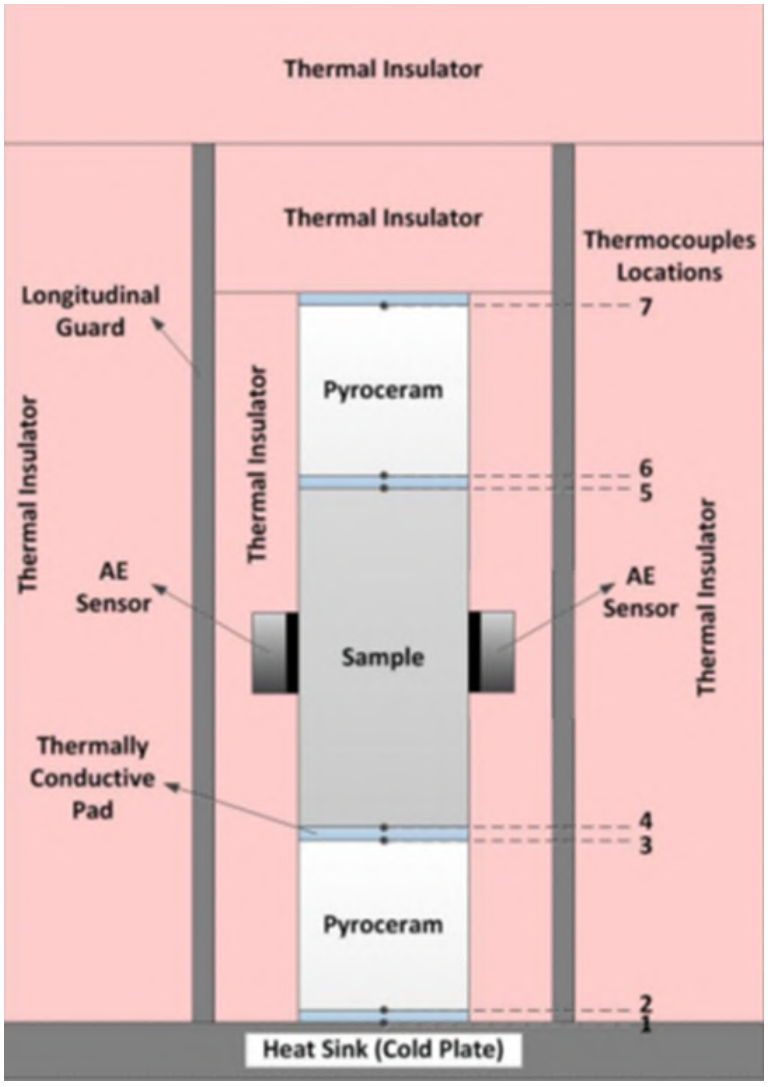


**Figure 49.** LGCC and AE sensors laboratory experimental set-up.

### 3.3.3. Testing Configuration

As water filled voids in concrete freeze and expand, they result in internal pressure that causes crack formation and internal concrete damage. The extent of the damage is inversely related to the DOS. When the DOS exceeds the critical value ($DOS_{cr)}$, freeze–thaw damage occurs. This approach has been largely used to explain and predict freeze–thaw damage. The experimental approach exposed samples with varying DOS to 3 freeze-thaw cycles with a temperature range of 10 °C to -20 °C. The temperature profile for each conducted experiment is demonstrated in **Figure**

**50**. The temperature gradient was configured at a rate of 2 °C/hr. Damage was expected when sample experiences temperature around -5 °C.

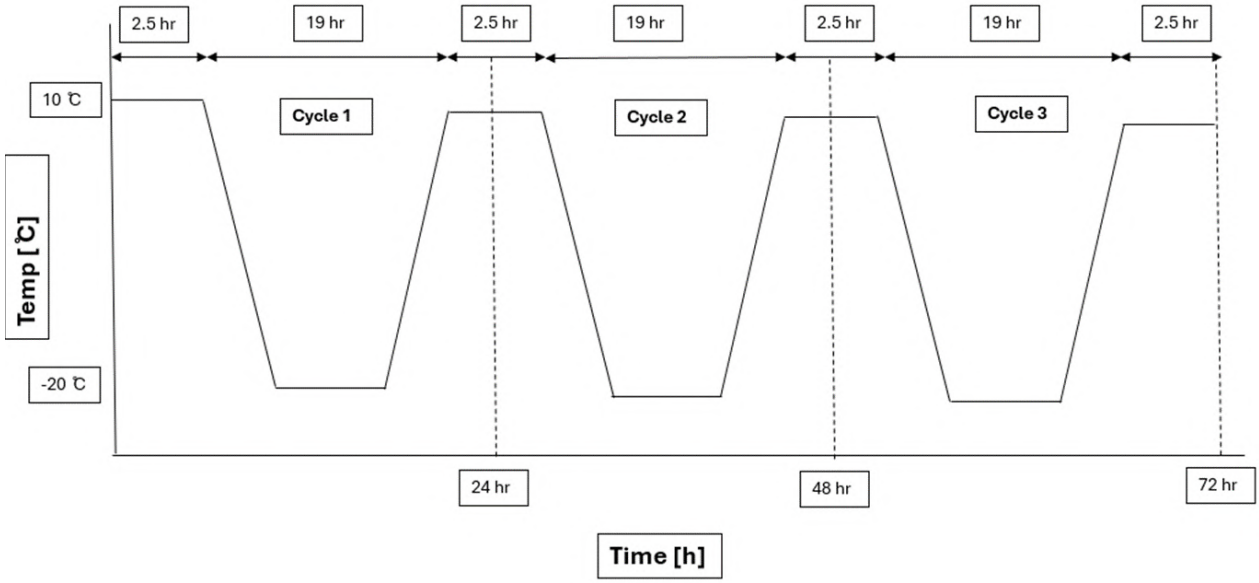


**Figure 50.** Temperature profile for freeze-thaw cycle experienced during testing.

### 3.3.4. Results and Conclusion

The DOS according to the samples rate of absorption were correlated and plotted as a function of DOS over time (**Figure 51**). This indicates the amount of time necessary for concrete continuously exposed to water to reach specific DOS. The secondary rate of increase in DOS curve (**Figure 52**) was fitted with a linear function to estimate the amount of absorbed water over a long period of time. This allows for a direct correlation between predicted DOS and $DOS_{cr}$.

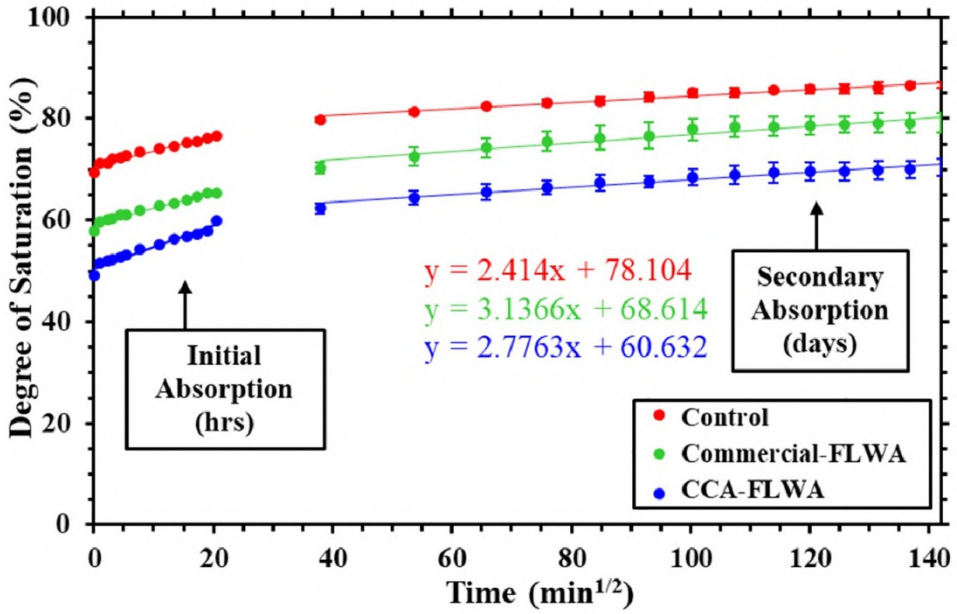


**Figure 51.** DOS as a function of time.

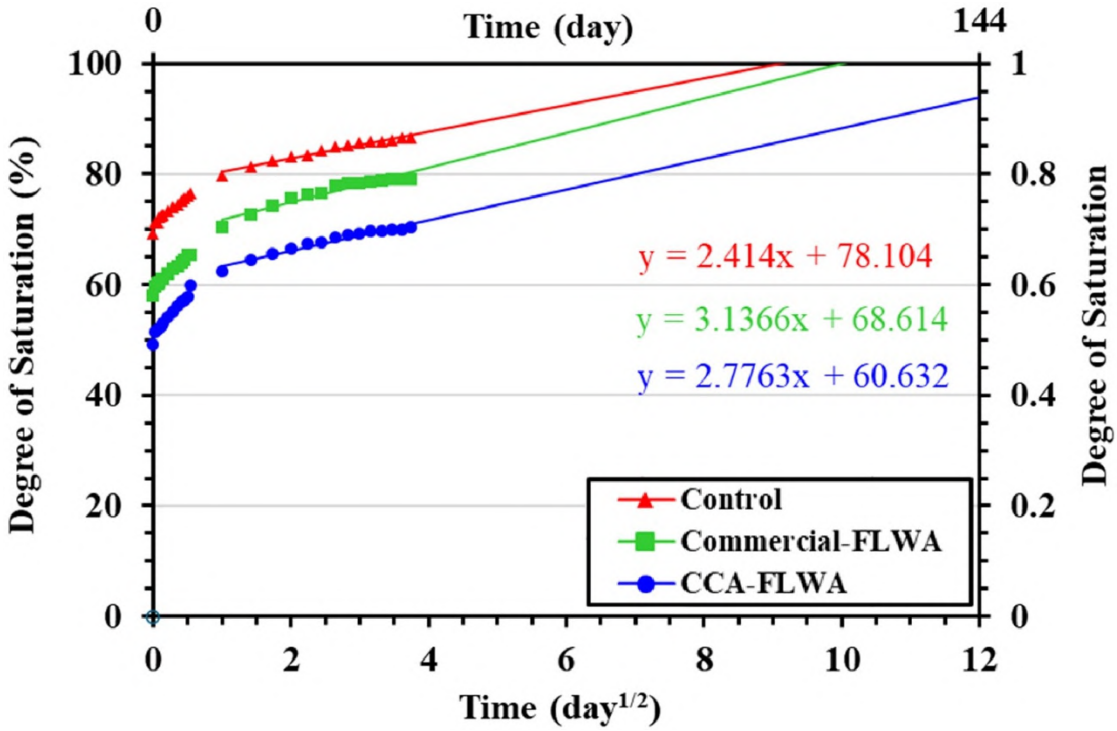


**Figure 52.** Predicted DOS as a function of time.

The freeze-thaw testing for samples manufactured with CCA-FLWA, Commercial-FLWA, and control concrete with DOS of 100, 95, 90, 85, 80 % were documented and plotted as a function of

acoustic emission and fracture energy over time. Acoustic emission demonstrated in ***Figure 15-17*** for all samples at varying DOS presented the peak amps (dB) collected during freeze-thaw cycle. An expected decreasing trend in acoustic emission is noticed for all samples as the DOS is lowered. This can be explained by the amount of void available for internal freezing water expansion. It is concluded that as the DOS decreases, more emptier voids are available, providing more space for freezing water to expand and therefore reducing the amount of internal stress and cracking. Another trend was noticed during each test, as samples are exposed to 3 freeze-thaw cycles, the detected energy activity decreases linearly from the first freeze-thaw cycles to the last. This can be further explained by the amount of damage experienced. When a sample is exposed to a freeze-thaw cycle, water in saturated voids expands and causes internal cracks. These cracks increase the number of voids within a sample and thereby reducing the impact of freezing water expansion due to more voids, during the second and third freeze-that cycle. Furthermore, it was also noticed that CCA-FLWA concrete samples demonstrated the least amount of acoustic emission and Commercial-FLWA concrete demonstrated lower acoustic emission in comparison to the control sample. This was hypothesized to result from two reasons. The first explanation is attributed to internal curing resulting in further internal hydration leading to a denser matrix and lower porosity which reduces the amount of voids and water retention that results in freeze-thaw damage. The second reason is that the CCA-FLWA containing closed isolated pores may provide more voids during freeze-thaw damage and reduce its impact, however, this requires further investigation.

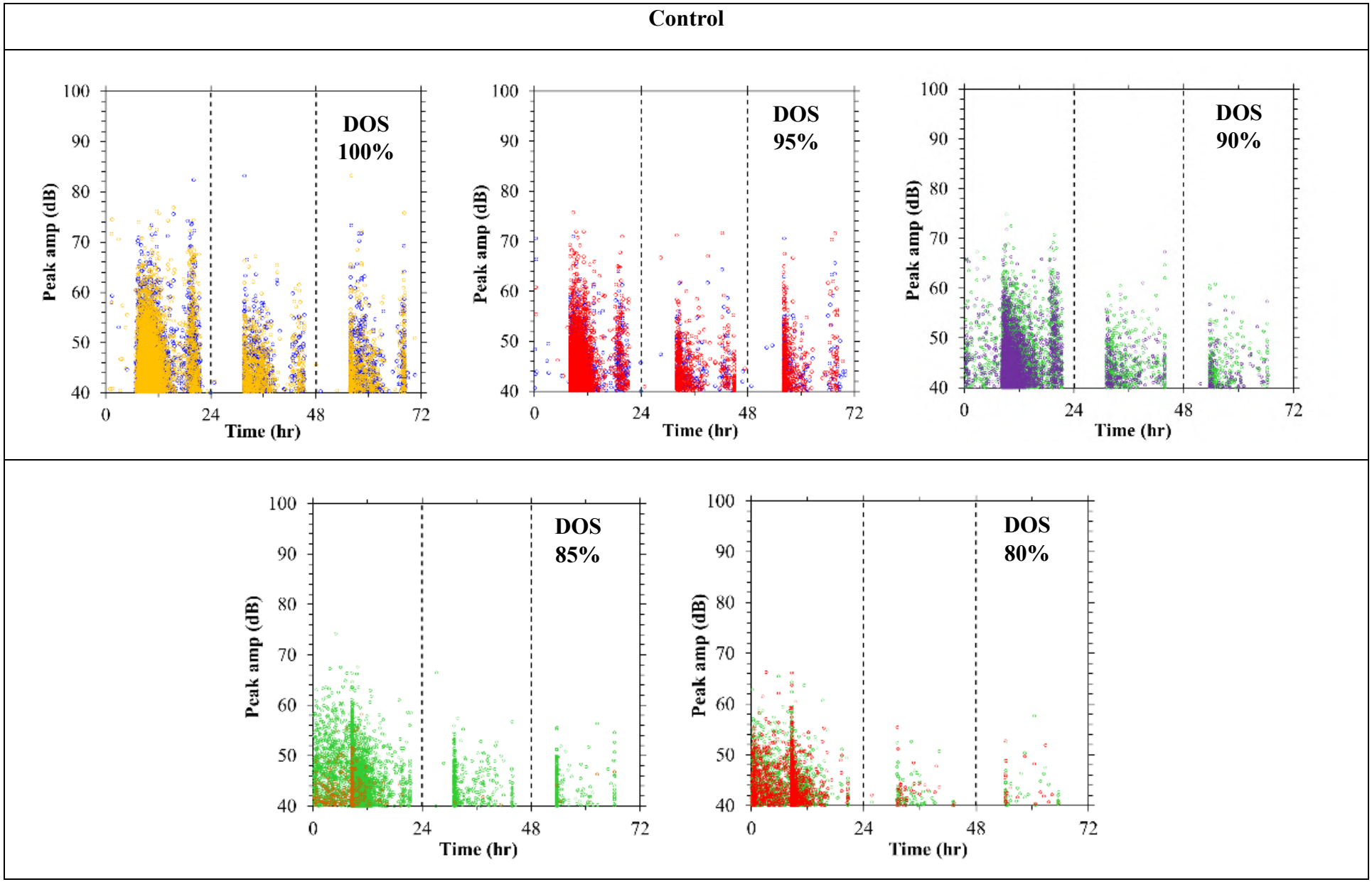


**Figure 53.** Control Specimen acoustic emission, peak amp [dB] as a function of Time [hr].

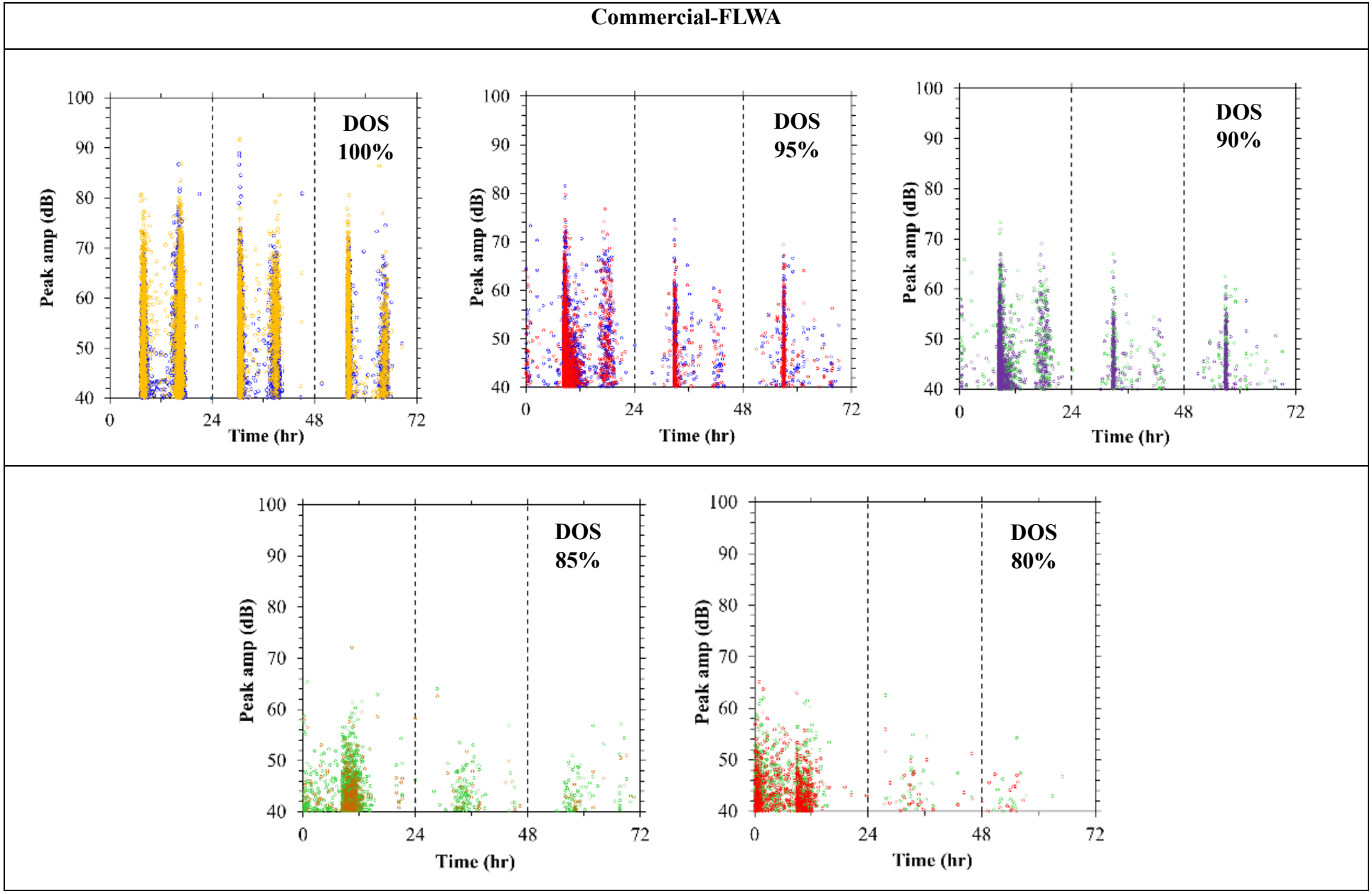


**Figure 54.** Commercial-FLWA specimen acoustic emission, peak amp [dB] as a function of Time [hr].

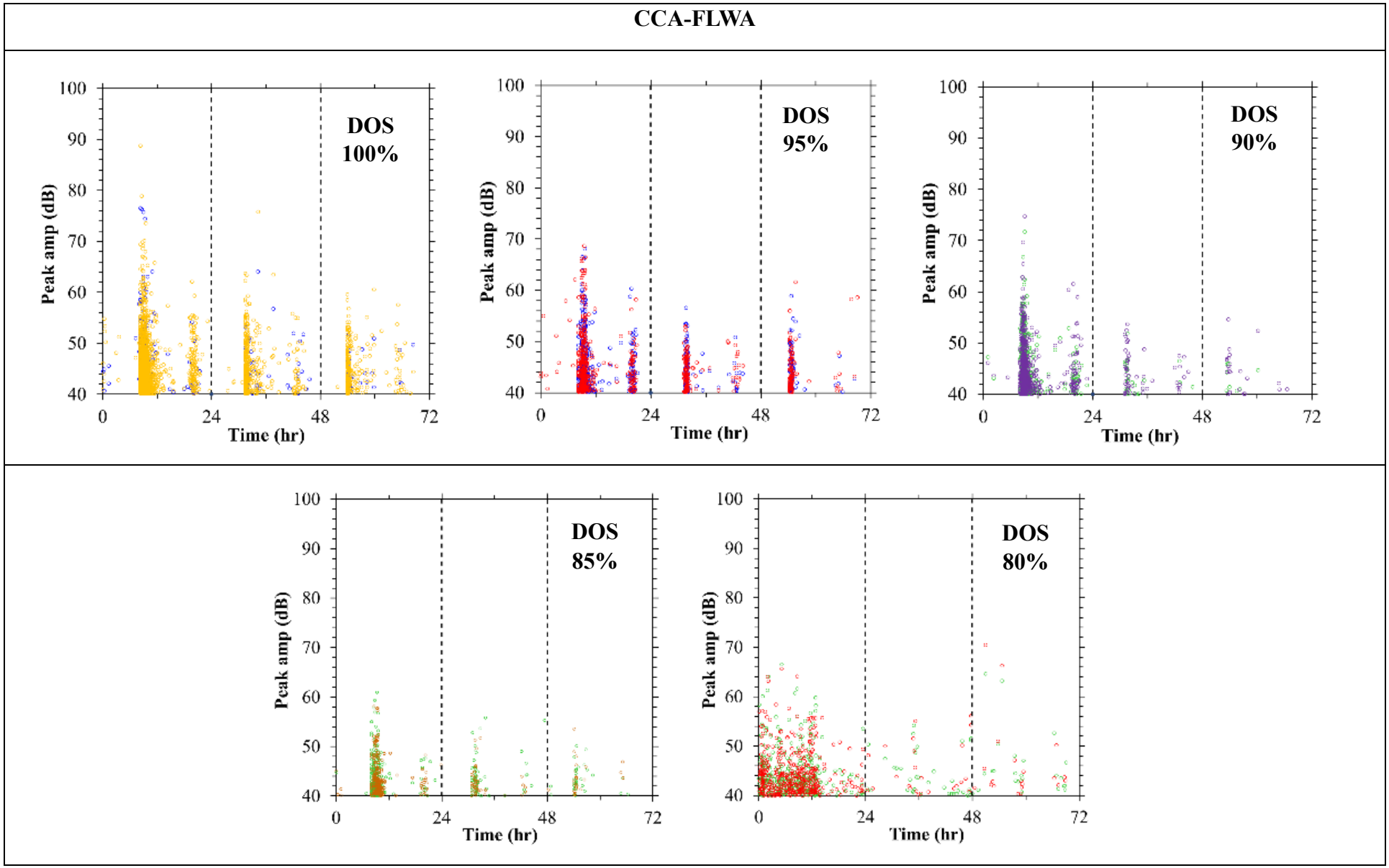


**Figure 55.** CCA-FLWA acoustic emission, peak amp [dB] as a function of Time [hr].

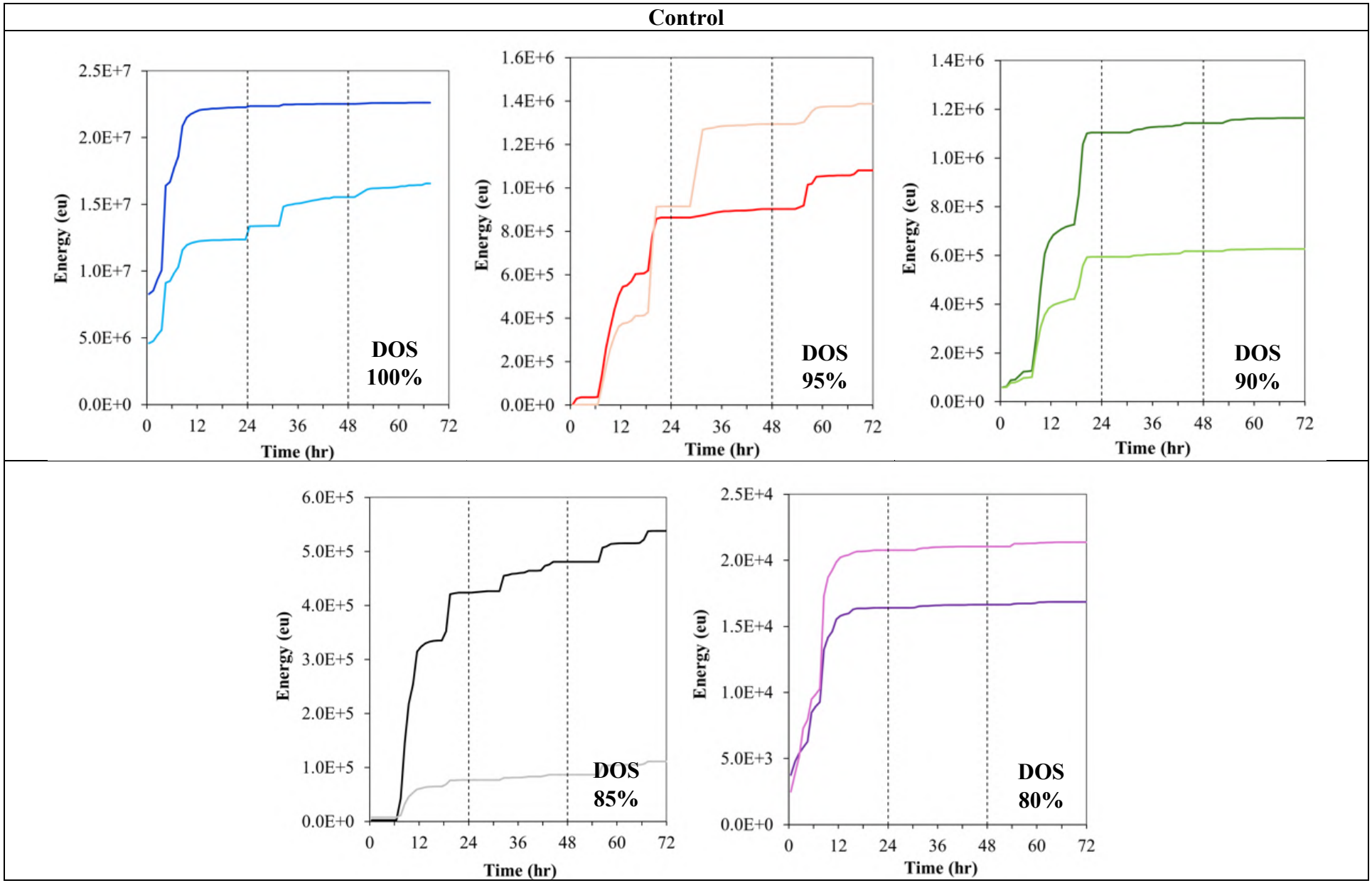


**Figure 56.** Control specimens cumulative fracture energy, energy [eμ] as a function of Time [hr].

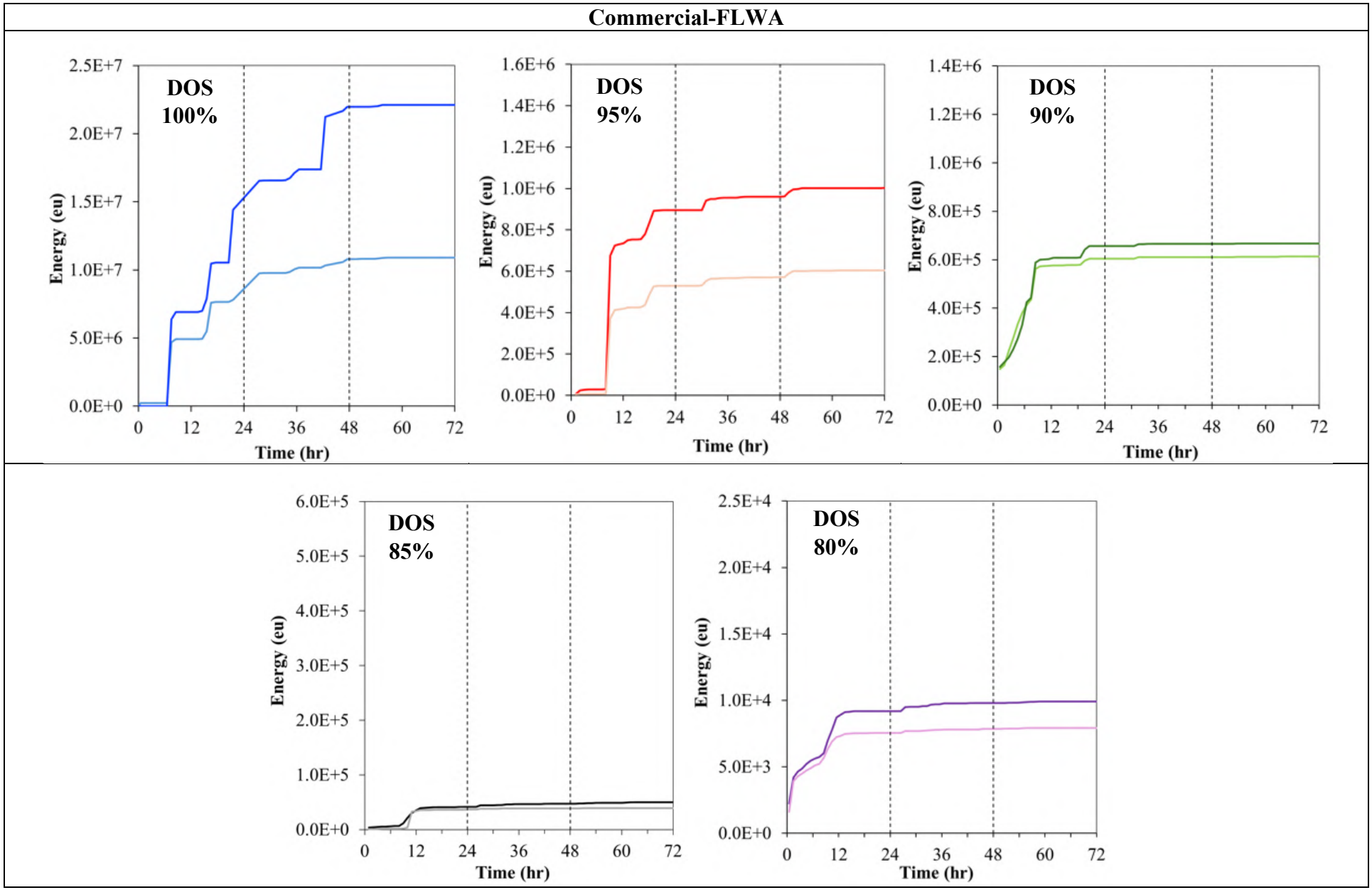


**Figure 57.** Commercial-FLWA specimen cumulative fracture energy, energy [eμ] as a function of Time [hr].

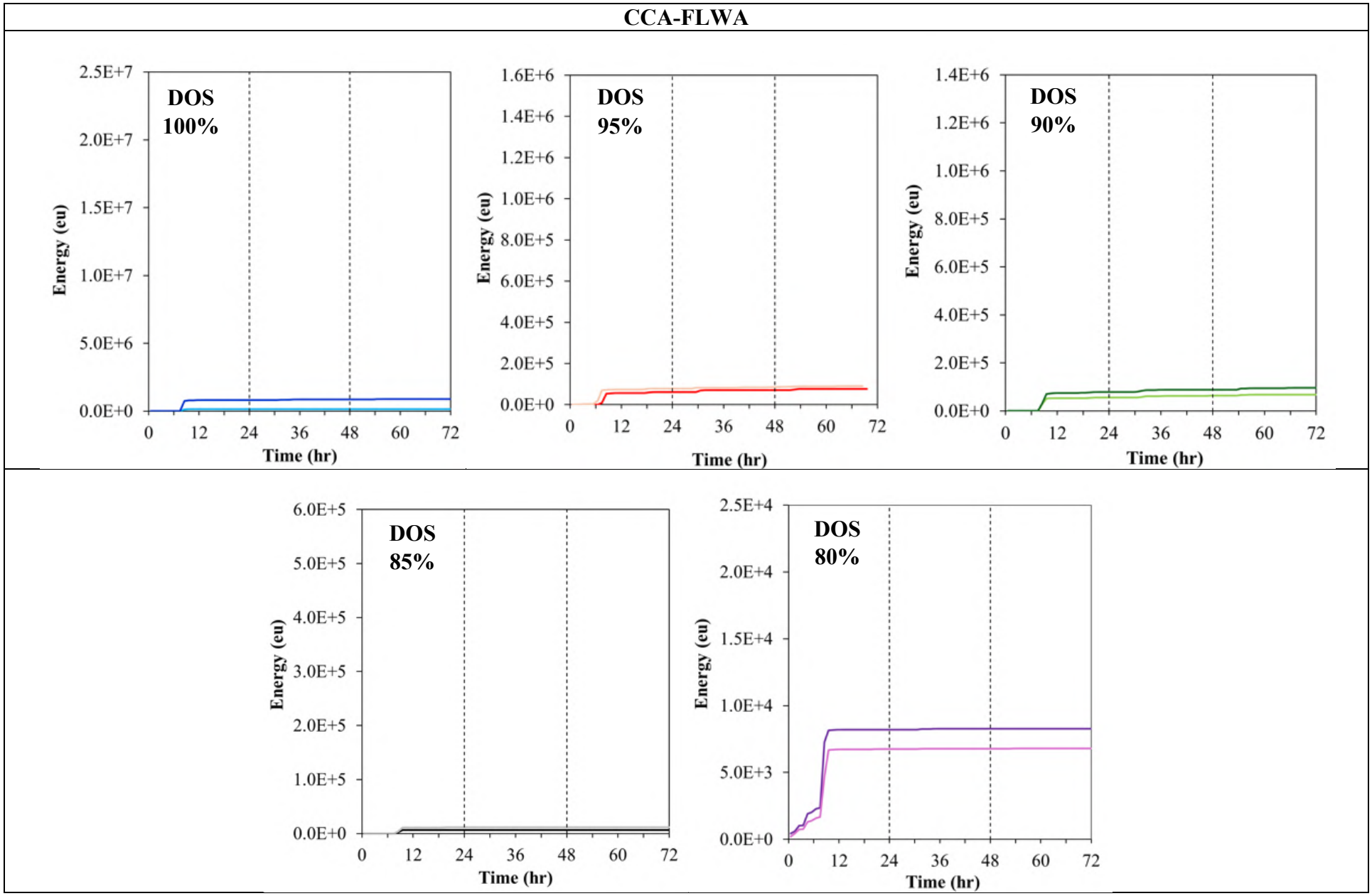


**Figure 58.** CCA-FLWA specimen cumulative fracture energy, energy [eμ] as a function of Time [hr].

AE energy can be proportionally correlated with the fracture energy during freeze-thaw cycles [54]. To observe the magnitude of the fracture energy the cumulative energy from the acoustic emission data was plotted in ***Figure 58*** as a function of energy [eμ] over time [hr]. It can be noted that the same decreasing trend noticed in the acoustic emission graphs ***(Figure 15-17)*** was also observed. Interestingly, at the same magnitude of energy measures, CCA-FLWA demonstrates a significantly lower degree of fracture energy in comparison to Commercial-FLWA concrete and control concrete.

The damage index of the sample exposed to freeze-thaw cycles was measured using UPV and correlated with DOS to identify the $DOS_{cr}$ and $t_{cr}$. The damage index was plotted as a function of DOS and results for CCA-FLWA, Commercial-FLWA, and control concrete are presented in ***Figure 59***. It was revealed that the $DOS_{cr}$ according to the damage index measured was between 78-80 % DOS. This indicates that when samples possess a DOS $\geq$ 78-80 % and undergo a freeze-thaw cycle, the sample will experience freeze-thaw damage. The $DOS_{cr}$ was then correlated with the predicted time required to achieve DOS for all samples to identify $t_{cr}$ ***Figure 60***. It was noted that control concrete reached $t_{cr}$ after 1 day of saturation exposure, Commercial-FLWA concrete reached $t_{cr}$ after 13 days of saturation exposure, and CCA-FLWA concrete reached $t_{cr}$ after 47 days of saturation exposure. This indicates that CCA-FLWA concrete will require significantly longer moisture exposure before reaching $t_{cr}$ (unlikely to occur) and therefore, reducing the potential risk of freeze-thaw damage.

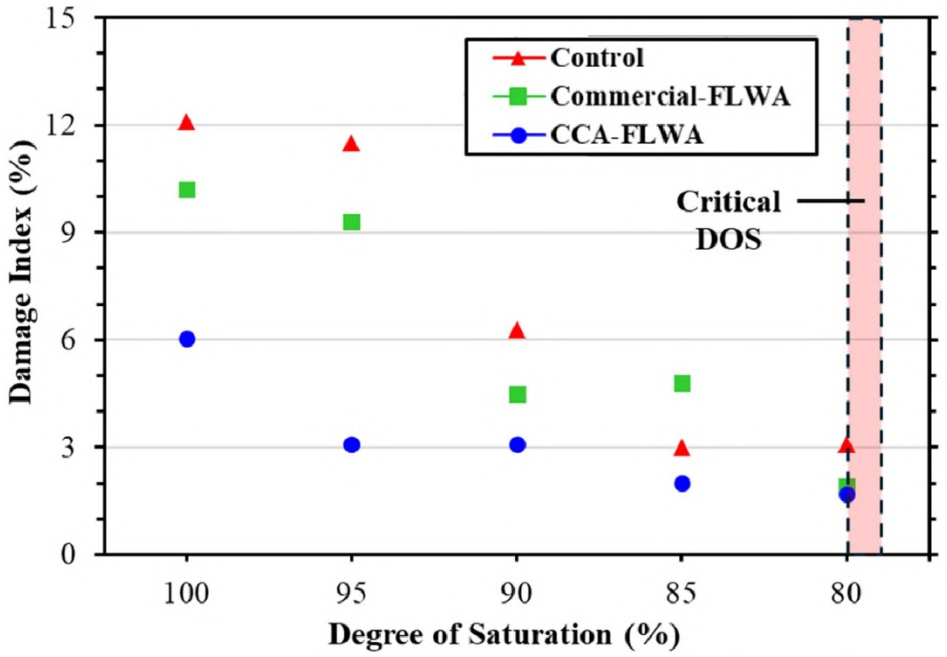


**Figure 59.** Damage index (%) plotted as a function of DOS (%).

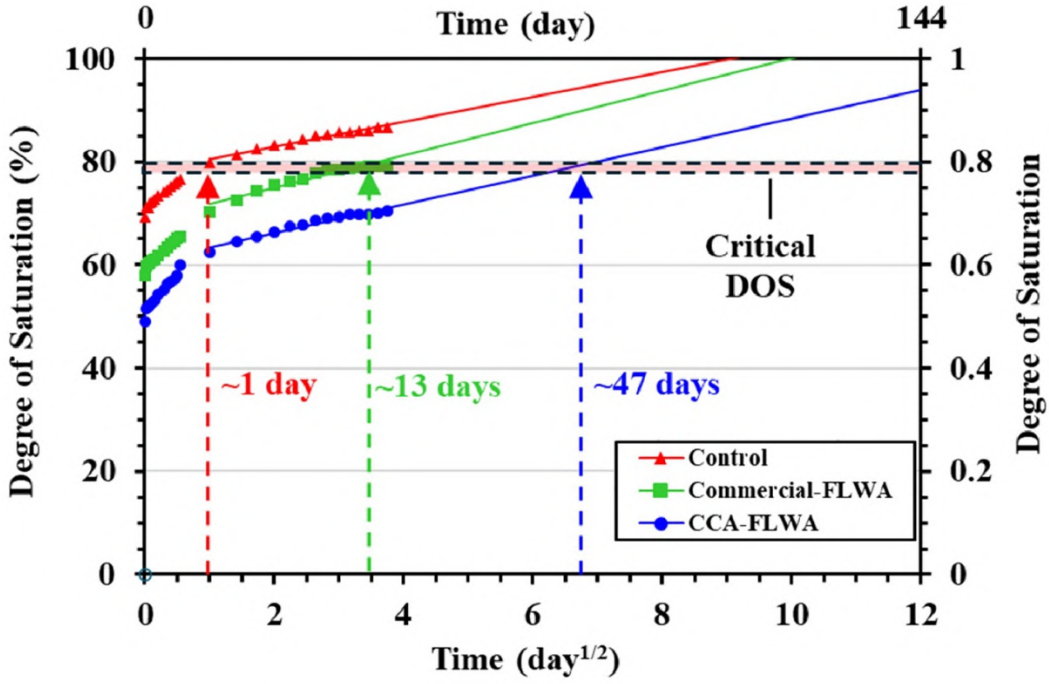


**Figure 60.** $DOS_{cr}$ (%) mapped on the curve representing DOS (%) as a function of time [day], to identify $t_{cr}$

### 3.4. Evaluation of Leaching Potential of Constituent of Potential Concern (COPC)

Unsuitable CCAs derived from electric power industry waste materials may contain COPC (e.g., heavy metals (including e.g., chromium (Cr), lead (Pb), selenium (Se), and antimony (Sb)), it is important to characterize the leachability of COPC in concrete made using CCA-FLWA. For evaluation of leaching potential, Test Method 1315 [57] from Leaching Environmental Assessment Framework (LEAF) [58] test methods was followed in this sub-task to obtain the leaching potentials of COPC. This test method is an EPA-validated and recommended test method for waste solid materials testing in monolithic form (e.g., concrete). Concrete samples were exposed to a continuous reagent water-saturated environment in an eluent-filled tank with periodic renewal of the leaching solution. This protocol is a semi-dynamic, tank-leaching procedure where the sample was exposed to eluate for a series of 9 leaching intervals interspersed with eluent exchanges **Figure 61**. The chemical composition of each eluate was determined as a function of cumulative leaching time.

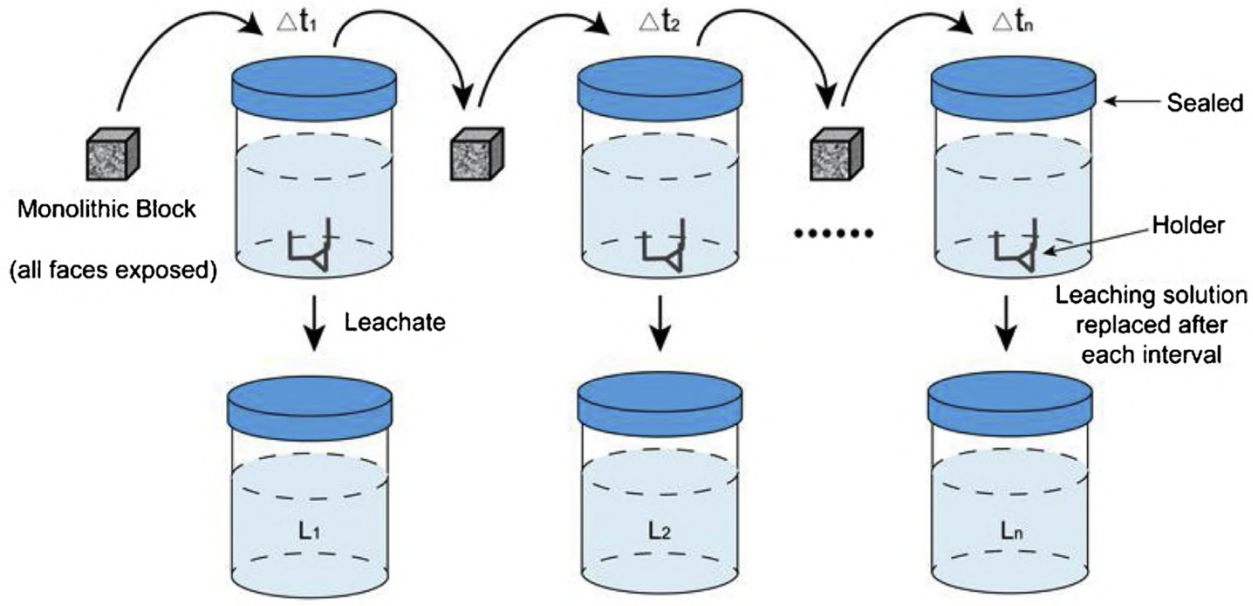


**Figure 61.** Semi-dynamic, tank-leaching procedure, sample exposed to eluate for a series leaching intervals interspersed with eluent exchanges.

### 3.4.1. Sample Conditioning and Experimental Set-up

This leaching characterization method provides intrinsic material parameters for release of inorganic species under mass transfer-controlled leaching conditions. This test method is intended as a means for obtaining a series of eluents which are used to estimate the diffusivity of constituents and physical retention parameters of the solid material under laboratory conditions. Monolithic samples are suspended in the leaching fluid such that at least 98% of the entire sample surface area is exposed to eluent and the bulk of the eluent (e.g., a minimum of 2 cm between any exposed surface and the vessel wall) is in contact with the exposed sample surface. The eluent used in this characterization method is deionized (DI) water. Samples are cylindrical form with dimensions of 2 inch in diameter and 4 inch in height. A leaching vessel with required volume of DI water quantified based on a minimum L/A of 9 $\pm$1 mL/cm$^2$ where L = required unit volume of DI water and A = exposed surface area of sample. The sample was carefully placed on the holder in the leaching vessel so that the sample is centered in the eluent. Submersion was gentle enough so that the physical integrity of the monolith was maintained and scouring of the solid was minimized. The sample was exposed to eluate for a series of 9 leaching intervals interspersed with eluent exchanges. The eluent was vacuum filtered after every interval using a filter membrane with an effective pore size of 0.45 μm. The eluent pH and conductivity [μs/cm], as well as the monolithic samples mass [g] were measured before and after every eluent exchange **Table 11**.

**Table 11.** Series of 9 leaching intervals with eluent exchange measuring pH, conductivity, and sample mass.

| Date | Interval Duration | Cumulative Leaching Time (d) | pH | | Conductivity (µs/cm) | | Mass (g) | |
|---|---|---|---|---|---|---|---|---|
| | | | Before | After | Before | After | Before | After |
| 11/30/2023 | 2 hr ± 0.25 | 0.08 | 7.5 | 11.2 | 1.03 | 227.5 | 408.01 | 426.3 |
| 11/31/2023 | 23 hr ± 0.5 | 1 | 7.28 | 11.99 | 0.99 | 937.1 | 421.56 | 4325 |
| 12/2/2023 | 23 hr ± 0.5 | 2 | 7.73 | 11.68 | 0.97 | 514 | 429.88 | 432.5 |
| 12/7/2023 | 5 d ± 0.1 | 7 | 7.55 | 11.86 | 1.45 | 789 | 431.07 | 433.6 |
| 12/14/2023 | 7 d ± 0.1 | 14 | 7.06 | 11.80 | 1.8 | 689 | 430.7 | 434.1 |
| 12/28/2023 | 14 d ± 0.1 | 28 | 7.02 | 11.84 | 1.62 | 718.1 | 431.83 | 433.31 |
| 1/11/2024 | 14 d ± 0.1 | 42 | 7.36 | 11.81 | 3.76 | 645.6 | 436.27 | 436.30 |
| 1/18/2024 | 7 d ± 0.1 | 49 | 7.03 | 11.60 | 1.78 | 459 | 433.55 | 437.13 |
| 2/1/2024 | 14 d ± 0.1 | 63 | 7.20 | 11.72 | 1.20 | 532.2 | 433.57 | 436.91 |

### 3.4.2. Results and Conclusion

The evaluation of leaching for constituents of potential concern (COPC) was performed by measuring the concentration and cumulative release of major COPC such as As, Se, Cr, Ag, Cd, Ba, and Pb for CCA-FLA concrete. A comparison was performed between raw coal ash, CCA-FLWA, and CCA-FLWA Concrete **Table 12**. Detection of the cumulative concentration limits is documented as a function of mass per leaching time.

**Table 12.** L.E.A.F. Testing for concentration [mg/l] for raw coal ash, CCA-FLWA, and CCA-FLWA Concrete.

| **Major COPC** | **LEAF Testing** | | |
|---|---|---|---|
| | Raw Coal (mg/L) | CCA-FLWA (mg/L) | CCA-FLWA Concrete (mg/L) |
| **As** | 7.6 | 0.964 | 0.0034 |
| **Se** | 0.64 | 0.0337 | 0.0091 |
| **Cr** | 0.361 | BDL | 0.0304 |
| **Ag** | BDL+ | BDL | BDL |
| **Cd** | 0.019 | 0.00093 | BDL |
| **Ba** | 6.382 | 1.737 | 0.0214 |
| **Pb** | 0.0537 | 0.008 | BDL |

*BDL – Below Detection Limit

The concentration of leaching constituents was plotted as a function of leaching time according to the 9 intervals specified by L.E.A.F. (**Figure 62**). Selenium and Arsenic demonstrated leaching

concentrations below the lower limit of quantification (LLOQ) and above the max detection limit. Both Selenium and Arsenic are major elements of concern and detecting lower concentrations of these elements leaching into the eluent demonstrates the low risk of elemental leaching in practice. The cumulative release of these elements over cumulative time was plotted to document the potential for leaching in sever conditions where concrete is continuously exposed to water, increasing leaching potential. Lower cumulative release of Selenium and Arsenic were observed in comparison to raw coal ash after cumulative exposure to eluent for 63 days. This was believed to be a result of both the sintering mechanics of CCA-FLWA creating a stronger bond between elements and reducing the potential for leaching, as well as the encapsulation of the CCA-FLWA in concrete with low permeability reducing direct exposure to the eluent. Finally, the cumulative elemental release of CCA-FLWA concrete was compared to control concrete samples manufactured with ordinary Portland cement (OPC). It was observed that slightly lower traces of both Selenium and Arsenic were documented after exposure to a longer leaching time of 63 days. This indicates that concrete manufactured using CCA-FLWA does not demonstrate leaching of COPC and can be utilized in practical practice.

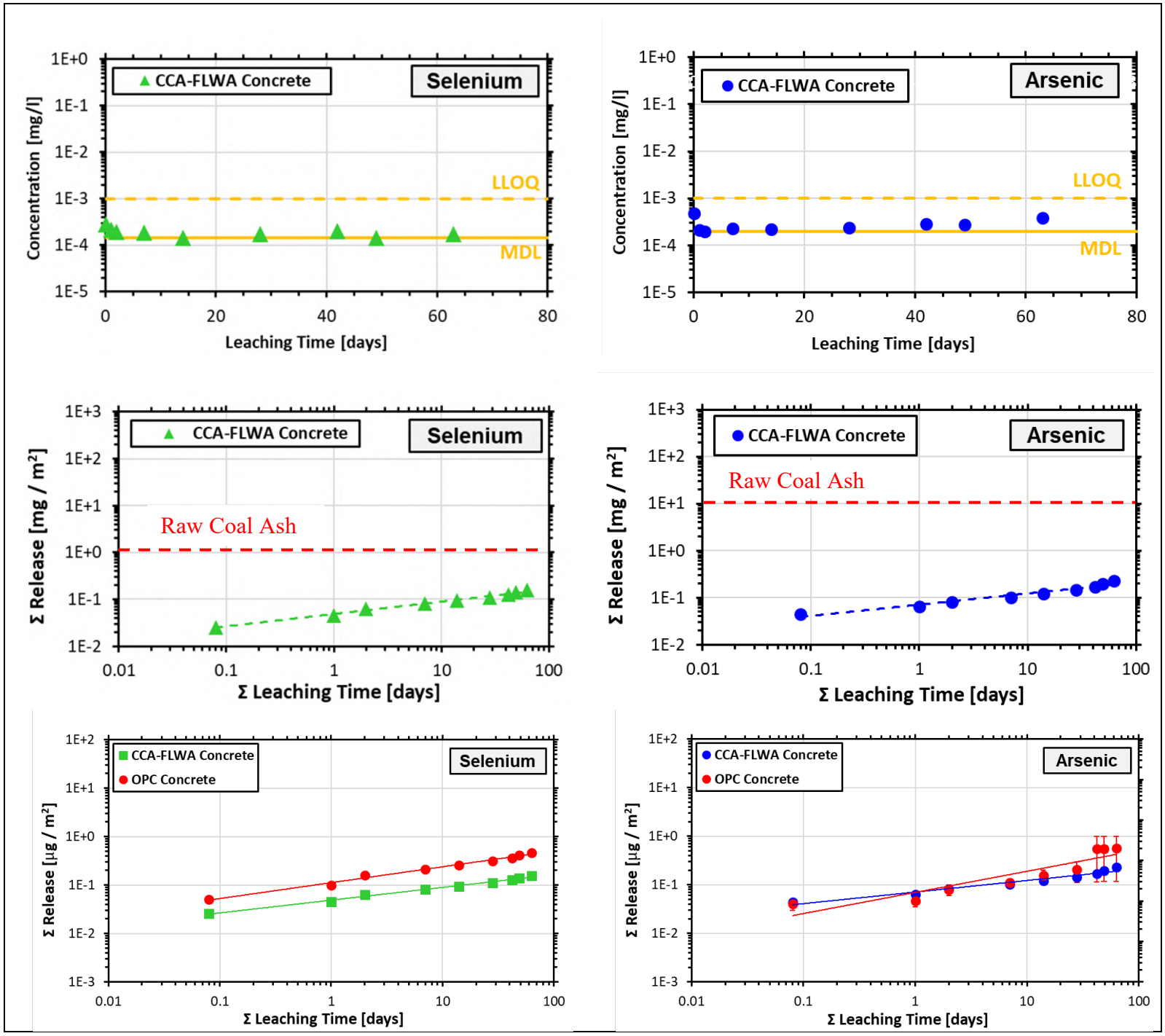


**Figure 62.** Leaching evaluation of Selenium and Arsenic, documenting release concentration, cumulative release (compared to raw coal ash), and comparison between CCA-FLWA concrete and control concrete (OPC).

### 3.5. Summary of Task 2

The report studied the performance of concrete internal curing manufactured using CCA-FLWA and compared it to commercial-FLWA concrete and control concrete specimens. Theoretical calculations were made for quantifying the necessary amount of CCA-FLWA inclusion for successful internal curing of concrete. Concrete mix design was calculated based on material characterization and PennDOT bridge deck design criteria. CCA-FLWA, Commercial-FLWA, and Control concrete samples were made and cast according to specimen testing dimension and then cured according to required curing age and conditions. Finally, the samples were tested according to an experimental program evaluating fresh properties, hardened properties, freeze-thaw evaluation, and leachability of COPC. Major outcomes in task 2 are summarized below:

Task 2.1: Concrete samples were prepared using CCA-FLWA from Task 1, Commercial-FLWA, and NWA. The fresh properties of concrete paste were measured for slump, air content, and density. Hardened properties were evaluated, testing the compressive strength of concrete cured at 14, 28, and 56 days. The results indicate that CCA-FLWA concrete had similar gained strength at 14 days of curing relative to Commercial-FLWA and control concrete of ~28-29 MPa. As curing progressed to 28 days and 56 days the compressive strength of CCA-FLWA concrete gained (35.4 MPa) was superior to both Commercial-FLWA and control concrete (~32 MPa). This was attributed to internal curing providing efficient internal hydration. Furthermore, flexural strength was also measured for the same curing age. It was noticed that control concrete had slightly high flexural strength at 14 days of curing, however, as the curing age progressed to 56 days, both CCA-FLWA and Commercial-FLWA gained similar strength of control concrete specimens with a modulus of rupture of ~7.5 MPa. This was concluded that internal curing requires time to achieve optimum strength leading to a delay in strength achieved in flexural strength. Additionally,

shrinkage of concrete made using CCA-FLWA, Commercial-FLWA, and NWA was measured. Results indicated that CCA-FLWA concrete experienced lower strain as curing progressed. This was attributed to internal curing through the increase in the degree of hydration anticipated and significantly reducing chemical and drying shrinkage. The rate of absorption of all three concrete typologies was measured and evaluated. It was revealed that concrete made using CCA-FLWA experienced lower absorption rate when exposed to water at various curing ages. This was attributed to a decrease in capillary pores and densification of ITZ. The reduction in capillary pores reduces capillary suction and therefore reduced the concrete absorption rate. The comparison analysis of fresh and hardened properties assessed that concrete made using CCA-FLWA possessed superior performance capability due to internal curing advancing internal hydration and thereby enhancing the concrete internal microstructure and overall durability.

Task 2.2: The evaluation of freeze-thaw performance was performed for CCA-FLWA, Commercial-FLWA, control concrete specimens. The rate of absorption of samples was measured to assess permeability and to identify the degree of saturation (DOS) as a function of time. Samples were conditioned and prepared for freeze-thaw testing based on various DOS (100, 95, 90, 85, and 80 %). Freeze-thaw cycles were evaluated by measuring acoustic emission through acoustic sensors and UPV before and after freeze-thaw cycle exposure. Acoustic emission and fracture energy were evaluated, and the damaged index was measured to identify the critical degree of saturation ($DOS_{cr}$). It was noticed that CCA-FLWA concrete demonstrated lower acoustic emissions than Commercial-FLWA concrete and Commercial-FLWA concrete demonstrated lower acoustic emissions than control concrete. The same trend was noticed when measuring the cumulative fracture energy and damage index. The $DOS_{cr}$ was correlated with the rate of absorption to identify the critical time ($t_{cr}$) for all measured samples. The analysis revealed that the

$DOS_{cr}$ for the control concrete would be achieved after 1 day of water exposure. The $DOS_{cr}$ for Commercial-FLWA concrete would be achieved after 13 days of water exposure and CCA-FLWA concrete would be achieved after 47 days of water exposure. The delay in reaching the $DOS_{cr}$ demonstrates the ability for CCA-FLWA concrete to withstand freeze-thaw damage under severe water exposure conditions.

Task 2.3: The leaching test was performed following L.E.A.F. test method 1315, measuring the release of inorganic species under mass transfer-controlled leaching conditions. The test measured the concentration of elements of potential concern of samples exposed to eluate for a series of leaching intervals interspersed with eluent exchanges. The concentration and cumulative release of concerning elements were documented and compared to raw coal ash, CCA-FLWA, and control samples (OPC). The elements considered include As, Se, Cr, Ag, Cd, Ba, and Pb, and it was identified that CCA-FLWA concrete demonstrated concentrations of leaching COPC when compared to CCA-FLWA, and CCA. Furthermore, CCA-FLWA concrete demonstrated low risk of leachability of major COPC when compared with OPC concrete with both Selenium and Arsenic levels being very similar in release concentrations at various eluent exposure revealing that CCA-FLWA is suitable for practical practice.

The evaluation of internal curing of CCA-FLA concrete in Task 2 demonstrates promising performance to be used in practical practice for bridge deck construction. Additionally, a cost analysis and feasibility study will be performed later in the project to assess implementation measures for utilizing landfill condition CCA to manufacture FLWA for the internal curing of concrete.

## 4. Cost Analysis and Feasibility Study of Implementing CCA-FLWA (Task 3)

Assessing the industrial practicality of converting coal combustion ash (CCA) into fine lightweight aggregates (FLWA) for concrete use requires both cost analysis and feasibility of implementation study. This section builds on information obtained in previous tasks and literature to study practical implementation methodologies to apply CCA-FLWA to existing or new concrete structures and pavements for internal curing. Additionally, a comprehensive cost analysis is determined in this task. Due to the anticipated reduction in CCA disposal and displacement of natural aggregates, CCA-FLWA is expected to reduce landfilled waste and cost by eliminating the need to extract and process natural FLWA or manufacture FLWA from synthetic resources, with high transportation costs [59]. The system boundaries consider sourcing, processing, refining, storing, and transporting FLWAs, for use in functionally equivalent concrete mixes. Accumulated data are used to account for processing inputs needed to manufacture CCA-FLWA. The results of this task will enable the research team to identify a platform for proposing a robust implementation plan to produce FLWA from local resources in Pennsylvania for concrete internal curing applications.

This study examines three fundamental factors essential for the industrial-scale implementation of CCA-FLWA for practical application. Firstly, it examines the successful production of CCA-FLWA within an industrial setting, serving as a benchmark for comparison by analyzing variances with traditional FLWA industrial processes. This entails an evaluation of manufacturing procedures and associated costs, followed by an analysis of fresh concrete performance relative to both CCA-FLWA and traditional FLWA. Subsequently, it assesses the final concrete product. Secondly, the study explores the utilization of CCA-FLWA for internal curing in concrete applications, encompassing an examination of delivery methods and the challenges they entail. These challenges include design considerations, delivery mechanisms, existing precedents, and

property performance. Lastly, the study addresses risk assessment concerning the industrial implementation of CCA-FLWA. This involves investigating aspects such as CCA landfill security, reproducibility, and potential technical issues, along with strategies for mitigation. By exploring these three key factors, the study aims to provide a fundamental analysis, identifying preliminary considerations for cost assessments, and feasibility studies pertaining to the industrial utilization of CCA-FLWA.

## 4.1. Practical Implementation Methodology

### 4.1.1. Production/Innovation

The production flow model for manufacturing CCA-FLWA follows a series of steps including material characterization, thermochemical modeling, material proportioning, and experimental configuration (***Figure 63***) [60]. Through a partial sintering process, the oxide compounds of CCA are partially melted and subsequently combust the residual carbon to create a porous material, LWA, encapsulated by a glassy layer that exhibits pozzolanic reactivity. We achieve this novel process by using thermodynamic modeling principles and experimental validations to obtain phase equilibria to identify a desired blend of CCA, an appropriate fluxing agent (NaOH), and an appropriate elevated temperature to partially melt CCA. Our research driven by thermodynamic-based methodology indicated that a large portion of waste CCA can be converted into FLWA [60]. Drexel University is currently working with companies within the state of Pennsylvania to establish a licensing agreement to produce CCA-FLWA in PA.

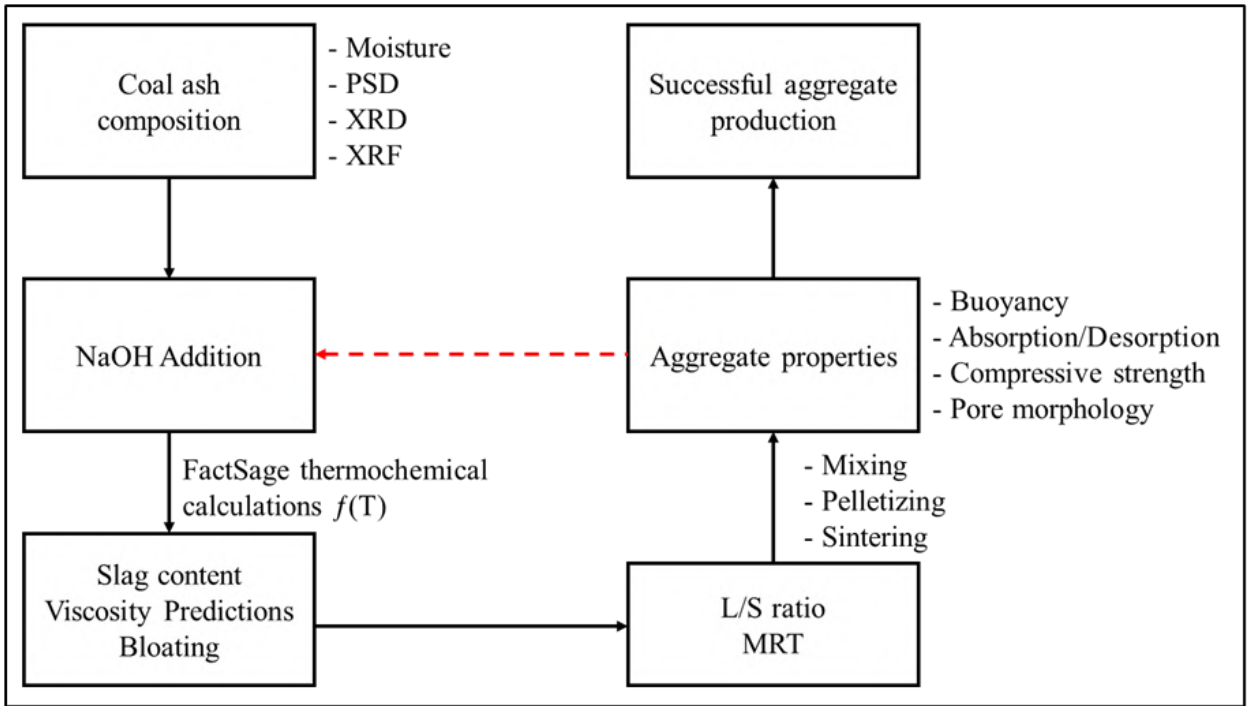


**Figure 63.** Summary of production flow model methodology for CCA blending and flux addition, Factsage calculations render, addressing minimum criteria requirements, experimental configuration, and FLWA requisite properties for internal curing application.

### 4.1.2. Considerations

Practical implementation analysis requires three main considerations i) evaluating the security (availability) of suitable CCA within the region, ii) assessing the facility requirements for hosting production lines, and iii) project personnel for successful execution.

i) The main components for the manufacture of CCA-FLWA include landfill condition CCA, fluxing agent (NaOH), and water. Landfill condition CCA currently inflicts financial burdens and ecological risks for energy power plants in PA and the US in general. Plants are required to provide storage impoundments/landfills, perform maintenance, and regulatory inspections impose undesirable obligations [61]. Production of a value-added product from CCA, i.e., CCA-FLWA, can be a reliable and interesting source for landfill owners to provide a secure source of feed materials.

ii) The second consideration for assessing the facility requirements for hosting the CCA-FLWA production line includes four primary sectors for the successful establishment of a CCA-FLWA plant including 1) industrial space (owned or rented), 2) industrial machinery, 3) daily operation cost, and 4) a research and development sector (R&D).

1. Operation facilities require a controlled environment with minimum external weather influence, appropriate ventilation, and a safe working environment for production and execution. The approach proposed for converting CCA into FLWA delivers an on-site manufacturing procedure. This implies that the operation and equipment for manufacturing are situated in relative proximity to the CCA landfill. This reduces additional shipping costs and with prior agreement energy power plants can facilitate designated empty facilities for CCA-FLWA manufacturing. If on-site facilities are not available for CCA-FLWA manufacturing renting an off-site industrial facility will be necessary.
2. The industrial scale machinery for the three stages of CCA-FLWA manufacturing consisting of material mixing, pelletizing, and sintering requires an industrial mixer, large-scale pelletizer, pellet feeder with discharge rate control, conveyor belt for assigned pellet delivery to a furnace, and rotary furnace.
3. The daily cost of operating the facility will cover all expenses related to facility costs, machinery operation/maintenance, and assigned personnel. A detailed breakdown of these expenses will be provided in subsequent sections of the report.
4. The R&D sector involves the utilization of the technology proposed and reproducing successful CCA-FLWA for industrial applications. This requires knowledge in characterization testing for CCA characterization including moisture analysis, x-ray fluorescence (XRF) to identify elemental composition, x-ray diffraction (XRD) for

measuring chemical oxide composition, particle size distribution (PSD) for measuring size proportions and range, and thermogravimetric analysis (TGA) for understanding gas release under elevated temperatures. Additionally, knowledge of the software used for thermodynamic modeling (Factsage®) is essential. This software allows for the input of elemental and oxide composition of the CCA along with fluxing agent (NaOH) concentrations for slag content predictions and successful CCA-FLWA production. This department extends to formal personnel training for comprehending the scientific and technological processes involved in converting CCA to FLWA. Experience in mechanical and observational consideration experience is necessary for addressing technical difficulties and executing successful CCA-FLWA.

iii) The final consideration for practical implementation consists of the project personnel involved for successful execution. Execution purposes require an established personnel team that can function in a coherent environment and perform assigned tasks and deliverables accordingly. The team structure typically includes a designated team leader responsible for project oversight and coordination, a junior research scientist involved in experimental design and data analysis, an industrial technician focused on equipment operation and maintenance, and a logistics officer managing resource procurement and project scheduling. The dynamic and scale of execution will dictate the number of team members required for project execution.

## 4.2. Cost Analysis and Market Opportunity

### 4.2.1. Core Material

The main components for the manufacture of CCA-FLWA include landfill condition CCA, fluxing agent (NaOH), and water (**Table *13***). Throughout laboratory investigations, CCA was acquired from the TALEN energy station in Brunner Island, PA [62]. Their attention to finding a solution

for this waste material incentivizes them to provide CCA at minimum to no cost, to mitigate its economic impact on the power plant and negative environmental effects. The fluxing agent NaOH was supplied from Macron Fine Chemicals with a Sodium Hydroxide concentration of more than 95 % [63]. The NaOH properties include molecular weight of 39.997 (g/mol), boiling point: 1390 ºC, melting point: 323 ºC, density: 2.13 g/cm$^3$, grade – ACS, category R, and physical form pellets. Market-available sodium hydroxide in pellet or flask form is considered adequate and according to various analytical sources [64–67] the US market price stability index and trend forecast indicate an annual fluctuation of 4-6% signifying its stable market presence. The water utilized during material mixing was lab-grade deionized water. Industrial water supplied by the municipality is seen as adequate for manufacturing successful CCA-FLWA.

**Table 13.** Raw material rates per Pennsylvania availability.

| CCA-FLWA Components | Cost | Source |
|---|---|---|
| Landfill Condition Waste CCA | $0-5/ton | Coal-based Energy Power Plants, e.g., Talen Energy in PA [62] |
| Fluxing Agent NaOH | $120-300/ton | Maxi-Salt [68], Zimmerman Co. [69], Rock Salt USA [70] |
| Water | $10-24/1000 cf. *(Industrial Price)* | Pennsylvania Public Utility Commission [71], Philadelphia Water Department [72], Pittsburgh Water & Sewer Authority [73] |

### 4.2.2. Testing & Equipment

#### 4.2.2.1. Primary CCA and FLWA Assessment

A preliminary property assessment of the CCA intended for use is critical for the successful manufacturing of CCA-FLWA. Understanding the moisture content, elemental composition, chemical oxides, particle size range, and loss on ignition are all necessary parameters when using different CCA sources. The material characterization assessment provides essential information for modeling CCA-FLWA. The CCA-FLWA modeling requires material characterization information to input material chemical details and identify preliminary mixing proportions and

equipment configuration parameters. Once the design parameters are finalized a CCA-FLWA property assessment is necessary to validate their performance in concrete applications. Tests necessary for CCA-FLWA property assessment include ASTM specifications.

### 4.2.3. Market Assessment

In terms of the concrete industry, the demand for FLWA usage is increasing as the construction of lightweight concrete structures as well as internally cured concrete is growing. Currently, the availability of FLWA is limited to (1) natural LWA sources whose availability is limited, and (2) synthetic LWAs from Expanded Shale, Clay, and Slate (ESCS) FLWAs that use natural resources for LWA productions. Market alternatives are mainly FLWA manufacturers which are members of the ESCS institute. The development of CCA-FLWA offers a solution to the depletion of natural resources such as shale, clay, and slate by utilizing waste solid streams like CCA. The manufactured CCA-FLWA exhibits superior porosity, water absorption, and water desorption behavior in comparison with currently available FLWAs, providing a sustainable and high-performance alternative for construction applications. The developed CCA-FLWA has water absorption of ~25%, which is almost 2-2.5 times of water absorption of available FLWAs [60]. CCA-FLWA also has 25-40% higher water desorption, almost 3-4 times higher than traditional FLWAs. The performance capability of CCA-FLWA will directly affect the final quality used in lightweight concrete [60]. The spherical shape of the manufactured CCA-FLWA can also improve the workability of concrete by up to 15% in comparison to the natural shape FLWA available in the market [60].

The net cost analysis for the potential future commercialization of CCA-FLWA is reported in ***Table 14***. Comparison between net costs associated with traditional synthetic FLWA and the manufactured CCA-FLWA reveals that the expected net cost of our CCA-FLWA is comparable

to or even lower than traditional synthetic ESCS FLWA. In this calculation, the production cost of FLWA was assumed to be the sum of costs associated with raw materials feedstock, crushing/screening before sintering, processing (i.e., sintering), fluxing agent, and crushing after sintering. At this stage, the costs associated with capital costs and transportation were assumed to be similar and accordingly were not considered in the calculation for both traditional FLWA and manufactured CCA-FLWA. Key considerations include processing (sintering) costs for both traditional and CCA-FLWA production and selling price margins. Estimated processing (sintering) costs were found for cement-based industries which use a sintering temperature ranging between 1700-1800ºC, while both traditional and CCA-FLWA sintering temperatures range between 1000-1200ºC. This implies that processing (sintering) costs may be lower, increasing selling margins further. Both traditional and CCA-FLWA result in relatively similar net costs. If sold at the same prices, they would generate approximately 60% margins. This margin is considered adequate for covering capital cost payback, daily operational expenses (excluding sintering), and profit.

**Table 14.** Net cost analysis of producing LWA from CCA compared with traditional LWA (e.g., ESCS LWA); capital and shipment costs were not considered in the calculation.

| **Processes** | **Traditional FLWA ($/ton)** | **CCA-FLWA ($/ton)** |
|---|---|---|
| Feedstock (including mining) | 9 to 14 | 0 to 5 |
| Raw material (plant transport) | Negligible | Negligible |
| Crushing/screening | Negligible | Negligible |
| Processing (sintering) | 19 | 19 |
| Fluxing agents | 0 | 3-5 |
| Crushing | Negligible | Negligible |
| **Net cost (Sum)** | **28 to 33** | **22 to 29** |
| Approximate selling price | 100 to 130 | - |

*Data presented here is approximate and is based on values presented by Nguyen et al. [74], American Coal Ash Association [75,76], and the traditional LWA approximate selling price of around 100-130 $/ton [77–79].

### 4.2.4. Production line

The industrial product of CCA-FLWA involves an uninterrupted sequential manufacturing flow (***Figure 64***) after material characterization, modeling, testing, and specimen property evaluation are verified. As received landfill condition waste CCA is acquired from energy plant impoundments. Raw materials are mixed using a drum mixer and the CCA paste is transported to an industrial-size pelletizer that converts CCA paste to green CCA pellets. Green CCA pellets are then transported to a feeder which discharges a specified feed rate onto a conveyor belt that gradually delivers the CCA pellets to the rotary furnace. After green CCA pellets pass through the rotary furnace and are efficiently sintered they are then collected, packed, and stowed for industrial utilization. It is important to note that the traditional FLWA production line follows a relatively similar sequence of production. After site excavation and transport, the raw material is fed into a mechanical crusher. The crushed raw material is then transferred into a feeder that discharges a specified feed rate onto a conveyor belt that gradually delivers the CCA pellets to the rotary furnace. Sintering traditional FLWA results in large aggregates which require further crushing to achieve appropriate ASTM C330 gradation for concrete applications. After crushing, the traditional FLWA are packed and stowed for industrial utilization.

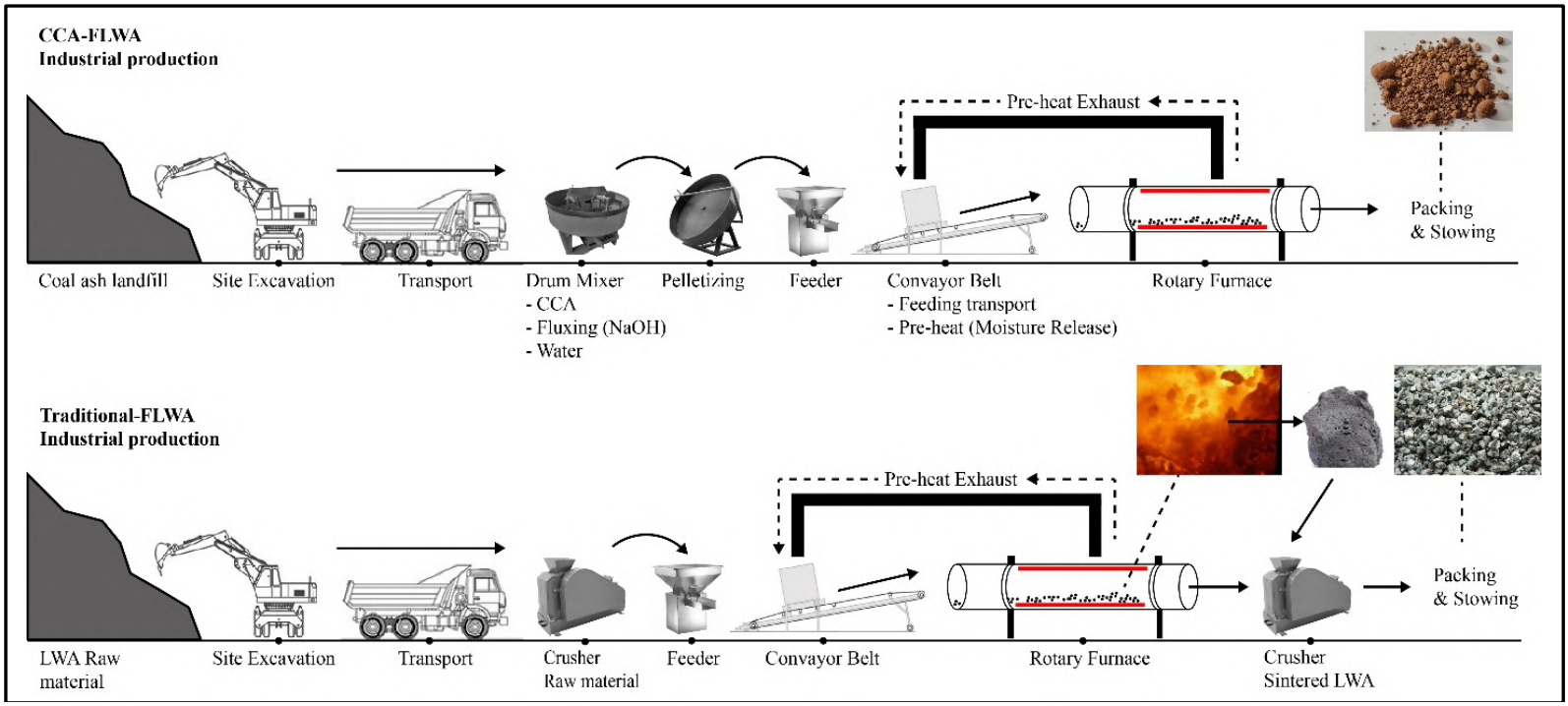


**Figure 64.** Industrial CCA-FLWA production flow

### 4.2.5. Manufacturing Equipment (Capital cost)

The equipment necessary for CCA-FLWA production follows the primary machinery proposed in the production sequence flow previously recommended (***Figure 64***). The machinery purchased or rented will impact cost-effectiveness for short- or long-term production. Rates for machinery suggested are an average based on availability within the Pennsylvania region. The major capital costs will cover an industrial mixer, pelletizer, conveyor belt, and rotary furnace (**Table *15***). Further machinery may be considered according to the desired industrial flow of production. The total capital cost for CCA-FLWA amounts to approximately $1,400,000, excluding shipping and installation expenses. Notably, the machinery cost for implementation is primarily dictated by the rotary furnace, which is utilized for both traditional and CCA-FLWA production. However, it is important to highlight that CCA-FLWA production necessitates a drum mixer and pelletizer within its production sequence, whereas traditional FLWA production does not require these machines. Instead, traditional FLWA production relies on two mechanical crushers, each with a purchasing

cost ranging from $100,000 to $200,000 per crusher (Specs: Jaw Crusher, 1100x650, 400 ton/h) [80]. This indicates that the CCA-FLWA production line does not impose significant additional financial burdens for additional or advanced required equipment. With a similar industrial operation sequence, it is implementable and expected to achieve a comparable success rate to existing LWA production plants within the USA.

**Table 15.** The capital cost of core machinery for preliminary industrial production flow for CCA-FLWA manufacturing.

| **Machinery** *(Industrial scale)* | **Specifications** | **Cost** |
|---|---|---|
| Mixer | Capacity 65 $yd^3$/hr.<br>Capacity 50-75 $yd^3$/hr.<br>Capacity 35-55 $yd^3$/hr. | $100,000-200,000 |
| Pelletizer | Diameter 10-15 ft<br>Sidewall 2-3 ft<br>Thickness 1-2 in | $50,000-100,000 |
| Conveyor Belt | Length 20-60 ft<br>Width 3-9 ft | $2000-8000 |
| Rotary furnace | Length 15-25 ft<br>Diameter 3-6 ft<br>Angle 0-7º | $500,000-1,000,000 |

*The data presented are based on quotations collected from various industrial companies and are priced according to machinery specifications [81–90].

### 4.3. Practical Applications *(Practice Implementation)*

#### 4.3.1. CCA-FLWA Design Considerations

This research investigates the utilization of CCA to manufacture FLWA used for internal curing of concrete. The design criteria adopted for the implementation of this technology consider conventional saturation techniques of immersing aggregates in water for 24 hr. to achieve saturated surface dry (SSD) conditions before concrete mixing. Centrifugal surface drying technique is adopted to achieve aggregate SSD conditions. The concrete mix design considered for verifying the internal curing of concrete using CCA-FLWA was performed according to the Pennsylvania Department of Transportation section 704 concrete bridge deck criteria. The design criteria

consider w/c 0.42, min f'c 5000 psi, slump 6 ±1 in, and air content 7 ±1%. The concrete mix design involved the addition of two admixtures: an air-entrainer and a water-reducing admixture. The performance of the proposed technology can be influenced by the saturation duration, SSD technique, concrete mix design criteria (w/c, min f'c, slump, air content), and additive dosage. To assess the internal curing of concrete using CCA-FLWA, sample batches are recommended for performance verification.

### 4.3.2. Case Study

Internal curing technology has found widespread use in various concrete blends across diverse applications, including bridge decks, pavements, transit yards, and water tanks. Field experiences have consistently shown improvements in concrete performance attributed to the incorporation of internal curing applications. The New York Department of Transportation (NYDOT) has successfully implemented internal curing in numerous bridge construction projects. In one field-cast project, the execution and performance of internal curing sites were evaluated to assess field implementation. The study utilized 200 pounds of expanded shale and clay lightweight aggregate sourced locally, possessing an absorption capacity of 15%. A pre-wetting technique involving sprinklers on the stockpile was adopted, ensuring 48 hours of saturation duration. Saturation surface dry (SSD) conditions were achieved following method NY 703-19E, employing 3×6 feet dry brown paper towel drying. Concrete mixing was carried out using a normal concrete mixer, and the concrete was pumped onto the deck. Although no significant differences in pump-ability or finish-ability were observed, the contractor noted that mixes with internal curing were less sticky than traditional mixes. Air content testing was conducted using a pressure meter. Initial concerns regarding flow difficulty were anticipated; however, no such issues were encountered during casting. The structures were subjected to various climates, traffic loadings, and exposure to

de-icing chemicals. This underscores the fact that the use of pre-wetted lightweight aggregate (LWA) for internal curing does not necessitate advanced machinery or testing equipment for delivery in field applications.

Concrete mix design was executed with a water-to-cement (w/c) ratio of 0.4, for two mix designs including and excluding internal curing agents (pre-saturated LWA) (**Table *16***). For concrete without internal curing, the addition of a water reducer agent was necessary. Performance evaluation conducted after 56 days of curing revealed that both types of concrete yielded relatively similar compressive strength of approximately 5900 pounds psi. It was further observed that concrete without internal curing had a density of 137.8 pcf, whereas concrete with internal curing exhibited a slightly lower density of 133 pcf. Discussions with the NYDOT indicated no visible drawbacks associated with internal curing on tested bridges. Evaluations of three internally cured decks after 1 to 3 years revealed minimal issues, with only a very small crack observed in the negative moment region of one internally cured bridge. In contrast, parapet walls and sides constructed with concrete lacking internal curing exhibited several larger cracks. Despite anticipated wear, the decks are performing satisfactorily, and the NYDOT permitted the use of these concretes for pumping without reported problems.

**Table 16.** Concrete mix design and performance evaluation of high-performance (HP) concrete with and without internal curing (IC) application inclusion.

| | Class HP | Class HP-IC |
|---|---|---|
| Cement – Blended with 7% Silica Fume | 538 lbs. | 548 lbs. |
| Fly Ash – Type F | 137 lbs. | 125 lbs. |
| Fine Aggregate – Natural Sand | 1187 lbs. | 810 lbs. |
| Fine Aggregate – LWAF 22.2% moisture | 0 lbs. | 250 lbs. |
| Coarse Aggregate – No. 1 Stone | 862 lbs. | 870 lbs. |
| Coarse Aggregate – No. 2 Stone | 849 lbs. | 840 lbs. |
| Water | 270 lbs. | 270 lbs. |
| Air Entrainment – BASF MB-VR Standard | 18.2 oz | 17.5 oz |
| Retarder – BASF Pozzo-Lith 100 XR | 13.5 oz | 34.0 oz |
| Water Reducer – BASF Poly-heed 997 | 20.2 oz | - |
| Average 7-day Compressive Strength | 3,720 psi | 3,335 psi |
| Average 28-day Compressive Strength | 5,040 psi | 5,273 psi |
| Average 56-day Compressive Strength | 5,900 psi | 5,853 psi |
| Concrete Density | 137.8 pcf | 133.0 pcf |
| Air Content | 5.7% | 7.2% |
| Slump | 3.5” | 4.5” |

### 4.3.3. Comparative Analysis

Following the assessment of both the laboratory delivery process of CCA-FLWA and the case study involving the NY bridge deck, a comparative analysis assessed the viability of practical implementation for CCA-FLWA. Evaluating design considerations, execution, and performance assessment revealed that CCA-FLWA used in concrete achieved optimal saturation for internal curing within 24 hours of complete submersion in water. The NY case study achieved aggregate pre-wetting by direct sprinkling on the stockpile after 48 hr. While this is a viable pre-wetting technique for CCA-FLWA, further assessment is needed to determine the duration required to achieve optimum saturation levels. The method of achieving SSD conditions, as per method NY 703-19E (dry brown paper towel drying), is acceptable for LWA and can be effectively utilized for CCA-FLWA. CCA-FLWA possessed a compressive strength of 47.5 kN, indicating sufficient structural resistance for on-site delivery via concrete pumping [91]. The mix design for CCA-FLWA concrete incorporates admixtures within the supplier dosage range and was consistent with

the admixtures used in the NY case study mix design. The employing of pre-saturated LWA in the NY case study did not necessitate additional machinery beyond the traditional delivery method also employed in laboratory execution for CCA-FLWA concrete. Evaluation of fresh and hardened properties for the NY case study demonstrated similarities to CCA-FLWA concrete. The site analysis revealed that a mixed design with a w/c ratio of 0.4, slump of 4.6 ±1 inch, and air content of 7.2 ±1%, achieved a density of 133 pcf and compressive strength of 5,853 psi after 56 days of curing. Comparatively, CCA-FLWA concrete with a w/c ratio of 0.42, a slump of 6 ±1 inch, and air content of 7 ±1%, achieved a concrete density of 125 pcf, and a compressive strength of 5,562 psi after 56 days of curing. These findings suggest that the mixed design, delivery approach, and performance for CCA-FLWA concrete are comparable to those of the NY bridge deck internally cured concrete, indicating its feasibility for practical implementation.

## 4.4. Feasibility study, Risk Assessment, & Mitigation Plan Recommendations

### 4.4.1. Accessibility & Market Demand

The accessibility of construction FLWA is becoming increasingly challenging for concrete industries in the US due to difficulties in [92] accessibility in different regions, [93] increasing market demands, and [94] shipment costs due to the distance from the quarry to the site. Synthetic LWA is a growing industry, and its market alone is a $5+ billion industry per year in the US [95]. This study proposes to produce CCA-FLWA from waste coal combustion ash (CCA) that is abundantly available in many regions in the US. This will increase the accessibility of FLWA in various US states, it will also increase the availability of FLWA in the market, impacting prices along with shipping cost reduction for large suppliers. The produced FLWA can be used as a fine aggregate substitution for the internal curing of concrete. The industries that will benefit from this technology are electric power (to manage coal ash), aggregate, and concrete industries.

Fundamental customers include large-size ready-mixed and precast concrete producers with more than 100 cubic yards of concrete production per day (a $50+ million/year market size for our FLWA only in PA) [95].

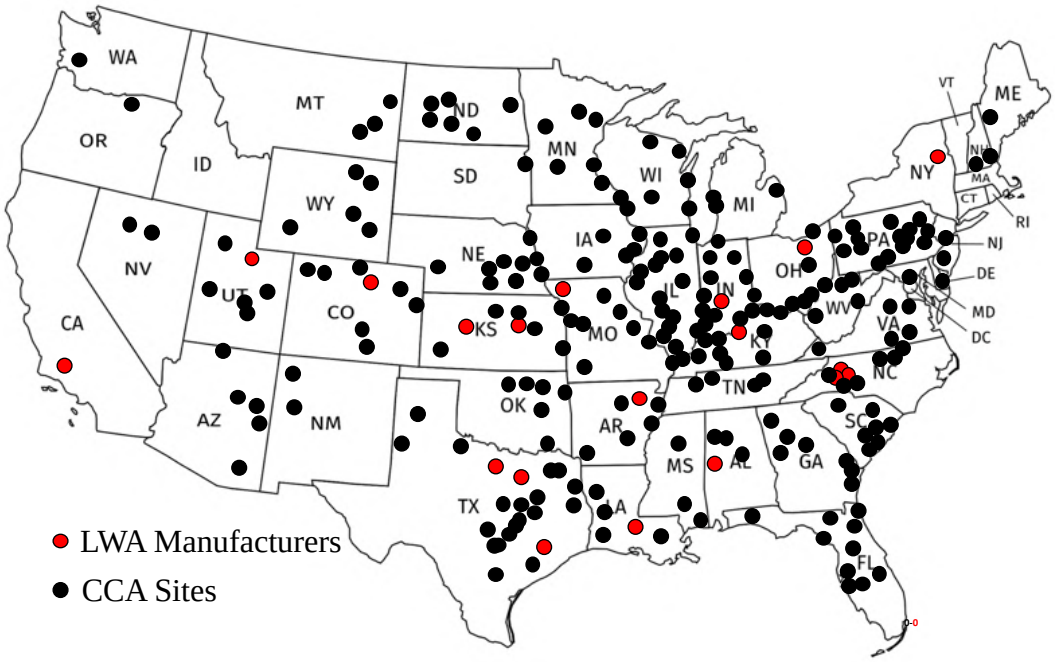


**Figure 65.** Distribution of LWA manufacturers and CCA sites in the United States [96].

Unfortunately, FLWA manufacturers are available in a few locations in the US due to their dependency on suitable natural materials (***Figure 65***). For example, ready-mixed concrete producers in Pennsylvania (PA) and New Jersey (NJ) are required to import FLWA from upstate New York (NY) or North Carolina (NC) spending extra for shipment costs [95]. Therefore, effectively converting CCA into FLWA at CCA sites in the US will provide further access and lower costs, distinctly decreasing shipping costs and prices. Establishing a CCA-FLWA manufacturing plant near Philadelphia can be beneficial for ready-mixed and precast concrete producers in PA and NJ. As illustrated in ***Figure 65***, like PA and NJ, the technology has opportunities to be applied to other states such as MN, ND, SD, NE, NV, NM, FL, AZ, GA, VA, WY, and IL which have ample supply of CCA to manufacture FLWA for ready-mixed and precast

concrete producers that do not currently have close access to FLWA manufacturers. Initiating manufacturing plants for CCA-FLWA in these states will provide lower prices by eliminating shipping costs and addressing this stream of waste through a circular economy approach.

### 4.4.2. Value Proposition

Three major value propositions make CCA-FLWA a superior selling candidate than traditional FLWA: (1) CCA-FLWA is a green product since it uses waste CCA and accordingly customers may potentially receive ~ $2-5/ton tax remission from the government [97,98]; (2) since waste CCA is available in most locations/states in the US, CCA-FLWA can be produced in closer proximity to customer markets, saving customers ~ $90-120/ton on shipping cost which is nearly 70-90% of FLWA original price; and (3) through task 1 and 2, it was demonstrated that CCA-FLWA has superior properties, such as 100-150% increase in water absorption capacity and 200-350% increase in water desorption capacity, in comparison with traditional FLWAs available in the market. The proximity and localization of manufacturing can provide a commercial opportunity for supplying competitive CCA-FLWA locally. In the Pennsylvania region, there are currently 8 active coal ash landfills and 13 active surface impoundments, or ash ponds, housing millions of tons of unrecycled CCA [99,100]. This significant reservoir of CCA indicates that there is ample feedstock available to support the establishment of a CCA-FLWA industrial plant in the area. Furthermore, it was also verified that CCA-FLWA possessed superior properties when used in concrete. Pre-wetted CCA-FLWA used in concrete demonstrated higher compressive strength, comparable flexural strength, lower shrinkage and rate of absorption, higher freeze-thaw durability, and lower to no leaching of constituents of potential concern (COPC) [60].

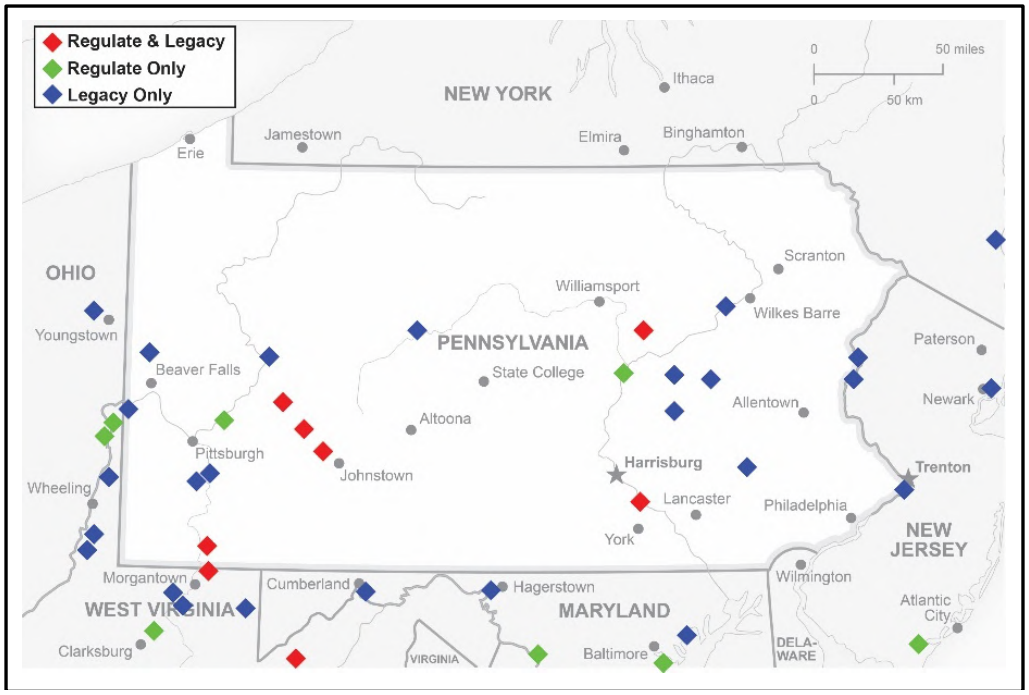


**Figure 66.** Locations of CCA landfill across the PA region [99,100].

### 4.4.3. Capital cost *(Produce/Sell in PA)*

The capital cost of the proposed machinery needed for CCA-FLWA production aligns with existing LWA manufacturers. The machinery proposed does not extend beyond the traditional industrial LWA manufacturing equipment. This implies that the capital cost for CCA-FLWA manufacturing does not impose significant economic burdens on the industrial framework of aggregate production. Unlike LWA companies that require excavating or milling raw material which may add costs, the proposed processes utilize waste feedstock available on-site reducing both extracting and transporting costs. The proposed machinery is suggested to be transportable (mobile) for relocation purposes once the CCA landfill site is fully used. This could reduce both transportation costs and preliminary costs once relocation is necessary.

### 4.4.4. Technical Challenges

The use of waste CCA to produce LWA has unfortunately suffered major challenges to several factors based on their sources/sites due to variations in their physical conditions as well as their

chemical composition [101]. CCA may be wet, dry, ponded, or landfilled in their sites, may contain different chemical compounds (different calcium oxide/silica/alumina contents (Class C or Class F) and percentage of amorphous phase), or may be impacted by the process and types of coals (such as by activated carbon sorbents, by sodium- and calcium-based sorbents, or by heavy metals) [14]. All these factors/variations may complicate the production of CCA-FLWA and need holistic technology for the successful industrialization of FLWA production from CCA. Otherwise, the production of FLWA will not be effective and efficient in consuming a large portion of waste CCA [102,103]. The technology and flow of production presented in the Task 1 report are based on a thermodynamic methodology that can target a wide range of CCA with various physical conditions and chemical compositions. Previous studies performed by the research group verified that the proposed sequence of modeling and production was successful for various types of coal ash including two types of bottom CCA: low calcium and high calcium, two types of fly ash: class F (low calcium) and class C (high calcium), and as received landfill condition CCA. The research group studies were able to validate that with a partial sintering process, the oxide compounds of CCA can be partially melted and subsequently combust the residual carbon to create a successful porous ceramic, FLWA [6,7,9–13]. The major technological hurdles that need to be addressed to develop a market-driven large-scale technology to produce FLWA from CCA are related to its chemical/physical composition. The chemical compositions and physical conditions of several power plants in the US were studied [104–107]. These investigations concluded variations in four main parameters in CCA: oxide contents, moisture, particle size, and lack of sufficient amount of glass content. These parameters accordingly need to be studied and validated on a large scale using the thermodynamic methodology proposed, and if needed alternative solutions such as using a

proper fluxing agent, changing the kiln temperature or duration, and using a CCA blend should be provided to further develop and confirm successful CCA-FLWA production.

#### 4.4.4.1. Appropriate CCA

Finding CCA samples from appropriate CCA sites in the US with desired properties is critical for successful CCA-FLWA production. It is recommended that CCA acquired from local power stations is utilized, due to preliminary validation of successful CCA-FLWA production. Most power stations host multiple basins with millions of tons of CCA. This access to appropriate feedstock will ensure a considerable supply of raw materials for industrial-scale CCA-FLWA production.

#### 4.4.4.2. Modeling and Design Configuration

Some challenges associated with modeling and design configurations are (1) reaching the sintering temperature lower than 1200°C, since kilns with a temperature above will be very costly and energy-consuming, (2) reaching the slag and viscosity needed for successful LWA production (a minimum requirement in design considerations – task 1), and (3) reaching a total LWA production cost less than 33 $/ton to be able to compete our competitors (attributed to costs of feedstock, energy consumed, and fluxing agent dosage required to achieve necessary CCA-FLWA properties). Various types of fluxing agents can be alternatively used to lower the risks; however, this requires prior validation testing to ensure a delicate balance between CCA-FLWA performance and overall costs is achieved.

#### 4.4.4.3. CCA-FLWA Verified Performance

Achieving the desired engineering properties of CCA-FLWA is necessary for successful implementation and use in concrete for internal curing purposes. This step requires refinement tuning of material proportioning, fluxing agent dosage, sintering duration, and particle size. These

parameters can directly affect the strength and engineering properties needed. Verified performance checks are required for two stages subsequently, following CCA-FLWA production and succeeding concrete implementation.

#### 4.4.4.4. Industrial Scale-Up

Associated challenges in successfully scaling up the technology to an industrial scale are achieving a successful flow of production and comparable CCA-FLWA results to the pilot scale study. Technical challenges in scale-up include physicochemical property variation, heat/mass transfer issues, and reproducibility. To mitigate the scale-up risk it is recommended to verify the proposed technology at sample production quantity and perform a quality assessment after batch production. This can be performed by working with industrial manufacturers with similar production lines that are compatible with the proposed technologies' manufacturing process.

### 4.5. Summary of Task 3

The study conducted a comprehensive cost analysis and feasibility assessment of implementing CCA-FLWA with a thorough comparison with traditional FLWA plants. The practical implementation study underscored the importance of understanding the innovative technological framework, alongside licensing considerations. Three critical elements were examined: ensuring CCA security, determining facility requirements, and identifying necessary personnel for planned CCA-FLWA implementation. The cost analysis and market opportunity study evaluated the pricing of core materials associated with CCA-FLWA production. The market assessment revealed that the overall net cost of traditional FLWA was comparable to that of CCA-FLWA. Assigning the selling price for CCA-FLWA equivalent to traditional FLWA would yield a theoretical 60% margin, sufficient to cover capital costs, daily operations, and generate profit. A comparison of production line costs between CCA-FLWA and traditional FLWA showed relatively similar

capital expenditures, with rotary furnaces being the primary cost determinant. Importantly, no advanced or expensive machinery was required, alleviating potential capital cost burdens. This suggests that there are no significant financial burdens or risks, with normal operation indicating implement ability, with similar success rates as current LWA companies. A case study conducted by NYSDOT demonstrated that the practical implementation of pre-wetted LWA as an internal curing agent did not require additional considerations or advanced machinery beyond standard field operations. The proposed CCA-FLWA was found to need similar machinery as the case study, imposing no risk. The feasibility study, risk assessment, and mitigation plan highlighted a growing market demand for LWA. This prior analysis indicated the potential successful establishment of a CCA-FLWA Plant in the PA region. Risk assessment through an R&D sector within the company could replicate the technological approach for CCA-FLWA production post-licensing. Initiating a CCA-FLWA plant in regions with abundant CCA landfills and no CCA-FLWA plants would present a value proposition by offering a closer supply to the area, thereby reducing shipping costs and a longer-term solution to this stream of waste material. In addition, it would yield a product with superior properties while repurposing waste material with negative environmental impacts to manufacture a valuable green product for industrial applications.

## 5. Conclusions and Recommendations

This study evaluated the potential utilization of waste coal combustion ash (CCA) to manufacture fine lightweight aggregate (FLWA), hereafter referred to CCA-FLWA, suitable for internal curing concrete. Waste CCA was obtained from a landfill in the state of Pennsylvania. The utilized CCA for this study consisted of higher concentrations of fly ash along with bottom ash and field debris. Thermodynamic modeling revealed that a minimum of 35% liquid phase and 100 kPa were necessary to achieve sufficient liquid phase during sintering to manufacture desired CCA-FLWA.

The loss on ignition (LOI) of 8% in CCA was also found sufficient for producing enough gas to achieve the required FLWA porosity appropriate for internal curing. To produce CCA-FLWA, 2% sodium hydroxide (NaOH) was found to achieve the required mechanical properties of FLWA intended for concrete applications. The manufactured CCA-FLWA were characterized according to ASTM and European standards, where they possessed an appropriate pore structure with various pore morphology facilitating superior absorption and desorption capabilities, and sufficient mechanical properties for concrete applications. To evaluate internal curing performance of CCA-FLWA, three factors were assessed: (1) how much water can be stored in CCA-FLWA, this is mainly influenced by the LWA absorption and storage capability; (2) how water can be desorbed from CCA-FLWA to the surrounding environment, this depends on the CCA-FLWA desorption capability; and (3) how CCA-FLWAs are spatially distributed within the concrete matrix, this depends on the particle size distribution and volume of the CCA-FLWA in concrete matrix. The manufactured CCA-FLWA in this study demonstrated promising internal curing performance meeting all three factors in accordance with ASTM. They were able to absorb and retain enough water (more than 5% by mass defined by ASTM). They showed adequate desorption capabilities to release water into its surroundings (more than 85% moisture released at 94% RH per initial 24 h moisture absorption). FLWA also met the ASTM gradation for FLWA.

The internal curing performance of CCA-FLWA was also evaluated using concrete samples made with pre-wetted CCA-FLWA and they were compared with concrete samples made with Commercial-FLWA and normal-weight aggregates. The concrete made with CCA-FLWA showed desirable fresh concrete properties (i.e., slump, air content and fresh density) when compared to commercial-FLWA and normal-weight concrete. Additionally, mechanical strength evaluations were performed. Concrete made using CCA-FLWA revealed a comparable gained strength at early

curing age relative to concretes made with Commercial-FLWA and normal-weight aggregates. As curing progressed, CCA-FLWA concrete gained comparatively higher compressive strength to both Commercial-FLWA and normal-weight aggregates. This was attributed to superior internal curing performance of CCA-FLWA providing efficient internal hydration. Furthermore, flexural strength was also measured where it was observed in early curing age, the concrete made with normal-weight aggregate had slightly high flexural strength. However, as the curing age progressed, both CCA-FLWA and Commercial-FLWA concrete gained similar strength to normal-weight aggregate concrete. It can be concluded that internal curing requires proper curing time to meet strength of normal-weight concrete.

Concrete shrinkage evaluation was conducted, and it was found that CCA-FLWA concrete experienced lower strain in comparison to both commercial-FLWA and normal-weight concrete as curing progressed. This was attributed to internal curing through the increase in the degree of hydration where both chemical and drying shrinkage can be alleviated. The rate of absorption of concrete was evaluated. It was revealed that concrete made using CCA-FLWA experienced a lower absorption rate when exposed to water at various curing ages. This was attributed to a decrease in capillary pores due to further internal curing. The reduction in capillary pores reduces capillary suction and therefore reduces the concrete absorption rate.

Freeze-thaw evaluation concluded that concrete made using CCA-FLWA possesses enhanced freeze-thaw durability as opposed to Commercial-FLWA and normal-weight concretes. Examined concrete samples with varying degrees of saturation (DOS) indicated that CCA-FLWA concrete exhibited lower acoustic fracture energy and dynamic elastic modulus damage index after three freeze-thaw cycles as opposed to Commercial-FLWA and normal-weight concretes. The concrete samples DOS and rate of absorption were correlated with the damage index to identify the time it

takes for concrete samples to reach critical DOS where freeze-thaw damage initiates in concrete. It was revealed that normal-weight concrete would experience freeze-thaw damage way early in its service-life if exposed to moisture and freeze-thaw cycles. Both Commercial-FLWA and CCA-FLWA concrete showed promising freeze-thaw damage where concrete made with CCA-FLWA showed a superior behavior among all concrete types tested here. The extended duration to experience freeze-thaw damage demonstrates the ability of CCA-FLWA concrete to withstand freeze-thaw damage under severe water exposure conditions in comparison to Commercial-FLWA and normal-weight concrete. To evaluate the leaching potential of heavy metals from concrete made using CCA-FLWA, the leaching test was performed in accordance with the EPA LEAF method. It was found that CCA-FLWA revealed a low risk of leachability comparable with concrete made using normal-weight natural aggregates.

Finally, this study performed a feasibility and cost analysis of CCA-FLWA and found that the overall net cost of traditional FLWA was comparable to that of CCA-FLWA. Assigning the selling price for CCA-FLWA equivalent to traditional FLWA would yield sufficient theoretical margin to cover capital costs, daily operations, and generate profit. A comparison of production line costs between CCA-FLWA and traditional FLWA showed relatively similar capital expenditures, with rotary furnaces being the primary cost determinant. Importantly, no advanced machinery was required. This suggests similar financial strain, operational dynamics, and success rates as current LWA manufacturing companies, indicating the feasibility of the production of CCA-FLWA at industrial scale. The practical implementation study also revealed that the CCA-FLWA as an internal curing agent does not require additional considerations or advanced machinery beyond standard field operations used in the concrete industry. The feasibility study, risk assessment, and mitigation plan highlighted a growing market demand for FLWA. Initiating a CCA-FLWA plant

in regions with abundant CCA landfills and no accessibility to FLWA plants would present a value proposition by offering a closer supply to the area, thereby reducing shipping costs and a longer-term solution to this stream of waste material. In addition, it would offer a product with superior performance properties while repurposing waste material with negative environmental impacts to manufacture a valuable green product for industrial applications.

Overall, this study concludes that the conversion of CCA into FLWA for internal curing of concrete not only results in concrete with promising fresh and hardened concrete properties, but also is economical and implementable. While this study was performed in laboratory scale samples, future research may focus on evaluating the internal curing performance of CCA-FLWA in a scale-up work.

## 6. References


[1] EIA, Electric Power Annual, Eia.Doe.Gov 0348 (2010) 2. http://www.eia.doe.gov/ask/electricity_faqs.asp#efficiency.

[2] A. Deonarine, A. Kolker, M. Doughten, Trace Elements in Coal Ash, Usgs (2015) 1–6.

[3] C.W. TEPHEN K. RITTER, A new Life for Coal Ash, (n.d.) 10–14. https://ncejn.org/coal-ash/.

[4] Thomas H. Adams, Coal Ash Recycling Rate Increases Slightly in 2021; Use of Harvested Ash Grows Significantly , (2022).

[5] EarthJustice, Poisonous Coverup The Widespread Failure of the Power Industry to Clean Up Coal Ash Dumps, (2022). https://earthjustice.org/.

[6] Mohammad Balapour, Characterizing physical properties of lightweight aggregate made from waste coal ash using X-ray computed tomography, 2019.

[7] M. Balapour, R. Rao, S. Spatari, G. Hsuan, Y. Farnam, Engineering properties of fly ash-based lightweight aggregate, World Coal Ash (2019) 1–17.

[8] M. Balapour, T. Thway, N. Moser, E.J. Garboczi, Y. Grace Hsuan, Y. Farnam, Engineering properties and pore structure of lightweight aggregates produced from off-spec fly ash, Constr. Build. Mater. 348 (2022) 128645. https://doi.org/10.1016/j.conbuildmat.2022.128645.

[9] M. Balapour, M.H. Khaneghahi, E.J. Garboczi, Y.G. Hsuan, D.E. Hun, Y. Farnam, Off-

spec fly ash-based lightweight aggregate properties and their influence on the fresh, mechanical, and hydration properties of lightweight concrete: A comparative study, Constr. Build. Mater. 342 (2022) 128013. https://doi.org/10.1016/j.conbuildmat.2022.128013.

[10] M. Balapour, R. Rao, E.J. Garboczi, S. Spatari, Y.G. Hsuan, P. Billen, Y. Farnam, Thermochemical principles of the production of lightweight aggregates from waste coal bottom ash, J. Am. Ceram. Soc. 104 (2021) 613–634. https://doi.org/10.1111/jace.17458.

[11] M. Balapour, T. Thway, R. Rao, N. Moser, E.J. Garboczi, Y.G. Hsuan, Y. Farnam, A thermodynamics-guided framework to design lightweight aggregate from waste coal combustion fly ash, Resour. Conserv. Recycl. 178 (2022). https://doi.org/10.1016/j.resconrec.2021.106050.

[12] K.J. O'hare, G. Pizzulli, M. Torelli, M. Balapour, Y. Farnam, Y.G. Hsuan, P. Billen, S. Spatari, Life Cycle Assessment of Lightweight Aggregates from Coal Ashes: A Cradle-to-Gate Analysis, n.d.

[13] M. Balapour, W. Zhao, E.J. Garboczi, N.Y. Oo, S. Spatari, Y.G. Hsuan, P. Billen, Y. Farnam, Potential use of lightweight aggregate (LWA) produced from bottom coal ash for internal curing of concrete systems, Cem. Concr. Compos. 105 (2020) 103428. https://doi.org/10.1016/j.cemconcomp.2019.103428.

[14] S. Karimi, E. Jorjani, S. Chehreh Chelgani, S. Mesroghli, Multivariable Regression and Adaptive Neurofuzzy Inference System Predictions of Ash Fusion Temperatures Using Ash Chemical Composition of US Coals, J. Fuels 2014 (2014) 1–11. https://doi.org/10.1155/2014/392698.

[15] G.L. Fisher, B.A. Prentice, D. Silberman, J.M. Ondov1, A.H. Biermann1, R.C. Ragaini1, A.R. Mcfarland2, Physical and Morphological Studies of Size-Classified Coal Fly Ash, 1978. https://pubs.acs.org/sharingguidelines.

[16] J. Kamal, U.K. Mishra, Influence of Fly Ash Properties on Characteristics of Manufactured Angular Fly Ash Aggregates, J. Inst. Eng. Ser. A 101 (2020) 735–742. https://doi.org/10.1007/s40030-020-00461-5.

[17] L. Xiong, Z. Wan, Y. Zhang, F. Wang, J. Wang, Y. Kang, Fly ash particle size effect on pore structure and strength of fly ash foamed geopolymer, Adv. Polym. Technol. 2019 (2019). https://doi.org/10.1155/2019/1098027.

[18] D.P. Bentz, W.J. Weiss, Internal Curing : A 2010 State-of-the- Art Review, Civ. Eng. (2011).

[19] J. Castro, L. Keiser, M. Golias, J. Weiss, Absorption and desorption properties of fine lightweight aggregate for application to internally cured concrete mixtures, Cem. Concr. Compos. 33 (2011) 1001–1008. https://doi.org/10.1016/j.cemconcomp.2011.07.006.

[20] B. Akcay, M.A. Tasdemir, Effects of distribution of lightweight aggregates on internal curing of concrete, Cem. Concr. Compos. 32 (2010) 611–616. https://doi.org/10.1016/j.cemconcomp.2010.07.003.

[21] S. Zhutovsky, K. Kovler, A. Bentur, Efficiency of lightweight aggregates for internal curing of high strength concrete to eliminate autogenous shrinkage, Mater. Struct. Constr. 34

(2002) 97–101. https://doi.org/10.1007/bf02482108.

[22] B.R. Henkensiefken, J. Castro, H. Kim, D. Bentz, J. Weiss, C * Cs * A M, (2009).

[23] D. Cusson, T. Hoogeveen, Internal curing of high-performance concrete with pre-soaked fine lightweight aggregate for prevention of autogenous shrinkage cracking, Cem. Concr. Res. 38 (2008) 757–765. https://doi.org/10.1016/j.cemconres.2008.02.001.

[24] ASTM Committee C09.21, ASTM C1761-15 Standard Specification for Lightweight Aggregate for Internal Curing of Concrete, Annu. B. ASTM Stand. Vol. 04.02 (2015) 1–8. https://doi.org/10.1520/C1761.

[25] A. Paul, S. Murgadas, J. Delpiano, P.A. Moreno-Casas, M. Walczak, M. Lopez, The role of moisture transport mechanisms on the performance of lightweight aggregates in internal curing, Constr. Build. Mater. 268 (2021) 121191. https://doi.org/10.1016/j.conbuildmat.2020.121191.

[26] C. for R. in C. Thermochemistry, FactSage, (200AD). www.factsage.com%09%0A.

[27] G.J. Browning, G.W. Bryant, H.J. Hurst, J.A. Lucas, T.F. Wall, An empirical method for the prediction of coal ash slag viscosity, Energy and Fuels 17 (2003) 731–737. https://doi.org/10.1021/ef020165o.

[28] G. Urbain, Viscosity estimation of slags, Steel Res 58, 111–116. 58 (1987) 111–116.

[29] D.P. Kalmanovitch, An effective model of viscosity for ash deposition phenomena, Proc. Eng. Found. Conf. Miner. Matter Ash Depos. from Coal. 89–101 (1988).

[30] T.J. Krieger, I.M., Dougherty, A mechanism for non-Newtonian flow in suspensions of rigid spheres, Trans. Soc. Rheol. 3 (1959) 137–152.

[31] and Y.F. Y. Alqenai, M. Balapour, M. Zooyousefin, N. Shrestha, G. Hsuan, Evaluation of mean residence time of lightweight aggregates manufactured using waste coal-combustion ash, (n.d.).

[32] BSI Standards Publication, Part 11: Determination of compressibility and confined compressive strength of lightweight aggregates, 2013. www.techstreet.com.

[33] A.H.M.M.A.I. S. Hossain, Curing of Concrete: A Review of Literature, J. Civ. Eng. Archit. 8 (2014). https://doi.org/10.13140/RG.2.2.32095.07848.

[34] F. Aggregate, C. Aggregate, Section 704 — Cement Concrete, 1 (2016) 1–12.

[35] M.B. Solutions, MasterAir AE 90 air entraining admixture, (n.d.). https://www.master-builders-solutions.com/en-us/products/concrete-admixtures/air-entrainers-and-foaming-agents/air-entraining-admixtures/masterair-ae-90.

[36] M.B. Solutions, MasterSure Z 60 workability-retaining admixture, (n.d.). https://www.master-builders-solutions.com/en-us/products/concrete-admixtures/workability-retainers/mastersure-z-60.

[37] ASTM C127, Standard Test Method for Density, Relative Density (Specific Gravity), and Absorption of Coarse Aggregate, Annu. B. ASTM Stand. (2004) 1–5.

https://doi.org/10.1520/C0127-15.2.

[38] ASTM C128, ASTM C128: Standard Test Method for Relative Density (Specific Gravity) and Absorption of Fine Aggregate, Annu. B. ASTM Stand. i (2022) 1–6. https://doi.org/10.1520/C0128-15.2.

[39] Astm:C29/C29M-09, Standard Test Method for Bulk Density (“ Unit Weight ”) and Voids in Aggregate, ASTM Int. i (2009) 1–5. https://doi.org/10.1520/C0029.

[40] ASTM C33: Standard Specification for, (n.d.). https://doi.org/10.1520/C0033_C0033M-08.

[41] D.P. Bentz, K.A. Snyder, Protected paste volume in concrete: Extension to internal curing using saturated lightweight fine aggregate, Cem. Concr. Res. 29 (1999) 1863–1867. https://doi.org/10.1016/S0008-8846(99)00178-7.

[42] C.C. Test, B. Statements, ASTM C143 StandardTest Method for Slump of Hydraulic-Cement Concrete 1, (n.d.) 1–4. https://doi.org/10.1520/C0143.

[43] A. Drews, ASTM C231 Standard Test Method for Air Content of Freshly Mixed Concrete by the Pressure Method1, Man. Hydrocarb. Anal. 6th Ed. (2008) 545-545–3. https://doi.org/10.1520/mnl10913m.

[44] ASTM C-39, Standard Test Method for Compressive Strength of Cylindrical Concrete Specimens 1 - ASTM C39/C39M - Standard, Annu. B. ASTM Stand. 04.02 (2001) 1–7. https://doi.org/10.1520/C0039.

[45] C.C. Test, T. Drilled, C. Concrete, Standard Test Method for Flexural Strength of Concrete ( Using Simple Beam with Third-Point Loading ) 1, Hand C78-02 (2010) 1–4. https://doi.org/10.1520/C0078.

[46] A. C157, Standard test method for length change of hardened hydraulic-cement mortar and concrete, J. Hum. Evol. 04 (2018) 1–7. https://doi.org/10.1520/C0157.

[47] ASTM C1585-13, Standard Test Method for Measurement of Rate of Absorption of Water by Hydraulic Cement Concretes, ASTM Int. 41 (2013) 1–6. https://doi.org/10.1520/C1585-13.2.

[48] J. Castro, D. Bentz, J. Weiss, Effect of sample conditioning on the water absorption of concrete, Cem. Concr. Compos. 33 (2011) 805–813. https://doi.org/10.1016/j.cemconcomp.2011.05.007.

[49] R. Henkensiefken, D. Bentz, T. Nantung, J. Weiss, Volume change and cracking in internally cured mixtures made with saturated lightweight aggregate under sealed and unsealed conditions, Cem. Concr. Compos. 31 (2009) 427–437. https://doi.org/10.1016/j.cemconcomp.2009.04.003.

[50] G. Sant, P. Lura, J. Weiss, Measurement of volume change in cementitious materials at early ages review of testing protocols and interpretation of results, Transp. Res. Rec. C (2006) 21–29. https://doi.org/10.3141/1979-05.

[51] R. Henkensiefken, J. Castro, D. Bentz, T. Nantung, J. Weiss, Water absorption in internally cured mortar made with water-filled lightweight aggregate, Cem. Concr. Res. 39 (2009)

883–892. https://doi.org/10.1016/j.cemconres.2009.06.009.

[52] Astm C666/C666M, Standard Test Method for Resistance of Concrete to Rapid Freezing and Thawing, ASTM Int. West Conshohocken, PA 03 (2003) 1–6. https://doi.org/10.1520/C0666.

[53] Y. Farnam, D. Bentz, A. Sakulich, D. Flynn, J. Weiss, Measuring Freeze and Thaw Damage in Mortars Containing Deicing Salt Using a Low-Temperature Longitudinal Guarded Comparative Calorimeter and Acoustic Emission, Adv. Civ. Eng. Mater. 3 (2014) 316–337. https://doi.org/10.1520/ACEM20130095.

[54] Y. Farnam, H. Todak, R. Spragg, J. Weiss, Electrical response of mortar with different degrees of saturation and deicing salt solutions during freezing and thawing, Cem. Concr. Compos. 59 (2015) 49–59. https://doi.org/10.1016/j.cemconcomp.2015.03.003.

[55] Y. Shields, E. Garboczi, J. Weiss, Y. Farnam, Freeze-thaw crack determination in cementitious materials using 3D X-ray computed tomography and acoustic emission, Cem. Concr. Compos. 89 (2018) 120–129. https://doi.org/10.1016/j.cemconcomp.2018.03.004.

[56] Y. Qian, Y. Farnam, J. Weiss, Using acoustic emission to quantify freeze-thaw damage of mortar saturated with NaCl solutions, Proc. 4th Int. Conf. Durab. Concr. Struct. ICDCS 2014 (2014) 32–37. https://doi.org/10.5703/1288284315379.

[57] Tatiane Machado, L.E.A.F. METHOD 13151 MASS TRANSFER RATES OF CONSTITUENTS IN MONOLITHIC OR COMPACTED GRANULAR MATERIALS USING A SEMI-DYNAMIC TANK LEACHING PROCEDURE SW-846, 549 מים והשקייה (2017) 40–42.

[58] U. Epa, O. of Resource Conservation, Leaching Environmental Assessment Framework (LEAF) How-To Guide Understanding the LEAF Approach and How and When to Use It Leaching Environmental Assessment Framework (LEAF) How-To Guide Notice/Disclaimer & Acknowledgements i NOTICE/DISCLAIMER, 2019.

[59] L.C. Cost, ECONOMICS, (n.d.) 24–26.

[60] Y.M. Alqenai, B. Tejuoso, Yaghoob (Amir) Farnam, Internal Curing with Fine Light Weight Aggregates (FLWA) Created from Unsuitable Coal Combustion Ash (CCA) Task 2 – Report, (2024).

[61] EPA, Proposed Changes for Legacy Coal Combustion Residuals Surface Impoundments and CCR Management Units, (2023) 1–8.

[62] TALEN Energy, (2024). https://www.talenenergy.com/.

[63] Macron Fine Chemicals™ brand products | Avantor, (n.d.). https://www.avantorsciences.com/pages/en/macron-fine-chemicals (accessed July 28, 2022).

[64] M. Overview, R. Coverage, NaOH Pellets ( Sodium Hydroxide Pellet ) Market Size , Share & amp ; Trends Analysis Report By Application , Regional Outlook , Competitive Strategies , And S, (n.d.) 1–6.

[65] ChemAnalyst, Caustic Soda Price Trend and Forecast Get, Track Hydroquinone Price Trend Forecast Top 10 Lead. Ctries. Worlwide (2023) 1–5. https://www.chemanalyst.com/Pricing-data/hydroquinone-1392.

[66] Markets and Markets, Sodium hydroxide market, Mark. Mark. (2024) 1–12. https://www.marketsandmarkets.com/Market-Reports/sodium-hydroxide-market-91825689.html.

[67] Mike (Sodium Hydroxide), Sodium hydroxide price index, Businessanalytiq (2024). https://businessanalytiq.com/procurementanalytics/index/sodium-hydroxide-price-index/.

[68] R. Salt, F.O.R. Sale, A.T. Great, B. Rock, S. For, S. By, T.H.E. Ton, Braen Supply, (2014) 4–7. https://braensupply.com/rock-salt-for-sale-nj/.

[69] White River Salt, Zimmerman, (2019) 4–7. https://www.zimmermanmulch.com/products/ice-melt/bulk-road-salt/.

[70] M. List, F. Salt, B. Products, S. Sacks, L. Products, D. Control, C. Us, B.S. Calculator, Rock Salt USA, (n.d.) 1–5.

[71] Pennsylvania Public Utility Commission, (2024). https://www.puc.pa.gov/.

[72] Philadelphia Water Department, (2024). https://water.phila.gov/.

[73] Pittsburgh Water & Sewer Authority, (2024). https://www.pgh2o.com/.

[74] L. Nguyen, A.J. Moseson, Y. Farnam, S. Spatari, Effects of composition and transportation logistics on environmental, energy and cost metrics for the production of alternative cementitious binders., J. Clean. Prod. 185 (2018) 628–645. https://doi.org/10.1016/j.jclepro.2018.02.247.

[75] T.S. Butalia, W.E. Wolfe, Coal Combustion Products Extension Program, (2006) 74.

[76] C.R. Cheeseman, A. Makinde, S. Bethanis, Properties of lightweight aggregate produced by rapid sintering of incinerator bottom ash, Resour. Conserv. Recycl. 43 (2005) 147–162. https://doi.org/10.1016/j.resconrec.2004.05.004.

[77] E. Resources, About ESCSI STRUCTURAL EFFICIENCY WITH LW CONCRETE, (n.d.) 4–6. https://www.escsi.org/structural-lightweight-concrete/sustainability/structural-efficiency-with-lw-concrete/.

[78] M.C. Rukashaza-Mukome, Cost Comparison of Treatments Used to Maintain or Upgrade Aggregate Roads, Proc. 2003 Mid-Continent Transp. Res. Symp. (2003). http://www.ctre.iastate.edu/pubs/midcon2003/RukashazaTreatments.pdf.

[79] B.L. Drotleff, D. Eberly, B.R. Industries, About ESCSI SAFER , MORE COST EFFECTIVE ROADS : ESCS LIGHTWEIGHT AGGREGATE , USED IN CHIP SEAL SURFACE TREATMENTS , PROVIDED COST SAVINGS AND A HIGHER FRICTION NUMBER FOR LOUISIANA HIGHWAY 3147, (n.d.) 2–5. https://www.escsi.org/e-newsletter/safer-more-cost-effective-roads/.

[80] G. Started, Machinery Trader Co., (n.d.) 2–3. https://www.machinerytrader.com/.

[81] F. Service, HED International. Advanced Processing systems, (2024) 4–7. http://www.hed.com/site/.

[82] M.D.R. Motor, D. Rollers, B. Trolleys, B. Conveyor, C. Conveyor, C. Driven, L. Roller, C.F. Supports, C. Rollers, F. Conveyor, F. Rail, S. Wheels, C. Rail, Buy conveyors and parts, (1881) 1–5. https://www.ultimationinc.com/.

[83] D. Pelletizers, FEECO International Inc. Disc pelletizers, (n.d.) 5–11. https://feeco.com/disc-pelletizers/?gad_source=1&gclid=Cj0KCQjw_-GxBhC1ARIsADGgDjscMXvDXLN9_7NiafVz3T9tBwdc0CeLztmUJa0oCXALO3CvyZb7-XAaAu_SEALw_wcB.

[84] I.C. Solutions, C. Performance, Fives Group Co. Energy | combustion, (n.d.) 1–8. https://www.fivesgroup.com/energy-combustion.

[85] A. Us, Deltech Furnaces Co., (n.d.) 4–7. https://www.deltechfurnaces.com/.

[86] A.M. Heavy, D. Conveyor, S. Belting, Sparks A JSJ Buisness. Sparks Belting- D & D Belt Service, (n.d.) 1–6. https://www.sparksbelting.com/products/heavy-duty-conveyor-belting.

[87] C.T.H.E. Game, W.A. Proall, M. Truck, Pro ALL. A Terex Brand., (n.d.) 1–11. https://proallinc.com/.

[88] T. Oshkosh, Oshkosh Co., (1981) 24–26. https://oshkoshsseries.com/.

[89] M. Pelletizing, Diamond America Co. Pelletizing Machines, (n.d.) 5–7. https://daextrusion.com/equipment/extruders/pelletizing-machines/.

[90] Shumaker Industries Co., (1953) 1953. https://www.shumakerindustries.com/.

[91] T.Y. Shin, Y.H. Kim, C.B. Park, J.H. Kim, Quantitative evaluation on the pumpability of lightweight aggregate concrete by a full-scale pumping test, Case Stud. Constr. Mater. 16 (2022) e01075. https://doi.org/10.1016/j.cscm.2022.e01075.

[92] S. Aggregates, M.-I. Analysis, Synthetic Aggregates Market - Global Industry Analysis and, (2023) 1–6.

[93] T.W. Bremner, J.P. Ries, W.H. Wolfe, Achieving sustainability with lightweight aggregates, Proc. Int. Conf. Sustain. Constr. Mater. Technol. (2007) 13–17.

[94] Fior Markets, Global Lightweight Aggregates Market to Experience, GlobeNewswire (2022) 20–24. https://www.globenewswire.com/news-release/2022/05/12/2442567/0/en/Global-Lightweight-Aggregates-Market-to-Experience-Significant-Growth-of-USD-3-246-07-Million-By-2030.html.

[95] T. Impacts, S. Grant, A. Marshall, An official website of the United States government Here ’ s how you know I-Corps : Lightweight Aggregates from Waste Bottom Ash, (2019) 1–5.

[96] M. Balapour, Conversion of Waste Coal Combustion Ash to Value-Added Construction Lightweight Aggregates through A Holistic Thermodynamics-Guided Manufacturing Framework, Drexel University, 2021.

[97] O.P. Statement, C. Policy, A. All, Overview of environmental, social, governance (ESG) tax credit initiatives, (2023).

[98] U.S. EPA, Part One - The Multiple Benefits of Energy Efficiency and Renewable Energy, Quantifying Mult. Benefits Energy Effic. Renew. Energy A Guid. State Local Gov. (2018) 1–17. https://www.epa.gov/statelocalenergy/quantifying-multiple-benefits-energy-efficiency-and-renewable-energy-guide-state.

[99] R. Frazier, Report: Coal Ash contamination widespread in U.S., PA | StateImpact Pennsylvania, (2019) 1–9.

[100] D. Pdf, Toxic Coal Ash in Pennsylvania : Addressing Coal Plants ' Hazardous Legacy, (2024) 1–22.

[101] U. Symposia, About the ash library, (2017) 2017–2019. http://www.flyash.info/.

[102] D.C. Jansen, M.L. Kiggins, C.W. Swan, R.A. Malloy, M.G. Kashi, R.A. Chan, C. Javdekar, C. Siegal, J. Weingram, Lightweight fly ash-plastic aggregates in concrete, Transp. Res. Rec. (2001) 44–52. https://doi.org/10.3141/1775-07.

[103] M. Aineto, A. Acosta, J.M. Rincón, M. Romero, Production of Lightweight Aggregates from Coal Gasification Fly Ash and Slag, n.d.

[104] J.C. Van Dyk, S.A. Benson, M.L. Laumb, B. Waanders, Coal and coal ash characteristics to understand mineral transformations and slag formation, Fuel 88 (2009) 1057–1063. https://doi.org/10.1016/j.fuel.2008.11.034.

[105] W.C. McKerall, W.B. Ledbetter, D.J. Teague, Analysis of Fly Ashes Produced in Texas, (1982).

[106] B. Valentim, A. Guedes, D. Flores, C.R. Ward, J.C. Hower, Variations in fly ash composition with sampling location: Case study from a Portuguese power plant, Coal Combust. Gasif. Prod. 1 (2009) 14–24. https://doi.org/10.4177/ccgp-d-09-00017.1.

[107] J.C. Hower, A.S. Trimble, C.F. Eble, Temporal and spatial variations in fly ash quality, Fuel Process. Technol. 73 (2001) 37–58. https://doi.org/10.1016/S0378-3820(01)00193-X.